

RESEARCH ARTICLE

Astrobiology: resolution of the statistical Drake equation by Maccone’s lognormal method in 50 steps

E. Mieli¹ , A. M. F. Valli² and C. Maccone^{3,4} 

¹Via Oceano Pacifico, 2/A – 00071 Pomezia (Rome), Italy

²Istituto Italiano di Paleontologia Umana, Museo Civico di Zoologia, Via Aldrovandi 18, 00197 Roma (Italia), Société Scientifique du Bourbonnais pour l’Étude et la Protection de la Nature, Moulins-sur-Allier, France

³Istituto Nazionale di Astrofisica (INAF), Rome, Italy

⁴International Academy of Astronautics (IAA), Paris, France

Corresponding author: E. Mieli; Email: eugenio.mieli@gmail.com

Received: 20 January 2023; **Revised:** 25 April 2023; **Accepted:** 1 May 2023

Keywords: Drake statistical equation, galactic civilizations, lognormal distribution, Milky Way, transition from non-living to the living

Abstract

The authors use the mathematical tool of Maccone’s lognormal distribution to further factor the Drake equation, which calculates the number of advanced civilizations in the galaxy, from the seven original levels of the Drake equation to 49 levels of overall analysis. The Maccone approach, in fact, supported by the central limit theorem, becomes more reliable the more levels are introduced. The resulting study necessarily draws upon an array of disciplines ranging from astronomy, chemistry and geology to biology, palaeontology and futurology. The final result calculates the number of planetary systems suitable for life in its various stages of development: those which have probably hosted life in the past and those which still host it at its various evolutionary levels. The final evolutionary level is the so-called galactic civilization (often called ETC, or extraterrestrial civilizations). The number of resulting galactic civilizations is divided between *static* civilizations, which do not move around the galaxy and whose Kardašev rating is still low (<1.4), of which we find three examples (we ourselves plus, perhaps, two others), and potentially *dynamic* civilizations, which move around the galaxy and have a sufficiently high Kardašev rating (≥ 1.4), of which we find 2000.

Contents

Introduction	429
The phases and challenges	431
The Drake astronomical parameters: N_s, n_p and f_s	431
First Drake: the stellar number of the galactic disc for stars of spectral class K, G and F	433
Second Drake: number of planets per star, suitable for life in the habitable area (spectral classes F, G and K)	434
Third Drake: fraction of stable planets for 7 GY (lifespan of the star population)	434
The calculation of the third parameter from the composition of the nine challenges	440
Considerations on the first three parameters	441
The Drake biological parameters: f_i and f_l	441
Fourth Drake: the transition from the non-living to the living	443
Mario Ageno’s theory	444
The calculation of the fourth parameter f_l	446
Phases of transition from non-living to living	447
Evaluation of the probability of passing each stage	457

Considerations on the fourth parameter	459
Fifth Drake: the probability of intelligent life	460
The starting point; the stability conditions of a planet	461
Macro-interval A	461
The onset of the eukaryotic cell, phase by phase	466
Evaluation of the probability of passing each stage	472
Macro-interval B	474
The onset of metazoa, phase by phase	477
Evaluation of the probability of passing each stage	479
Macro-interval C	479
The birth of intelligence, phase by phase	483
Evaluation of the probability of passing each stage	491
Evaluation of the total probability: Drake's fifth parameter	492
The oxygen curve	494
Considerations on the fifth parameter	498
The Drake social parameters: f_C and f_L	499
Sixth Drake: fraction of planets where life decides to communicate	499
Seventh Drake: temporal fraction of a civilization's duration	499
The seven challenges of galactic civilizations (and plan B)	506
Considerations on the seventh parameter	514
The complete Drake equation	516
The Fermi paradox and conclusions	519
Appendix A: Summary of the 49 steps (plus one) of the Drake equation	530
Appendix B: Percentage of past planets and present for each stage of development	532
Appendix B1. Percentage of past planets and present for each stage of development	533
Appendix B2. Percentage of past planets and present for each stage of development	534
Appendix B3. Percentage of past planets and present for each stage of development	535
Appendix C: The calculation of the distribution function of the seventh parameter	536

Introduction

We will now take a brief introductory look at Maccone's work on the Drake equation and the number N of intelligent civilizations of the Milky Way. This approach is the main inspiration for what we attempt to do in this paper to estimate the number of planets suitable for life at various levels of evolution and the number of planets that have actually hosted it in the past and host it at present. To estimate the number of alien civilizations, Drake simply multiplied seven crucial factors (Drake, 1961, Menichella and Hack, 2002; Webb, 2015):

Original equation

$$N = R^* \times f_p \times n_e \times f_l \times f_i \times f_c \times L,$$

R^* , annual star birth rate in the Milky Way; f_p , fraction of stars with planets; n_e , number of planets suitable for life for each star; f_l , fraction of suitable planets where life develops; f_i , fraction of planets inhabited by intelligent life; f_c , fraction of planets where intelligent life decides to communicate; L , lifetime of the planet in which intelligent life persists.

It was soon noticed that this initial description was insufficient for obtaining concrete conclusions since the seven factors often oscillate between very distant minimum and maximum values and in some cases are completely unknown. We are referring above all to the points from 4 onwards, where

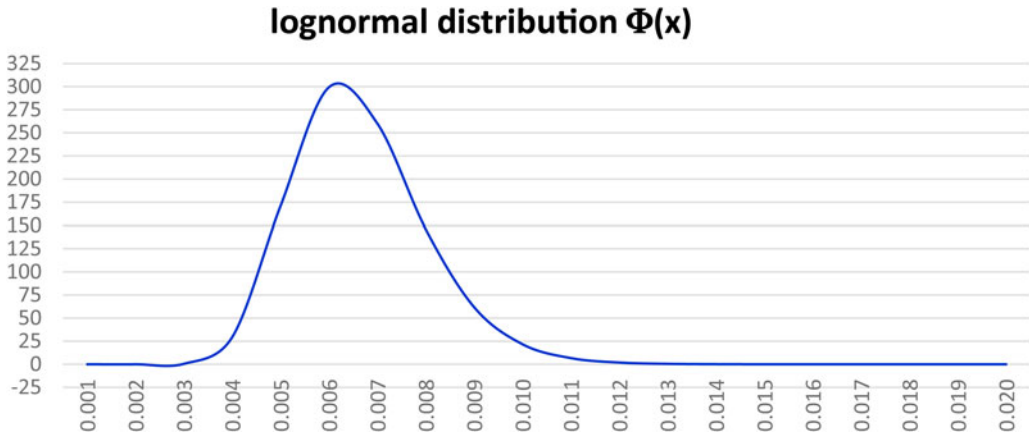


Figure 1. Example of lognormal distribution Φ : the distribution exists for $x > 0$ and is normalized to one with mean value, in the example reported, around 0.007 and standard deviation around 0.002.

astronomical knowledge is no longer helpful. In 2008, Maccone conceived of a powerful mathematical tool called the *statistical Drake equation* which, starting from the statistical distribution of the seven individual factors, calculates the statistical distribution of their product according to a curve called *lognormal*, or the distribution curve of a random variable whose logarithm is distributed normally.

This result is not obvious, and the more factors contribute to the calculation, the more correct are the result (Central Limit Theorem). An example of the lognormal function Φ is shown in Fig. 1.

As with many other authors, we have preferred not to refer to the classic Drake equation but to a variant of our own which is most suitable for our purposes. This being, in our case:

Changed equation

$$N = N_s \times n_p \times f_s \times f_i \times f_c \times f_L,$$

N_s , number of stars of the galaxy suitable for life (of spectral class K, G and F); n_p , number of planets per star in the habitable area (of spectral class K, G and F); f_s , fraction of planets stable in the habitable area (function of the duration ΔT); f_i , fraction of suitable planets where life actually develops; f_c , fraction of planets inhabited by intelligent life; f_L , fraction of the lifetime of the planet in which intelligent life persists with respect to the duration of the last stellar population I (HyperPhysics, 2014).

As can be seen, in the original Drake equation, the annual stellar formation rate in the Milky Way R^* appears as the first factor which is equal to $N_s/\Delta T_0$, where ΔT_0 is the average duration of the last stellar population which we set as equal to about 7 Gy (billions of years). Instead, in our equation, the first factor loses the denominator ΔT_0 , which instead is used to divide the last term L , which becomes f_L (fraction of the life time of the planet in which intelligent life persists with respect to the duration of the last stellar population). In this way, as we will see, we will also be able to use the first terms of the Drake equation to directly obtain information not only about advanced civilizations but also about life forms in general.

In addition, we made the choice not to delegate all the calculation effort onto the third of the first three Drake parameters (in the original equation, n_e , or number of planets suitable for life), but to also divide the work between the first two parameters: for this reason, the first N_s parameter has become the number of stars in the galaxy *only* if belonging to the spectral class K, G and F (Ledrew, 2001), which are those suitable classes for the development of life (Kunimoto and Matthews, 2020). Similarly, the second parameter has become n_p or the number of planets per star in the habitable area, thus absorbing the burden of discriminating *only* the planets of the so-called *Goldilocks zone* (keep in mind that the f_p parameter in the original equation trivially represented the fraction of stars with planets). In our

equation, this results in f_s , replacing n_e , that is, the number of planets suitable for life, specifically becoming the fraction of stable planets in the habitable zone, which is also a function of the duration ΔT which we take into consideration according to the phases of development of life considered. As mentioned above, this way of redefining the Drake equation will prove useful to us both in estimating each individual parameter and in the use of the entire equation which in addition to calculating the number of existing galactic civilizations can also be used to estimate the number of planets on which life develops at varying evolutionary levels.

Finally, Drake related the onset of intelligence to the fifth parameter and defined it as being technological and communicating in the sixth one. We have chosen, however, to define intelligence according to the more severe criterion of energy availability on the model of Kardašev: *intelligence is at least at our own technological level*, with a minimum parameter of $K = 0.7$. This factor defines the perimeter of the fifth parameter, while the sixth includes only those civilizations that *decide* not to communicate and remain in the shadows; the seventh, dealing with the duration of civilizations, also includes those cases in which the aforementioned civilizations *are induced or forced* to no longer communicate.

Without going into further detail, we can state that the advantages of our choice to redefine traditional parameters will become clearer over the explanation of the 49 (plus 1) steps of the Drake equation.

The phases and challenges

As we will see, the 49 steps in which we will carry out the Drake equation possess varying statistical characteristics which we will examine as they occur. The feature which is upstream of all the others, however, is the distinction between a step called a *phase* and a step called a *challenge*. The following analogy will give an immediate idea of the difference between them: imagine we must follow a route which presents various difficulties; for example

- (A) a maze from which to escape (prob. p_A)
- (B) a Tibetan bridge to cross (prob. p_B)

Both of these difficulties have an associated probability of success of p_A and p_B ; the statistical nature of these two parts of the route is the same, but is that really the case? No, in fact, *in relation to time*, the two steps behave in opposite ways, that is, the p_A probability of getting out of the maze increases over the time of permanence in the maze itself, while the probability p_B of crossing the Tibetan bridge decreases over the time spent on the bridge: the first, borrowing the language of relativity, is *covariant* over time and we will define the corresponding step as a *phase*, while the second is *contravariant* over time and we will define the corresponding step as a *challenge*.

If p_A and p_B do not have an explicit dependence with regard to time (this will only be true for us in the first approximation), then the respective transformation laws, going from a reference time interval ΔT_0 (with p_{A0} and p_{B0} probability) to any $\Delta T = n \times \Delta T_0$ (with p_A and p_B probability), will be the following:

A – <i>phase</i>	$p_A = 1 - (1 - p_{A0})^n$	Increasing with n
B – <i>challenge</i>	$p_B = (p_{B0})^n$	Decreasing with n

It is easy to see that when n increases, p_A approaches 1, while p_B approaches 0; in both cases exponentially with n .

If p_A and p_B have an explicit dependence as regards time then their trend is no longer simply exponential, even if they maintain their nature as phases or challenges.

The Drake astronomical parameters: N_s , n_p and f_s

At least in principle, the mathematical approach of the first three parameters is less difficult than for the biological ones, the fourth and fifth, because the astronomical events which we will refer to are now

largely independent of each other without there being any need to respect one particular sequence; the same thing will not be true for the fourth, fifth, nor for the seventh parameter, which deals with the fraction of extraterrestrial civilizations (ETC) duration compared to 7 Gy. The first three parameters were dealt with in Stephen H. Dole’s (1964) book *Habitable Planets for Man* and in Maccone’s paper, *Statistical Drake–Seager Equation for exoplanet and SETI searches* (Maccone, 2015).

We will now briefly describe the mathematical details relating to the Drake equation and the Maccone method; that is to say:

- (1) we will deal with the first two parameters of Drake, N_s and n_p without breaking them down into further factors but by directly using results that emerge overwhelmingly from the vast mass of experimental data available to us;
- (2) we will instead divide the process of the third parameter, f_s , into nine factors representing as many challenges to be overcome, all referring to the same time interval $\Delta T_0 = 7$ Gy (billions of years) which is the duration of the last stellar population;
- (3) we will therefore establish the input data for each individual challenge, that is the frequencies (fractions of overcoming the challenge) minimal and maximum a_j, b_j of the x_j random variable;
- (4) using Maccone’s lognormal formula $\Phi(x_0)$, we will obtain, from these single frequencies, $\langle x_0 \rangle$, the average frequency of the entire process of overall planetary survival and $\sigma(x_0)$ the standard deviation from the overall average over the period ΔT_0 (Maccone, 2010);
- (5) from the average frequency we will calculate the minimum value and the maximum value of the variable $\langle x_0 \rangle$ with the formula derived from the lognormal (Maccone, 2010):

$$\langle x_0 \rangle_{\min} = \langle x_0 \rangle - \sqrt{3} \times \sigma(x_0),$$

$$\langle x_0 \rangle_{\max} = \langle x_0 \rangle + \sqrt{3} \times \sigma(x_0),$$

we will extend the $\langle x_0 \rangle_{\min}$ and the $\langle x_0 \rangle_{\max}$, from the ΔT_0 period of 7 Gy set to any ΔT period, thus obtaining the final survival frequencies $\langle X_0 \rangle_{\min/\max}(\Delta T)$ of the stable planets in function of time ΔT . To do this we set:

$$\left\{ \begin{array}{l} m = \frac{\Delta T}{\Delta T_0} \\ \langle X_0 \rangle_{\min}(\Delta T) = (\langle x_0 \rangle_{\min}(\Delta T_0))^m \\ \langle X_0 \rangle_{\max}(\Delta T) = (\langle x_0 \rangle_{\max}(\Delta T_0))^m \end{array} \right.$$

In this way, the new $\langle X_0 \rangle_{\min/\max}(\Delta T)$ (contravariant over time) values will be referred to the new time ΔT which is m times the time Δs_0 . We observe that the above expressions can be written in the most familiar exponential form:

$$\left\{ \begin{array}{l} \tau_{(\min/\max)} \equiv \frac{\Delta T_0}{\ln\left(\frac{1}{\langle x_0 \rangle_{\min/\max}}\right)} \\ \langle X_0 \rangle_{\min}(\Delta T) = \exp\left(-\frac{\Delta T}{\tau_{\min}}\right) \\ \langle X_0 \rangle_{\max}(\Delta T) = \exp\left(-\frac{\Delta T}{\tau_{\max}}\right) \end{array} \right.$$

Figure 2 shows the trend that we expect from the calculation of $\langle X_0 \rangle_{\min/\max}$ according to ΔT (it was taken, by way of example, $\tau_{\text{med}} \sim 2.5$ Gy). As you can see, the three values $\langle X_0 \rangle_{\min}$, $\langle X_0 \rangle_{\max}$ and $\langle X_0 \rangle_{\text{mean}}$ have an exponentially decreasing trend as a function of the reference duration ΔT . This result will be useful later for determining the number of planets suitable for the various levels of life development.

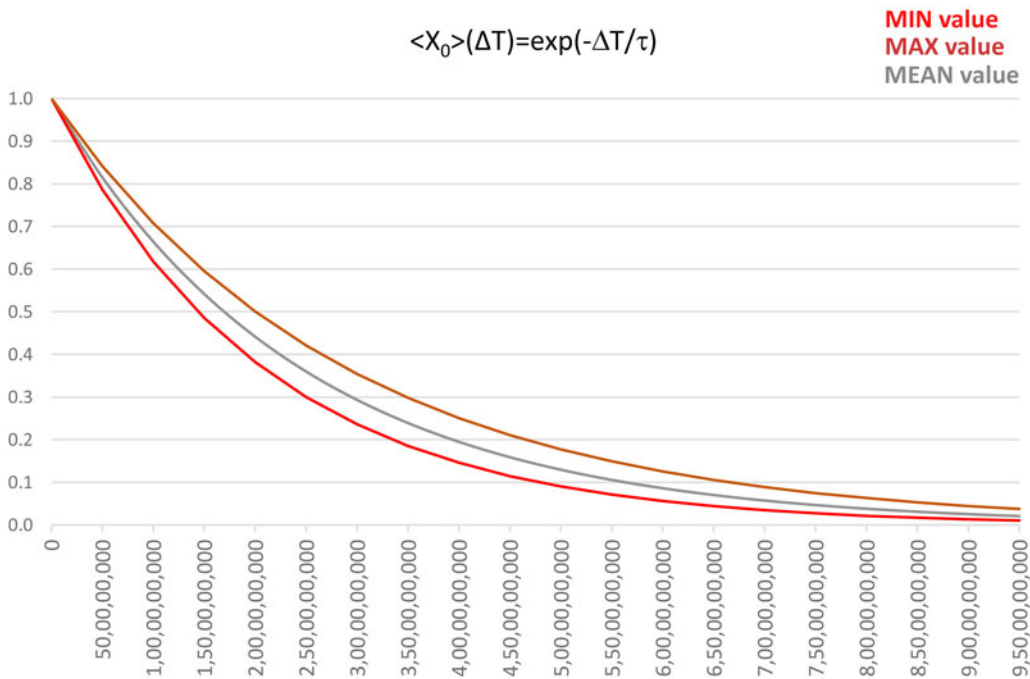


Figure 2. Trend expected by the calculation of $\langle x_0 \rangle_{min/max}$ according to ΔT with $\tau_{mean} \sim 2.5$ Gy.

First Drake: the stellar number of the galactic disc for stars of spectral class K, G and F

We will start with the first parameter of Drake, or the stellar number of the galaxy; also giving the parameter, however, the job of considering only the stars now considered suitable for the development of life, or those of spectral class K, G and F of the galactic disk (Erik, 2009; Kunimoto and Matthews, 2020). The reason for this choice, in addition to balancing the calculation effort between the parameters, as anticipated in the introduction, also has a mathematical advantage: if, for example, we now considered all the stars in the main sequence of the Milky Way (Salpeter, 1954), we should say that there are approximately between 2×10^{11} and 4×10^{11} , that is, on average, 3×10^{11} with a very large deviation of 10^{11} ; so, even if the underestimation/overestimation of the average value would then be reabsorbed by the second parameter, this would not be true for the deviation from the average value that would be unnecessarily large worsening the final calculation of the Drake equation. The exclusion of the numerous spectral class M (red dwarfs with masses between 0.08 and 0.45 M_{\odot} , solar masses) from this calculation depends on the current belief that these solar systems are highly unstable from the point of view of the nuclear activity of the star; because of its slow stellar evolution due to its small mass, this has frequent and lethal flares for the first part of the life of the planets (Crossfield *et al.*, 2022). The planets of these stars have in turn synchronous rotations (always presenting the same face to the star) due to the strong tidal forces of the habitable area. These two factors, especially the first, makes this type of star unsuitable for hosting life for a long period of time, despite the recent discovery of wonderful and apparently habitable planetary systems around these stars.

The same reasoning was applied to the galactic bulge, considered too crowded and therefore subject to frequent violent phenomena such as supernovas or gamma flashes, lethal for the development of life (Margalef-Bentabol *et al.*, 2018; Gonzalez *et al.*, 2001; Gonzalez, 2005; Sanders, 2014). With the above in mind, let us consider the data of Table 1, which reports all the star types divided by areas of the galaxy:

Obviously, we are only interested in the stars of the classes F, G and K belonging to the galactic disk (McMillan, 2011): the sum of these three sets is equal to 1.10×10^{10} stars; despite the presence of three significant figures in the mantissa, for this value we assign to the first parameter of Drake a prudential uncertainty of approximately 10%, namely:

Table 1. *Stellar number of the Milky Way divided by localization and spectral type (Picaud and Robin, 2004; McMillan, 2011; data taken from the site <https://ilpoliedrico.com/2015/12/quante-stelle-ci-sono-nella-via-lattea.html>)*

Spectral class	Mass interval (M_{\odot})	% of stars in the disc	Bulge stars ($2.40 \times 10^{10} M_{\odot}$)	Disk stars ($3.79 \times 10^{10} M_{\odot}$)	Halo stars ($2.40 \times 10^8 M_{\odot}$)	Main seq. stars ($6.43 \times 10^{10} M_{\odot}$)
O	≥ 16	0.00001%	8.57×10^1	1.35×10^2	The production of new stars in the halo ceased 10 billion years ago and only small population of the population II are still in the main sequence. The others got extinct	2.21×10^2
B	2.1–16	0.13%	2.99×10^6	4.71×10^6		7.70×10^6
A	1.4–2.1	0.60%	6.40×10^7	1.01×10^8		1.65×10^8
F	1.04–1.4	3.00%	5.43×10^8	8.58×10^8		14.00×10^9
G	0.8–1.04	7.60%	1.97×10^9	3.11×10^9		5.09×10^9
K	0.45–0.8	12.10%	4.47×10^9	7.06×10^9	1.71×10^9	1.32×10^{10}
M	0.08–0.45	76.45%	6.44×10^{10}	1.02×10^{11}	2.27×10^9	1.68×10^{11}
Total stars present in the Milky Way			7.14×10^{10}	1.13×10^{11}	3.97×10^9	1.88×10^{11}

Drake 1

N_s min	N_s max
1.0×10^{10}	1.2×10^{10}

Second Drake: number of planets per star, suitable for life in the habitable area (spectral classes F, G and K)

We will also evaluate the second parameter directly from what we find in the literature (Schulze-Makuch *et al.*, 2020). In this case, the abovementioned 2020 work of Michelle Kunimoto and Jaymie M. Matthews, which is based on an independent catalogue of extrasolar planets carried out on about 200 000 stars, directly provides the result we need.

For planets with dimensions 0.75–1.5 R_{\oplus} , terrestrial masses, orbiting in a conservative habitable area (0.99–1.70 UA) around G-type stars, Kunimoto defines an average value of 0.18 star planets with an uncertainty of 10%. That is to say:

Drake 2

n_p min	n_p max
0.16	0.20

Third Drake: fraction of stable planets for 7 GY (lifespan of the star population)

With the third parameter, we finally enter the calculation through the division of the process into several challenges (in this case nine) which the planet survives with a certain minimum and maximum probability for each. The use of the Maccone formula collects all the input data and provides the minimum and maximum values of the third overall Drake parameter.

The nine challenges, which represent the astronomical dangers to which the planet is subjected, are the following:

- (1) multiple star systems
- (2) supernova less than 40 ly away
- (3) gamma-ray bursts less than 5000 ly away
- (4) superflares of their own star
- (5) transit of the gas giants on internal orbits
- (6) prolonged meteoric bombardment
- (7) instability of rotation axis
- (8) absence of the carbon cycle
- (9) absence of the magnetic field

Challenge 1: multiple star systems

Until a few years ago, the possibility of existence of planets around multiple star systems was considered residual. Today, we have some concrete feedback (Andrade-Ines *et al.*, 2016; Tokovinin, 1997), the most famous of which is the exoplanet *Proxima Centauri b* which is also the closest to us. Together with Alpha Centauri A and B, Proxima Centauri is actually a triple system: Alpha Centauri A and B revolve around the common centre of mass at close range, while Proxima Centauri (a red dwarf of spectral class M5v that we are only using here by way of example) revolves around the preceding couple at much greater distance. *Proxima Centauri b*'s planetary system is called a type S planetary system, which means that the planets orbit around a practically isolated star because it is very far from its companion (or in this case from its companions). Systems of this type are quite common and do not preclude the formation of lifeforms, each type S system having its own area of habitability scarcely influenced by the orbiting star at a great distance. The opposite case is that of type P planetary systems, called *circumbinary* (Shevchenko *et al.*, 2019), which are composed of a pair of stars rotating at a close distance and a planetary system that revolves at a great distance around them (like the imaginary planet Tatooine in 1977's movie, *Star Wars*); these systems have an area of dynamic ovoid habitability, which follows the motion of the couple of stars and which very rarely adapt to the orbits of the planets. We therefore prefer to exclude these systems from those that could host lifeforms.

In conclusion, we must exclude the number of short distance multiple systems (which could therefore have type P planetary systems) from the number of spectral class F, G and K. As indicated by Charles J. Lada in the *Stellar Multiplicity and the IMF: Most Stars Are Single* (Lada, 2006), for stars with mass similar to the sun the study gives a percentage of 56% of single stars and 44% of double or multiple stars; from this 44% of multiple stars we must estimate how many are short distance systems that would give rise to type P planetary systems: we prudently say between 10 and 30%; therefore, the fraction of those of the F, G and K spectral classes suitable for life is between 70 and 90%.

Challenge 1	
a_1	b_1
0.7	0.9

Challenge 2: supernova at less than 40 ly away (safety distance)

We can quickly calculate the risk factor due to supernovae through the following considerations:

- (A) from indirect assessments, about three explosions of supernova per century are estimated in the Milky Way (Harrington *et al.*, 2008)
- (B) the Milky Way, during the last stellar population of 7 Gy, therefore experienced about 200 000 000 explosions, or one every 1000 stars, approximately

Assuming a random distribution of these events, the average distance of a supernova from any star is about $1,000^{1/3} = 10$ times the average distance between stars, which in the galactic disk is equal to about 5 ly (see [Appendix B](#)). Therefore, the average distance of a supernova from another star is about 50 ly. Obviously this is only an average value from which there are deviations every now and then: it is estimated that there is a supernova explosion within 50 ly of the Earth which involves damage to a part of the ozone layer with partially lethal effects on the biosphere every 250 000 000 years (Chavanis *et al.*, 2019). For these reasons, we have assigned a probability of escaping the risk of a supernova explosion as about 70% with a 10% deviation. That is to say:

Challenge 2	
a_2	b_2
0.6	0.8

Challenge 3: gamma-ray bursts less than 5000 ly away (safety distance)

There is a rich literature dedicated to investigating the causes and potential effects on the planets affected by the imposing phenomena of gamma-ray bursts: it is estimated that in a few seconds they emit an amount of energy equal to 10^{44} – 10^{45} J, the same as that emitted by the sun over its entire existence (Tajima, 2009; Modjaz *et al.*, 2016; Zhang, 2018).

Being extremely powerful phenomena, they are also detected at distances on the borders of the visible universe; this feature facilitates our task because, for this reason, without looking further into their nature and methods of issue (isotropic emission or collimated beams), we can draw up statistics directly from the experimental number of these phenomena recorded on Earth. That is to say:

- (A) roughly one gamma-ray burst a day in the direction of the Earth from the observable universe is detected;
- (B) thus, over the last star population of 7 Gy, there were about 2.5×10^{12} gamma-ray bursts in our direction;
- (C) there are about 10^{23} stars in the observable universe;
- (D) therefore, there was a gamma-ray burst every 4×10^{10} stars in the direction of the Earth from the observable universe;
- (E) the volume defined by the safety distance of 5000 ly from the nearest gamma-ray bursts is $(5 \times 10^3)^3 = 1.25 \times 10^{11} \text{ ly}^3$;
- (F) the density of the galactic disk is approximately $5^3 = 125 \text{ ly}^3$ per star;
- (G) within the safety volume area there are 10^9 stars; this corresponds to an average number of gamma-ray bursts within the safety volume area during the last stellar population, equal to $10^9 / (4 \times 10^{10}) = 2.5 \times 10^{-2}$: thus, a very low value. It has, however, been hypothesized that the mass extinction of the Ordovician–Silurian was due to a gamma-ray burst (Melott *et al.*, 2004).

As in the previous case, we cautiously place ourselves a little above this margin of risk, let's say at 5×10^{-2} , again with a deviation of 5×10^{-2} which takes into account the great uncertainty around these phenomena. The complementary value to this, which indicates the probability of overcoming the risk of gamma flashes, is therefore:

Challenge 3	
a_3	b_3
0.9	1.0

Challenge 4: superflares of the own star

We now consider the dangers coming directly from your planetary system. The common definition of stellar superflare is that of a violent eruption of matter that explodes from the photosphere of a star, with an energy equivalent to a million times or more that characteristic of the common solar flares (Doyle *et al.*, 2020; Trail *et al.*, 2020).

One of the characteristics of the sun-type stars on which superflares have been observed is a faster rotation and greater magnetic activity than those of the sun. It has been hypothesized that these explosions are produced by the interaction of the stellar magnetic field with that of a hot Jupiter-type planet in narrow orbit (Rubenstein and Schaefer, 2000); however, no confirmation of this theory has been provided even from the search for any hot Jovian planets belonging to stars presenting the phenomenon of superflares. In one study (Maehara *et al.*, 2012), 83 000 stars similar to the sun were analysed using the data of the Kepler space telescope, finding 365 superflares from 148 stars, lasting an average of 12 h, over a period of 120 days. This is a statistically very high value, but one should also take into account how these phenomena are distributed.

Despite this, the absence of mass extinctions associated with this kind of phenomena makes us believe that no superflare of the sun has occurred in the past. We therefore associate with these phenomena an intermediate risk and a consequent probability of survival of just over 50%:

Challenge 4	
a_4	b_4
0.5	0.7

Challenge 5: transit of gas giants on internal orbits

Until the discovery of the first exoplanet, mathematical models of planetary evolution were relatively simple and stable, being able to refer to the only known example, namely the solar system (Pollack *et al.*, 2009). The scenario was as tidy as a display in a museum, with the rocky and massive planets in the internal band (but still not too close to the sun) and the gas giants in the most external one; there was even a transition area between the two, the belt of asteroids which, exactly as expected, had not been able to form a planet due to the powerful gravity of nearby Jupiter.

Then we began to receive the first data on the observed exoplanets (Kenyon *et al.*, 2016) and understood that our orderly Solar System was an exception and that most planetary systems were instead as chaotic as a teenager's bedroom: gas giants at ridiculous distances from their star: 0.05 AU or even less (Dawson and Johnson, 2018); gigantic super-earths of dozens of terrestrial masses positioned almost everywhere relative to the other planetary masses (King *et al.*, 2018). In short, the model needed completely redoing, or rather, completely corrected, taking into account the new data. It seems that planetary systems are intrinsically unstable and only rarely remain in their *natural positions*, if they actually exist, as is the case in our system (Chambers, 2006; Johansen *et al.*, 2019). Despite all this, however, one thing is certain: the immense mass of a gas giant in the area disrupts if not the formation of other planets (as in the case of the asteroid range) certainly the trajectory of meteor objects in transit which would be dangerously attracted to internal orbits close to other rocky planets in the habitability band (Bonomo *et al.*, 2017).

Through the observation of exoplanets we can say that this event is not uncommon (Izidoro, 2022); however, we must not fall into the trap of considering the statistics collected on exoplanets directly comparable with a galactic planetary reality, given that some types of planet – the hot Jupiters – are the most easily observable ones both with the transit and with that of the radial speeds method which are the most commonly used. For this reason, we will give the average probability of the transit of hot Jupiters on internal orbits as 20% with a 10% deviation; which, with respect to the complementary value of the probability of survival of life on a planet in the habitability band, translates into the following values:

Challenge 5	
a_5	b_5
0.7	0.9

Challenge 6: prolonged meteor bombardment

There is no reason to think that the typical meteor bombardment that accompanies the formation of rocky planets must be prolonged beyond the initial stages of the life of the planet (Gomes *et al.*, 2005; Berkeley, 2022), especially if we have already excluded the presence nearby of gas giants which can attract objects of various sizes from the external bands of the asteroids (for the solar system, the Kuiper band and the Oort cloud). However, as we have seen, the solar system is not a typical example of a planetary system; therefore, we cannot exclude the possibility that, for example, a particular provision of super-earths in the habitability band or in its vicinity can determine gravitational resonance phenomena with eventual asteroid belts. We have no experimental data on this topic but wish in any case to give a statistical weighting, even if low, to this potential risk:

Challenge 6	
a_6	b_6
0.8	1.0

Challenge 7: instability of the rotation axis

Normally, the rotation axes of the planets do not have a stable inclination but rather vary chaotically due to the interaction between their orbits (Simon *et al.*, 1994). Typical variability periods are of the order of a few million years (see Mars) and the oscillation intervals are very large (60° – 90°). Apart from very small variations of the inclination of the axis, the Earth does not have this characteristic because its heavy satellite – the Moon – acts as a natural stabilizer (Smulsky, 2011).

But how important is this characteristic for the development of life? Given the imposing climatic impacts that a chaotic inclination of the planetary axis would entail, it is plausible that this situation, although not completely compromising the development of life, would limit its evolution to the most resistant and primitive forms.

Even if the data relating to the presence of *exomoons*, in the systems that are being discovered daily, are at the moment completely absent, in this case it is justifiable to assume that moons are a characteristic of gas giants and not of the small rocky planets and therefore a situation like that of the Earth is rare. The following survival values are therefore:

Challenge 7	
a_7	b_7
0.1	0.3

Challenge 8: absence of the carbon cycle

Stability of temperature is maintained not only by a stable and moderate inclination of the planetary axis, but also by appropriate mechanisms of elimination and restoration of greenhouse gases in the atmosphere of the planet, in particular CO_2 . On Earth, an effective natural thermostat is provided by the so-called *carbon cycle*, or the dynamic exchange between geosphere, hydrosphere, biosphere and atmosphere through chemical, physical, geological and biological processes (Krissansen-Totton

and Catling, 2020). In summary, the terrestrial mechanism of thermostation due to the carbon cycle is made up of this (Foley and Fischer, 2017):

Carbon capture cycle in the form of CO₂

- (a) The planet is initially located in the habitability band with liquid water and average temperatures of around 20°.
- (b) Volcanism (or animals or other activities) adds CO₂ to the atmosphere, causing an initial imbalance.
- (c) CO₂ increases the planet's temperature.
- (d) Thermal increase intensifies the evaporation of the seas and the consequent rains.
- (e) The rains capture excess CO₂ and carry it back into the oceans.
- (f) The carbon present in the CO₂ is carried to the seabed.
- (g) The subduction phenomena of the seabed carry the carbon back into the geosphere.

Carbon restoration cycle in the form of CO₂

- (a) Impoverished of CO₂, the atmosphere does not retain heat and the planet cools down (glaciation).
- (b) Volcanism restores CO₂ without causing further rains as long as the temperature remains low.
- (c) The temperature increases by virtue of greenhouse gas and returns to the starting levels (point a).

The terrestrial carbon cycle is thought to have developed since the formation of our planet in ways which have varied over time (Dasgupta, 2013). It is clear that the main driver of this mechanism is the geothermal activity that acts in combination with the other three components; therefore, the essential condition for a thermally stabilized planet is active plate tectonics.

Paradoxically, the planets that present this feature are medium-sized rocky ones. The reason for this lies in the fact that small planets – those half the size of the Earth, to give an idea – have greater thermal dispersion and therefore exhaust their supply of internal thermal energy sooner. At that point, the planet cools, the crust solidifies in a uniform way and the geological activity stops together with the carbon cycle. This is what happened to Mars which, in addition to not having sufficient gravity to retain a fairly dense atmosphere, does not have a carbon cycle that maintains its constant temperature in the habitability band. On the contrary, the so-called recently discovered *super-earths* – a rich class of rocky planets of size equal to or greater than the Earth – would be excellent candidates in this respect due to their tectonics probably being more active than those on Earth. A theoretical model has recently been developed: it calculates whether a carbon cycle is present on the exoplanets once the mass, the size of the nucleus and the amount of CO₂ are known (Oosterloo *et al.*, 2021). In any case, the super-earths are very common and ensure that the risk of not finding geologically active planets is fairly low. Thus:

Challenge 8

a_8	b_8
0.7	0.9

Challenge 9: absence of the planetary magnetic field

There is another problematic aspect which has been little studied: the analysis of the deep part of the planets, and their magnetic fields. We know that magnetic fields shield the planet from the solar winds of charged particles and therefore are as necessary for life as the ozone barrier which blocks ultraviolet (UV) rays. In the case of the super-earths, a 2021 study conducted by the Earth and Planets Laboratory of Carnegie (Fei *et al.*, 2021), a private scientific institute based in Washington DC, simulated extreme pressure exercised on a magnesium silicate to better understand the dynamics of the interior, in particular the mantle, of the rocky exoplanets most similar to the Earth in order to ascertain if these planets might have a magnetic field similar to ours and, therefore, could host life. The conclusions were divided thus: in some geological scenarios the super-earths might generate a *geodynamo* similar to

the terrestrial one at the beginning of their evolution, and then lose it over billions of years during which cooling slows down magnetism. A recommencement of magnetic activity could be triggered by the movement of lighter elements through the crystallization of the internal nucleus.

Given the uncertain situation, we decided to assign this challenge an intermediate probability of 50%:

Challenge 9	
a_9	b_9
0.4	0.6

The calculation of the third parameter from the composition of the nine challenges

At this point, we can collect all the data that we have so far described in a single summary tab which we will insert in our algorithm of the Maccone lognormal (Table 2 and Fig. 3).

In conclusion, for the third parameter of Drake, over the time of the entire stellar population of 7 billion years, we obtained:

Drake 3	
$f_s \text{ min}$	$f_s \text{ max}$
5.8×10^{-3}	3.1×10^{-2}

At this point, we can insert precise values in the formula for the final survival frequencies $f_{s(\text{min/max})}(\Delta T)$ of the stable planets according to the stability time ΔT . That is to say:

$$\left\{ \begin{array}{l} \tau_{(\text{min/max})} \equiv \frac{\Delta T_0}{\ln \frac{1}{f_{s \text{ min/max}}}} \\ f_{s \text{ min}}(\Delta T) = \exp\left(-\frac{\Delta T}{\tau_{\text{min}}}\right) \\ f_{s \text{ max}}(\Delta T) = \exp\left(-\frac{\Delta T}{\tau_{\text{max}}}\right) \end{array} \right.$$

Table 2. Third Drake: entry of a_j , b_j and ΔT_0 data in the lognormal formula

	a_j	b_j	μ_j	σ_j^2	ΔT_0	μ	σ^2	$\langle X_0 \rangle$	$f_s \text{ min}$	$f_s \text{ max}$
1	0.70	0.90	-0.2258	0.0052	7 Ga	-4.07	0.15	1.84%	0.58%	3.11%
2	0.60	0.80	-0.3601	0.0069						
3	0.90	1.00	-0.0518	0.0009						
4	0.50	0.70	-0.5155	0.0094						
5	0.70	0.90	-0.2258	0.0052						
6	0.80	1.00	-0.1074	0.0041						
7	0.10	0.30	-1.6547	0.0948						
8	0.70	0.90	-0.2258	0.0052						
9	0.40	0.60	-0.6999	0.0136						

In light grey, the intermediate calculations of the logarithmic average and logarithmic variance are shown

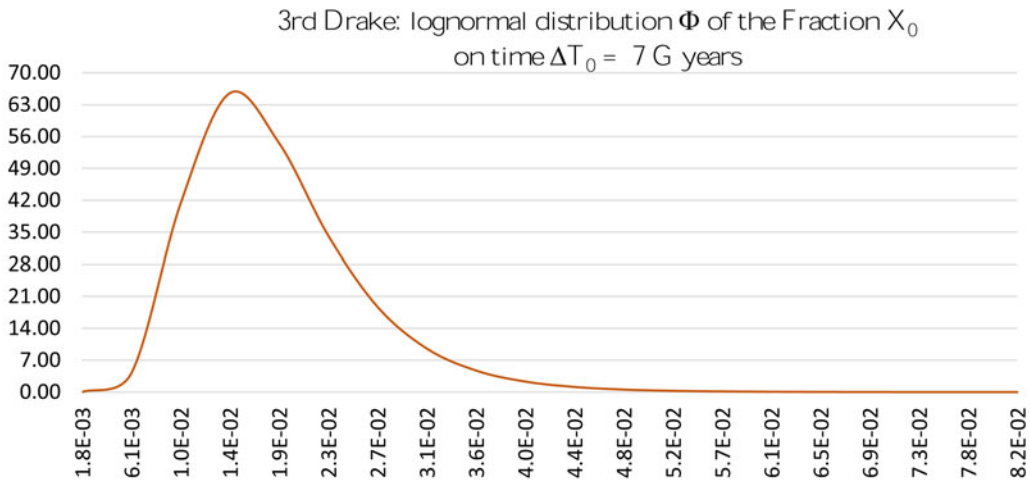


Figure 3. Third Drake: trend of the lognormal curve for the nine input values. The average valour found for the third parameter is therefore about 1.9% (between 0.6 and 3.1%).

which in our case will be (adding also τ_{mean}):

$$\begin{aligned} \tau_{\text{min}} &= 1\,359\,230\,076 \\ \tau_{\text{max}} &= 2\,016\,147\,681 \\ \tau_{\text{mean}} &= 1\,752\,672\,805 \end{aligned}$$

Considerations on the first three parameters

Figure 4(a) shows the survival probability of the stable planets according to the time ΔT over the life-span of the stellar population of 7 Gy. Figure 4(b), on the other hand, is nothing more than the probability of habitability at the current moment obtained by multiplying the previous value by $\Delta T/(7 \text{ Gy})$. These trends, associated with the remaining parameters of Drake, will be useful, in a subsequent discussion, to count the planets at different levels of development both of life and of ETC.

For the third Drake parameter, we found that, despite the substantial skimming effected with the first two parameters for the stars and planets suitable for the development of life, the $f_s(\Delta T)$ planetary stability curve of the third parameter quickly drops to zero. In the case of systems of a stable duration of at least 7 billion years which allow with reasonable certainty the development of intelligent civilizations, the value of the f_s probability drops to the decidedly modest value of 1.84%.

The Drake biological parameters: f_i and f_l

It goes without saying that the mathematical approach to the so-called *biological* parameters, the fourth and fifth, must necessarily be more articulated than for the first three for the reason that biological and evolutionary processes must almost always respect a rigid sequence and delicate environmental conditions.

To statistically simulate such a scenario through a division into *phases* (we will call them thus rather than *challenges*, as they do not now represent a risk to overcome, but an evolutionary opportunity, which from time to time presents itself) and using the Maccone lognormal, we will proceed as follows:

- (A) we will divide the phenomenon (with the relative associated parameter, for example, the fourth parameter for the onset of life) into the appropriate stages;

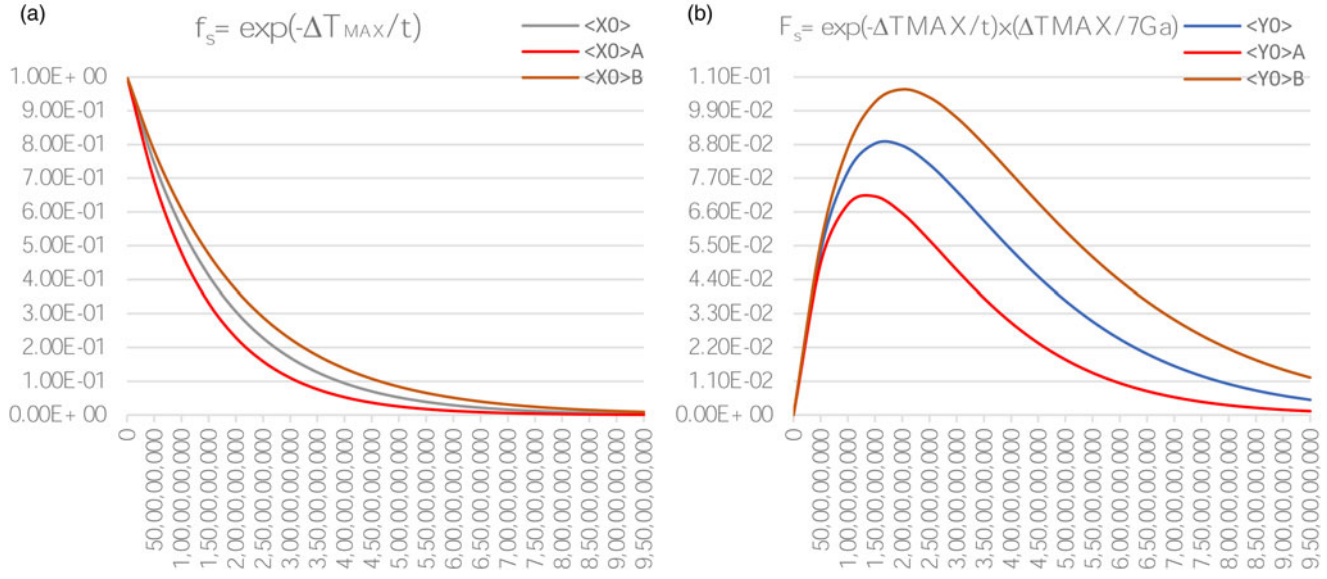


Figure 4. (a) Third Drake: calculated trend of the probability of habitability f_s $_{min/max}$ as a function of ΔT with $\tau_{mean} = 1.75$ Gy; (b) third Drake: probability of habitability at the current moment F_s $_{min/max} \equiv f_s$ $_{min/max} \cdot \Delta T/7$ Gy.

- (B) we will establish ΔT_j observation time intervals for each phase and the relative maximum and minimum a_j and b_j frequencies (relating to the x_j random variable) of the realization of phase j ;
- (C) we will define the maximum time intervals ΔT_{0j} of *micro-catastrophe* for each phase j , or the times beyond which the environmental conditions change and in fact prevent the phase from occurring;
- (D) we will transform all a_j and b_j frequencies into their corresponding A_j and B_j values (random variable X_j) compared to the times ΔT_{0j} of *micro-catastrophe*;
- (E) we will add all the times ΔT_{0j} obtaining the order of magnitude of the duration of the entire process of the n phases equal to ΔT_0 ;
- (F) we will calculate mean $\langle X_0 \rangle$ and standard deviation $\sigma(X_0)$ of the phenomenon formed by n phases, now temporally homogeneous, through the Maccone lognormal $\Phi(X_0)$ referring to time ΔT_0 , consequently obtaining $\langle X_0 \rangle_{\min}$ and $\langle X_0 \rangle_{\max}$;
- (G) we will define a maximum time interval ΔT of *macro-catastrophe* for all phases, or the time beyond which large planetary events occur that prevent the realization of the entire sequence of the n phases (e.g. the great extinction phenomena);
- (H) we will transform $\langle X_0 \rangle_{\min}$ and $\langle X_0 \rangle_{\max}$ in their f_{\min} and f_{\max} values, compared to the time ΔT of *macro-catastrophe*, which will be the minimum and the maximum of fourth and fifth Drake parameters.

We now observe that, once a phase or the entire cycle has been made, the arrival of a catastrophe is no longer lethal for the phase or the cycle itself. An example is the anomalous storms (*micro-catastrophes*) which periodically (e.g. every 10 years) occur in the quiet environment of the shallow lagoons, determining an improvised dilution of lipid bags: in this case, the concentration of the bags drops below the limit level of $n = 10^8$ per m^3 and this fact, as we will see in the next section, blocks the process described by Ageno to mix the content of the lipid bags, bringing its time of realization to over 30 years, i.e. not before the next storm. However, if the reaction takes place before the time limit of the 10 years, obviously it also remains after the arrival of the storm. The great mass extinctions (*macro-catastrophes*) that have reduced but not eliminated life on the planet are another example.

There is therefore a certain resilience of the different phases to trauma subsequent to their completion.

Fourth Drake: the transition from the non-living to the living

The origin of life and its possible occurrence outside our planet are one of the most exciting challenges facing modern science. It is not simply a question of formulating a consistent hypothesis on the transition from non-living to living, which is already a problem, but also one of being able to evaluate the possibility that this process can be realized elsewhere in the universe and with what probability.

Many hypotheses and theories on the origin of life have been formulated in the past (for a review, see e.g. Fry, 2000; Meinesz, 2008; Kauffman, 2011). However, the one that seems to us most interesting was advanced by the Italian physicist Mario Ageno, in the early 90s (Ageno, 1991, 1992a). His ideas will be briefly outlined in the next paragraph.

However, the theory of the transition from non-living to living that is currently better known is the one developed by the British biochemist Nick Lane (Lane, 2015). He also indicated six specific characteristics common to all living beings (Lane, 2015, pp. 90–91): a source of carbon (1) and energy (equal or different from the first) to feed metabolic processes (2), appropriate catalysts to encourage chemical reactions (3), the excretion of waste (4), a compartmentalization (the separation between the interior and the outside; 5) and, finally, the presence of hereditary material (6). It is easy to recognize in this the basic functions of a simple prokaryote cell (without nucleus nor organelles).

Lane located the process in the hydrothermal alkaline sources where, taking advantage of the difference of pH between the ocean waters, the chemical processes are very similar, both in polarity and in quantity, to those that take place in the self-trading living cells (Sojo *et al.*, 2016). His ideas are seductive: in fact, they integrate all recent discoveries and even allow for an explanation of how the

structural and evolutionary differences between bacteria and archaea would have come about through subsequent environmental specialization starting from a common ancestor. The latter would have been the famous LUCA (Last Universal Common Ancestor), the ancestor of all current terrestrial living beings (for information on LUCA, see e.g. Penny and Poole, 1999; Koonin, 2003; Forterre *et al.*, 2005; Theobald, 2010, and bibliography cited). However, despite this and despite the justified criticisms of other theories, of which it must be taken into account, his hypothesis presents one important defect. If the synthesis of biological molecules, as well as the oligomerization (production of short sequences of these molecules) is possible in hydrothermal systems (Colín-García *et al.*, 2016 and cited bibliography), the problem of nucleic acid filaments remains. In fact, in appropriate laboratory conditions, which reproduce those of the flues of the alkaline sources, only the appropriately activated adenine manages to form some short filaments a few units long. Unpaired adenine (AMP), on the other hand, only produces at best dimers, while the other nucleotides do not polymerize (Burcar *et al.*, 2015).

On the contrary, the processes hypothesized by Ageno, despite some still being devoid of an appropriate experimental verification, can theoretically allow for the production of triphosphate nucleotides, the active forms capable of reacting and forming a filament. In addition, the triphosphate nucleotides, in particular ATP, are the main molecules that act as organic batteries to make biological chemical reactions possible (Nelson and Cox, 2021).

Furthermore, as we will see, Ageno assumes that the first living beings were photosynthetic, because the only unlimited source of energy available all over the face of the Earth (up to a certain marine depth) was that provided by the sun. The importance of electromagnetic radiation for life, present and past, not only no longer requires demonstration (Green *et al.*, 2021), but photosynthesis, carried out by green plants and cyanobacteria is the only process that allows accumulation of the free oxygen in the environment and therefore the only process that allows the creation of a barrier – the ozone layer – to ionizing electromagnetic energy reaching the surface of a planet from space (Lane, 2002). Therefore, in the absence of photosynthetic beings capable of freeing oxygen, the ozone layer does not develop in the atmosphere; in the absence of ozone layer, water, after a certain time, is completely hydrolysed, meaning one of the indispensable resources of life is exhausted. Therefore, without photosynthesis, what happened on the planet Venus, where the oceans have all been consumed by this process (Kulikov *et al.*, 2006), happens. We therefore encounter the paradox that, if organisms are not formed among the first living beings capable of producing oxygen through the process of photosynthesis (or if they are not the first living beings), the life thus created cannot survive and vanishes quickly.

For these reasons, we consider Ageno's hypothesis to currently be the most plausible for explaining the steps necessary to evolve stable life forms on a planet. This will therefore be the common thread that we will follow to evaluate the numerical variables to be used in the calculations of Maccone's algorithm, in the absence of new discoveries that cast doubt on its effectiveness.

Mario Ageno's theory

The Italian physicist began by specifying what he meant by a living being (Ageno, 1991, 1992b). For Ageno, a living being is an open chemical system (i.e. a system within which chemical processes develop and which can exchange energy and materials), which is coherent (in which the processes are ordered in space and time) and equipped with a programme (in possession of an 'orchestra conductor' – DNA – which establishes what to do and when to do it). Although the author has specified that this definition is *one* of those possible to recognize all the lifeforms on Earth rather than *the* definitive definition, starting from his ideas it is easy to realize that at the basis of its idea of living being there is the biological cell, as for most modern specialists.

Starting from these bases, Ageno developed a hypothesis (1991, 1992a) based on a series of stages, whose transition from one to the other was considered to happen with an almost certain probability. Only in this way could we have a process capable of producing, starting with very specific conditions,

the transition from non-living to living. The idea originated from the classic prebiotic broth and lipid bags (supposed to turn into a protocell) formed into a small and particular environment, the shallow substrate – between 10 and 20 m – of a lagoon, to get to the formation of cells living.

Despite sharing a starting point with other previous theories, Ageno introduced two important novelties, making his hypothesis much more credible than what had been affirmed previously. By exploiting the properties of the components of the lipid bags, capable of merging and splitting without mixing their content with the external environment (Houslay and Stanley, 1982; Lipowsky and Sackmann, 1995), the Italian physicist stressed that it was not necessary to worry about following the fate of *a single bag*, but that the system capable of evolving into a living being was made up of the set of *all* the lipid bags present in the lagoon. In fact, if a particular reaction had taken place in a specific bag following a random collision between them, the product could have arrived in another, inside which the subsequent reaction could then have taken place; and so on, increasing the likelihood of going through the whole process.

Let us make a short digression to give a mathematical guise to this statement. We know that in a system of corpuscles (our protocells) of section equal to s and density equal to n per cubic meter, the average free path is:

$$\lambda = 1/(n \times s).$$

Therefore, defined v as the relative speed between corpuscles, the average time between one collision of the corpuscles and the next will be:

$$t = \lambda/v = 1/(n \times s \times v),$$

in fact, t is interpretable as the *first mixing time* of lipid bags. Knowing that:

$$s \sim 10^{-12} \text{ m}^2$$

$$v \sim 10^{-5} \text{ m/s},$$

it follows that:

$$t = 10^{17}/n$$

The latter value should always be kept under control because concentrations, for example, lower than $n = 10^8$ corpuscles per m^3 would produce mixing times exceeding 30 years which, as we will see, under certain variable and traumatic conditions of the system that houses the protocells, may be too long. It is true that for even a modest production of lipids distributed over the sea surface, for every m^2 of lipids there may be around 10^{12} lipid bags which, over a maximum depth of about 10 m (a value which allows, as we will see, the arrival of solar energy), would determine a value of $n = 10^{11}$. This discovery is quite comforting given that, in this case, the first mixing time would be $t = 10^6$ s, or around 10 days.

We will see later how, by periodically interfering precisely with the concentration of lipid pockets, marine meteorological agents often determine real temporal barriers (*micro-catastrophes*) for the realization of reactions inside the bags. Ageno's second hypothesis consisted of the mechanism capable of supplying energy for the system to function. According to Ageno, this derived from a simplified version of the photosynthesis of green plants: a lipid sac would trap a chlorophyll pigment capable of being excited by photons and losing electrons along a simple redox chain, included in the thickness of the membrane, comprising a molecule with double bonds between its carbon atoms. The latter would be capable of transferring H^+ protons inside the bags, making this system acidic. The acidity would favour the formation of polyphosphates, including biological energy batteries, molecules such as ATP and some chains of organic molecules such as those of oligonucleotides (simple strands of DNA, RNA and/or nucleotides and other molecules, such as amino acids)

starting from the precursors present in the prebiotic broth (regarding the possibility of synthesizing nucleotides and forming RNA and DNA filaments, see the synthesis of Yadav *et al.*, 2020 and its extensive bibliography). This would have been the first step towards the formation of all the chemical processes that characterize living beings.

To those who object that the photosynthesis of green plants, whose chlorophyll receives electrons directly from the water, requires a complicated apparatus and, for this reason, cannot be considered primitive, Ageno (1991, p. 271) reiterates that what is simplest is not always the most ancient: a simple apparatus can be a local adaptation of a system which was originally more complex. Some recent studies have underlined the importance of photosynthesis for all phenomena related to life on our planet (see e.g. Altamura *et al.*, 2017, 2020).

The calculation of the fourth parameter f_l

In Fig. 5, we show the entire calculation process, describing the various steps in detail:

Step 1. This step of the calculation process is the closest to our evaluation possibilities as it assigns frequencies starting from known data or, in any case, comparable with known data: each phase j is a necessary process for the development of life associated with a random variable x_j (fraction or frequency) to be estimated within the two maximum and minimum a_j and b_j values within the ΔT_j observation time. The phase must be carried out within a micro-catastrophe ΔT_{0j} time limit which, once exceeded, is consolidated and can be said to be realized. Ultimately, it is a question of providing the four $a_j, b_j, \Delta T_j$ and ΔT_{0j} values for each phase.

Step 2. In this passage of the calculation process, the assigned frequencies are translated into their time limit ΔT_{0j} from the transformation (covariant over time)

$$X_j(m_j) = 1 - (1 - x_j)^{m_j},$$

which transforms the frequency of an x_j event, relating to a certain ΔT_j time interval, in the X_j frequency relating to a ΔT_{0j} interval that is m_j times larger. In other words, if x_j is the probability of success of a single test, X_j is the probability of success of m_j consecutive tests, where $m_j = \Delta T_{0j}/\Delta T_j$. The same thing holds for the minimum and maximum a_j and b_j frequencies that are transformed into A_j and B_j according to the same law.

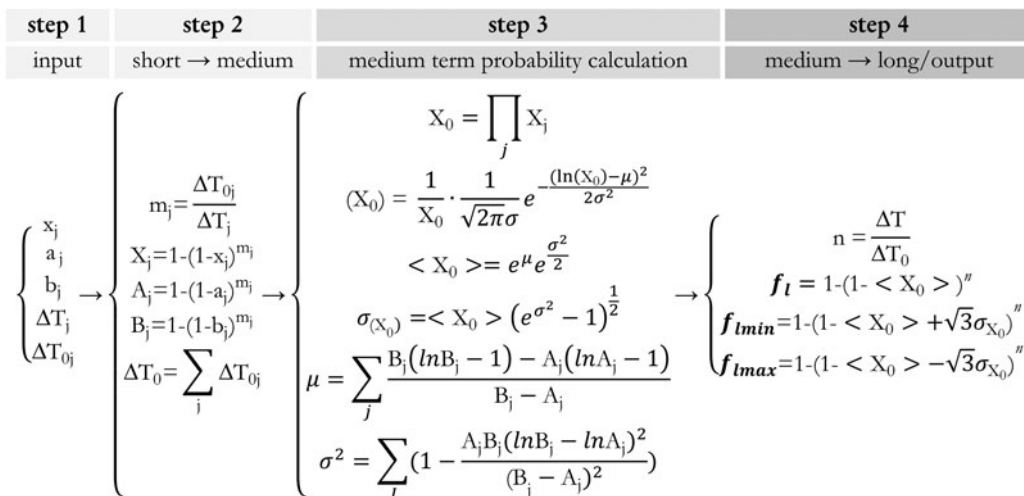


Figure 5. Fourth Drake: from step 1 to step 4, the information on individual processes in the short term gives rise to the probability in the medium and long term.

The sum of all the maximum times for micro-catastrophe gives rise to the overall medium ΔT_0 term necessary for achieving the entire process:

$$\Delta T_0 = \sum_j \Delta T_{0j}.$$

Step 3. In the medium term, the frequencies of the different X_j phases are temporally homogeneous and can be multiplied together, as with the Drake formula, to obtain the new medium-term variable X_0 whose distribution is calculated with the Maccone lognormal shown below:

$$\Phi(X_0) = \frac{1}{X_0} \cdot \frac{1}{\sqrt{2\pi}\sigma} e^{-\frac{(\ln(X_0)-\mu)^2}{2\sigma^2}},$$

where – note – μ and σ are the average and standard deviation of the logarithm of the random variable X_0 , while $\langle X_0 \rangle$ and $\sigma(X_0)$ are the average and standard deviation of the X_0 random variable.

Step 4. In this step of the calculation process, like in step 2, the obtained frequency $\langle X_0 \rangle$ is remodelled in the time limit of macro-catastrophe ΔT through the same algorithm used previously:

$$f_i(n) = 1 - (1 - X_0)^n,$$

where $n = \Delta T / \Delta T_0$

The two deviations from the average value $X_0 \pm \sqrt{3}\sigma(X_0)$ which give rise to $f_{i \min}$ and $f_{i \max}$, derive from the formula of the Maccone lognormal. We have now supplied the four a_j , b_j , ΔT_j and ΔT_{0j} values for each phase and obtained the final probability f_i with its $f_{i \min}$ and $f_{i \max}$ deviations in the time ΔT .

Phases of transition from non-living to living

We will divide the phenomenon of the onset of life related to the parameter f_i into the following ten phases:

- (1) the abiological synthesis of biological molecules
- (2) the concentration of the primordial broth
- (3) the formation of lipid bags
- (4) the inclusion in lipid membranes of chlorophyll
- (5) the ‘proton photopump’
- (6) the formation of nucleic acid filaments
- (7) the catalytic role of RNA
- (8) determination of roles
- (9) cell membrane formation
- (10) emergence of the genetic code

The starting point; the habitable planet

The basic conditions required for the transition from non-living to living on an Earth-like planet are summarized below.

First of all, the planet must be rocky and not gaseous, like the planets of the internal solar system Mercury, Venus, Earth and Mars.

Secondly, it must be found at such a distance from its star that it is neither too cold nor too hot. In particular, water in the liquid state must be present on the planet in question. This substance, in fact, is essential for life as we know it and as it has been previously defined (Chaplin, 2001; Lynden-Bell *et al.*, 2010; Ball, 2017), being, among other things, the solvent in which metabolic processes take place. Next, its gravity must be sufficient to retain an atmosphere which then also acts as a protective screen

against any bombardment of cosmic rays and UV radiation. The conditions described so far are continuously monitored and catalogued on thousands of exoplanets that have been identified continuously since the mid-1990s (<https://exoplanets.nasa.gov/>).

In addition, the atmosphere must not be oxidizing, like that of Earth now, but must be without free oxygen (O₂). This condition is easily achievable, as a stable and important presence of this gas in the air derives from photosynthetic processes that are undoubtedly the activities of living organisms (Lane, 2002; Holland, 2006). Water hydrolysis (e.g. by electromagnetic radiation) produces O₂, but the quantity obtained per unit of time is relatively low. In addition, the oxygen produced in this way tends to quickly oxidize the molecules present in the environment. Therefore, any celestial body without living beings is considered to have an atmosphere in which free oxygen is completely missing or is present only as a trace.

Finally, the planet must have a geothermal activity: energy (heat) produced inside, which moves towards the surface, to escape, giving rise to different phenomena (volcanism and vent fields).

All the fundamental characteristics described so far are analysed in the work of Southam *et al.* (2007).

Now we will discuss the various stages in which the process of transition from non-living to the living can be divided.

The first phase: the abiological synthesis of biological molecules

In order to start our process, the abiological synthesis of biological molecules and/or their precursors is essential. Today it is known that, under appropriate conditions (presence of energy and adequate chemical precursors), in the presence of a reducing atmosphere, simple organic molecules, including lipids, amino acids, nucleotides (Fig. 6) and hydrocarbons (Miller, 1953; Ageno, 1991; Green *et al.*, 2021; Ritson and Sutherland, 2012), can be produced. At its origins, the Earth did not have a completely reducing atmosphere (Trail *et al.*, 2011); however, it did not have free oxygen.

In a planet with the characteristics listed above, organic compounds can derive from meteoric contributions of molecules produced in space (during the Archean eon, hundreds of thousands of meteorites fell on Earth; Zahnle *et al.*, 2007) and from the synthesis that took place in hydrothermal vents (see e.g. Anders, 1989; Lazcano and Miller, 1996; Fry, 2000; Kwok, 2007; McCollom and Seewald, 2007; Kwok, 2017; Ménez *et al.*, 2018). It is therefore certain that in a planet with the characteristics we have defined it is possible to find organic molecules.

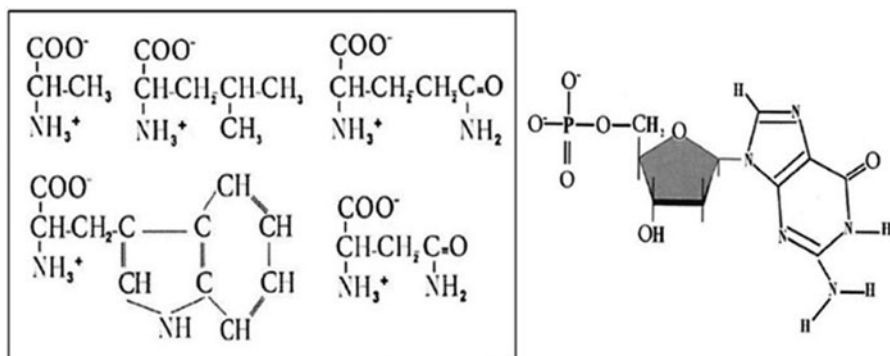


Figure 6. Fourth Drake: some of the biological molecules necessary for life: in the left box, 5 of the 20 fundamental amino acids (up, from left to right, alanine, leucine, glutamine; below, from left to right, tryptophan, asparagine); on the left, the monophosphate nucleotide obtained with the guanine base (figure modified by Valli, 2020).

In order to estimate the minimum and maximum formation frequency of biological molecules, we take as a reference of the two phenomena described (hydrothermal vents and meteoric phenomena), the slowest and less probable one, namely meteoric phenomena. During the Hadean and the Archean eons, the impact frequency of meteorites on Earth was remarkable. The recent work of Takeuchi *et al.* (2020) quantifies this phenomenon at about 10^{20} kg of meteorites that reached Earth in this period; a huge amount (the terrestrial mass is about 6×10^{24} kg) which widely justifies the presence of the molecules in question. We hypothesize that the phenomenon of distribution of the meteoric biological molecules affected between 90% (a_1) and 100% (b_1) of the planet on an observation period ΔT_1 of about 1 000 000 years. In addition, we will keep the maximum value of this observation ΔT_{01} (time of *micro-catastrophe* of phase 1) always equal to 1 000 000 years considering that the conditions of existence of hydrothermal vents (Chivers *et al.*, 2016) also have a limit value of that order of magnitude.

Phase 1			
a_1	b_1	ΔT_1	ΔT_{01}
0.9	1	1 000 000	1 000 000

The second phase; the concentration of the primordial broth

Agno locates the evolution of its system in a particular environment: the bottom of a sheltered lagoon at a depth of about 10 m (Agno, 1991, pp. 117–119 and 265). Details aside, what is important to underline is that the concentration of organic compounds must be consistent with a depth at which harmful electromagnetic rays (carrying too much energy and capable of destroying biological molecules and altering chemical reactions) are absorbed by the liquid, but such that the part of the spectrum used for photosynthesis is still accessible. The depth, therefore, depends on the particular composition of the atmosphere and the intensity of the light that reaches the surface of the planet.

How realistic is this picture? In a completely sterile environment (total absence of lifeforms), it is difficult to imagine phenomena capable of altering and destroying molecules. UV rays, such as the most energetic electromagnetic radiation, can, but beyond a certain depth are absorbed by the water molecules. Furthermore, if we add proximity to alkaline hydrothermal vents, we will be sure that we have ensured regular refuelling of organic material. Studies relating to vent fields show that though the majority of them are located between 2000 and 3000 m below sea level, they are also abundant near the surface at various other depths (Colín-García *et al.*, 2016), and this was probably true also in the past (Camprubí *et al.*, 2017). During the Archean eon, alkaline vent fields were present and widespread on our planet (see Sojo *et al.*, 2016 and its rich bibliography).

To estimate the probability of the presence of biological molecules in alkaline vent fields, we will take a minimum frequency of 5% and a maximum of 15%. These values are suggested by the distribution of the lagoons with these characteristics of depth (Colín-García *et al.*, 2016) on an adequate release time of about 100 years. The maximum lifetime of the lagoons in such optimal conditions is estimated at 10 000 years

Phase 2			
a_2	b_2	ΔT_2	ΔT_{02}
0.05	0.15	100	10 000

The third phase; the formation of lipid bags

Among the organic molecules present in the defined environment, lipids, with polar head and hydrophobic tail, are distinguished. These compounds are able to form thick double molecular layers on the surface (Fig. 7, at the top) and, in immersion, double-walled bags (Fig. 7, on the sides) in which the

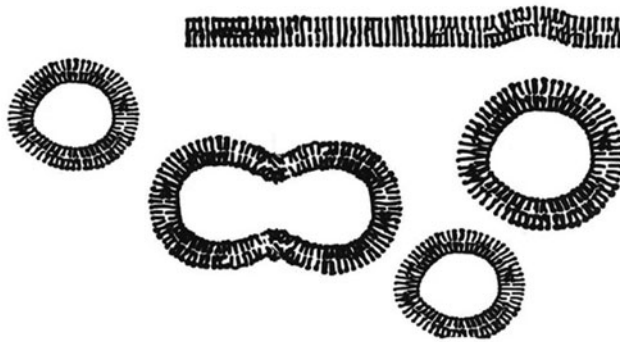


Figure 7. *Fourth Drake: top, double surface thick layer; on the sides of double-wall lipid bags; at the centre, fusion of two lipid bags (figure modified by Valli, 2020).*

polar ends of the molecules are in contact with the water while the hydrophobic ends are facing one another at the centre of the wall itself. These molecules are among the main components of the organic membranes, in particular of the cell membranes, of which all lifeforms are made (Nelson and Cox, 2021).

The double-walled lipid pockets thus formed are able to merge (Fig. 7, in the centre), by banging into one another, and to split in two when the volume of one of them turns out to be excessive, without mixing their content with the external environment (Houslay and Stanley, 1982; Lipowsky and Sackmann, 1995). In this way, it is possible to divide our system into two distinct spaces, the external one of the lagoon and the internal one which, as we have seen in the introductory section dedicated to Ageno, statistically includes the space in *all* the bags present. The bags formed in the lagoon referred to in the previous point can thus incorporate a part of the abiologically synthesized organic material. If a determined chemical compound is present inside a bag, due to the processes described above, at a certain point it will be able to come into contact with another, initially produced in a different bag, and react with it. In fact, due to the mergers and separations of the bags, the internal environment is unique and any molecule can, sooner or later, interact with the others.

The formation and dynamics of the bags depend on the concentration of lipids and the physical characteristics of the liquid (water) in which they are immersed. Since lipids are among the substances that can be easily synthesized in vent fields, they must therefore have been relatively abundant in our system. At this point, given their behaviour, the formation of the double lipid layers and bags was relatively probable and rapid: we set the frequency between 0.9 and 1 over a short period of 0.1 years. The limit time of the process, i.e. environmental crises capable of destroying the system, is the climatic events extreme enough to disturb the tranquillity of the lagoon, estimated at about 10 years.

Phase 3			
a_3	b_3	ΔT_3	ΔT_{03}
0.9	1	0.1	10

The fourth phase; the inclusion of chlorophyll in lipid membranes

In the prebiotic broth, there were not only amino acids, nucleotides and lipids. The abiological synthesis also allows the creation of other more or less simple molecules. For example, laboratory experiments (on the type of Miller, 1953) have demonstrated the abiotic synthesis of chlorophyll (Ageno, 1991 and cited bibliography), a pigment that allows green plants and cyanobacteria to carry out photosynthesis (see e.g. Tomitani *et al.*, 1999; Eggink *et al.*, 2001) using electrons removed from water molecules. Although complex, this molecule is very ancient: fossils of organisms capable of the

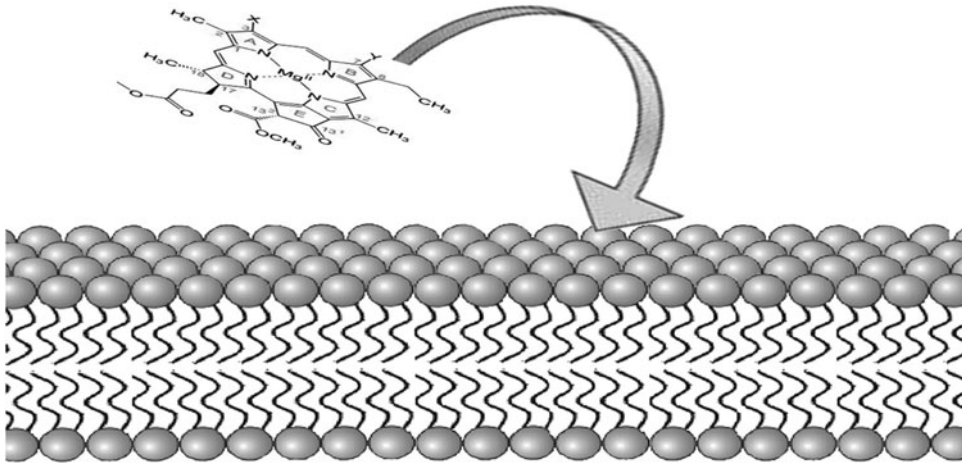


Figure 8. Fourth Drake: the trapping of chlorophyll (at the top left) in the double-wall lipid membrane.

photosynthesis carried out by green plants were found in Australian sedimentary layers from about 3.5 billion years ago (Schopf and Packer, 1987).

Chlorophyll is a pigment, a molecule that can become excited if stimulated by photons of an appropriate wavelength dependent on the pigment in question. The excitement causes the loss of one or more electrons that begin to travel a *redox chain* formed by various molecules contained in the photosynthetic membrane (Kiang *et al.*, 2007 and cited bibliography). Among these, the *quinones* stand out: particular molecules which, reducing themselves (accepting electrons), bind themselves to an equal number of protons (H^+). One of the peculiarities of these molecules is their alternating double bonds which are responsible for the characteristic mentioned above (Nelson and Cox, 2021). The simplest molecule with alternating double bonds (therefore, the properties of the quinones) is much simpler than numerous other compounds deriving from the abiological synthesis. Therefore, specimens of this substance were probably present in the prebiotic broth. As certain quinones, especially those that intervene in biological processes (Nelson and Cox, 2021), are liposoluble, some of them, or the alternated double bond molecules, could have been ‘trapped’ in the membrane of lipid bags formed in the prebiotic broth, retaining their essential properties for the photosynthesis process: the (reversible) reduction accompanied by the acceptance (reversible also) of protons.

If the temperature was not too low, these molecules could move inside the lipid membrane as in a two-dimensional liquid (Houslay and Stanley, 1982; Lipowsky and Sackmann, 1995), like the quinones in photosynthesis systems.

The trapping of chlorophyll (Fig. 8) and other components of the redox chain in the membrane would have allowed the passage of a flow of electrons through the membrane itself, powered by sunlight (Altamura *et al.*, 2020). It is important to underline that, for the operation of this function, the formation of the entire Redox chain is not necessary, only the presence of those elements that allow the passage of electrons through the quinone in order to carry out the transfer of protons. Chlorophyll and the molecules necessary for the Redox chain were certainly present in the primordial broth. Being liposoluble, they could penetrate the lipid double layer and remain trapped.

By assuming a not too high concentration of chlorophyll, we can assign a frequency between 10 and 20% of the pigment inclusion for an observation time of about 1 year. The phase can be compromised if the system of lipid bags dilutes; as in the previous case, we will set the time limit at 10 years

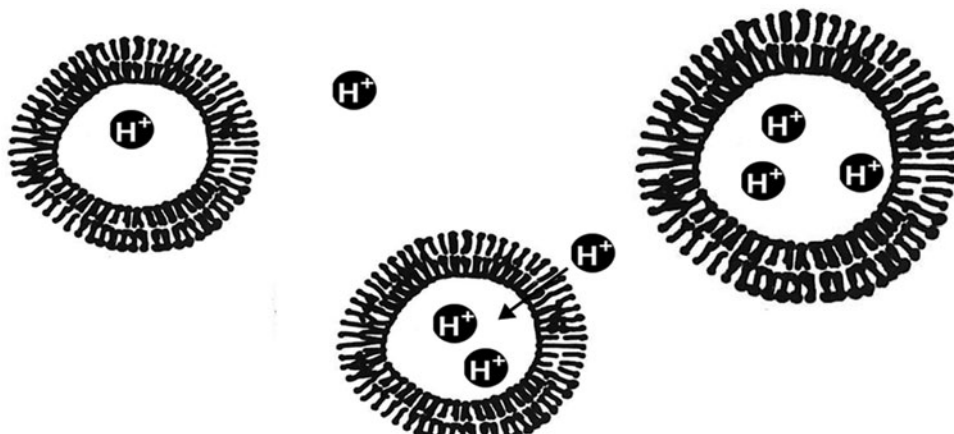


Figure 9. *Fourth Drake: the concentration of H^+ ions inside the lipid bag system increases the pH of this environment: the arrow indicates the entrance of an H^+ ion thanks to the ‘photopump for protons’ (a figure modified by Valli, 2020).*

Phase 4			
a_4	b_4	ΔT_4	ΔT_{04}
0.1	0.2	1	10

The fifth phase; the ‘photopump for protons’

Once present, in the lipid membrane, the set of the molecules indicated previously – Ageno’s ‘proton photopump’ (1991, page 278 and following) – can get to work. The combination of a pigment – in our case, chlorophyll, because it allows electrons to be obtained from water molecules – with an appropriate double bond molecule, will allow the first to pass the excited electrons to the second when the pigment receives appropriate photons. The polarity thus deriving will serve to keep the two molecules close to each other, inside the double lipid layer; and so on, for all the molecules belonging to the redox chain.

The reduction of the double bond molecule is accompanied by the acquisition, by the *external* environment, of protons which, upon the subsequent release of the electrons to another substance, are released, this time within the *internal* environment. There is therefore a probability that a system capable of concentrating protons in the internal environment will be generated, making the system acidic. Of course, there is also a probability that the opposite happens. However, in the first case, the system can evolve in the direction indicated by Ageno; in the second, however, the system stops.

Given the concentration of the prebiotic broth, multiple pigments and more double-tied molecules are likely to be trapped in the lipid membranes. Those capable of concentrating the protons inside (Fig. 9) will evolve in the sense indicated towards the subsequent phases, while the others will have no future. It should also be noted that the primordial ocean was probably more acidic than the ocean today (Morse and Mackenzie, 1998; Barge *et al.*, 2014; Krissansen-Totton *et al.*, 2018), which implies a greater concentration of protons in primordial marine waters.

To translate the above into a formal statistical phenomenon: chlorophyll, initially, with a 50% probability p , acidifies either the interior or the exterior of the lipid bag; however, this probability will have a binomial standard deviation equal to 25%, that is to say:

$$N \times p \times (1 - p) = N \times 1/2 \times 1/2 = N/4,$$

where N is the number of absorptions of photons over time of observation; it will be precisely this deviation from the average value which makes some of the lipid bags – those which are more acidic inside – capable of continuing the process in the next phase. Of course, the mergers and separations of the lipid bags can refurbish their content, but there is no doubt that Ageno's photopump (1991) would have been able to 'acidify' at least a part of the internal environment of our system. We set this fraction as between 10 and 20% in a period of observation of a few days, or 0.01 years and a time limit of 10 years, as in the previous two phases.

Phase 5			
a_5	b_5	ΔT_5	ΔT_{05}
0.1	0.2	0.01	10

The sixth phase: the formation of nucleic acid filaments

The acidification of the internal environment of the bags, or at least a part of it, allows us to solve one of the most important problems relating to the transition from non-living to lifeforms: the precipitation of phosphorus in the form of insoluble apatites. Phosphorus is an indispensable element for life because it plays a role in the formation of nucleic acids (DNA, RNA) and in biological energy batteries (whose most important, the ATP, is nothing more than the triphosphate form of the nucleotide of adenosine, one of the components of the ARN); and it is precisely the triphosphate forms of the nucleosides which can react to form the filaments of nucleic acids.

The acidification of the internal environment therefore allows the formation of polyphosphates and organic phosphates. In particular, it promotes the realization of two things essential for evolution towards life (Ageno, 1991):

- (1) The formation, starting from the basic components contained in the prebiotic broth and held inside the lipid bags, of DNA, RNA or hybrid filaments of nucleotides and amino acids;
- (2) The formation of ATP (Fig. 10, left), the most important biological 'battery' capable of allowing the evolution of endoenergetic chemical reactions.

Of course, the dynamics of lipid bags, with their merging and splitting, allowed the new material developed in the most acidic compartments to be available throughout the internal environment of the system.

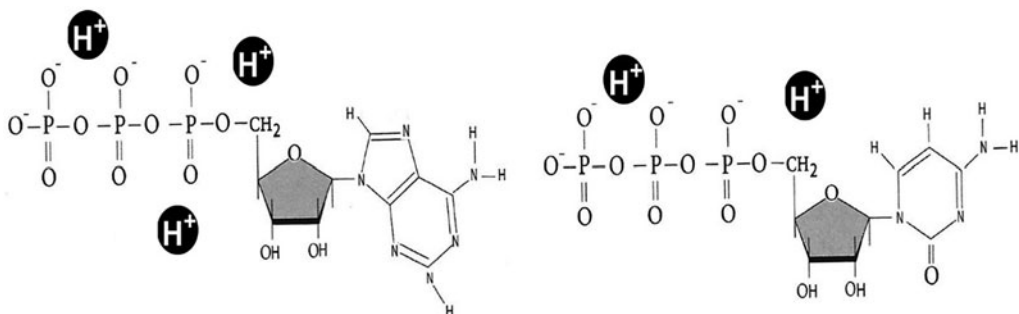


Figure 10. Fourth Drake: triphosphate nucleotides formed in the environment made acid by the H^+ ions (ATP, with the base adenine, left; CTP, with the cytosine base, right) (figure modified by Valli, 2020).

Given the complexity of this phase, we will assign them a low probability of between 2 and 3% over a time of 0.01 years (3–4 days) and a time limit of 1 year, beyond which variations of the seasonal conditions could represent an obstacle to the fulfilment of the phase.

Phase 6			
a_6	b_6	ΔT_6	ΔT_{06}
0.02	0.03	0.01	1

The seventh phase; the catalytic role of the RNA

The production of nucleic acid filaments (DNA, RNA and mixed chains of amino acids and nucleotides acids) and of triphosphate nucleotides in the ‘photopump’ system allows the slow further evolution of the system.

Starting from the filaments of nucleic acids, replicative processes dependent on the particular combinations present can start. By trial and error, certain filaments become more abundant than others. In parallel, the enzymatic activity, initially carried out by more or less isolated metal ions, becomes the prerogative of more complex molecules, including organic components. Is this perhaps the famous ‘RNA world’ (for more information on this concept and on the problems raised by it, see e.g. Bartel and Unrau, 1999; Neveu *et al.*, 2013) in which this molecule carried out both the enzymatic tasks related to inheritance? We don’t want to go into details. But let us remember that RNA, not being able to form the double helix, does not lend itself well to preserving genetic information, unlike DNA (Ageno, 1991, 1992a). Furthermore, there are no reasons to believe that the two types of nucleic acids were able to evolve in parallel or starting from a common ancestor (Cafferty and Hud, 2014). Since the hypothetical RNA world has left no traces in the current living world, we can reasonably consider DNA and RNA as two types of filaments in competition, but which rapidly ended up taking on different biological roles: DNA, with the double helix consisting of deoxyribonucleotides, has become the molecule with hereditary function.

On the other hand, the importance of the RNA in this phase of the process of the transition from non-living to the living should not be understated. The research highlighted an increasing number of RNA sequences capable of enzymatic activity (Higgs and Lehman, 2015; DasGupta, 2020). All this suggests that, at least initially, it was the RNA that carried out the principal enzymatic actions. We should also remember that in the most acidic environments of the internal compartment of the bags, triphosphate nucleotides could form, capable of ensuring energy for the synthesis of new molecules and of permitting the lengthening of the filaments of nucleic acids, the most active from the catalytic point of view.

It is now practically certain that RNA filaments can function as biological catalysts: the longer the filaments, the easier it is to find a reaction that they catalyse (see e.g. Higgs and Lehman, 2015; DasGupta, 2020) even if they are less effective than proteins. If the concentration is high, the times of the chemical reactions are quite short (hours), less short if the concentration is low (days-months). We will adopt the second case by placing the fraction of RNA molecules suitable between 90 and 100% in a time of 0.1 years (about a month) with a limit of about 1 year, as in the previous phase.

Phase 7			
a_7	b_7	ΔT_7	ΔT_{07}
0.9	1	0.1	1

The eighth phase; determination of roles

Our system, now equipped with catalytic molecules and energy batteries, has been able to begin to produce new biological molecules starting from an appropriate carbon source. Having mentioned

photosynthesis as the main engine of our process, it is natural to consider carbon dioxide (CO₂) as this source. On the other hand, this molecule, being liposoluble, could overcome the double lipid membrane and spread inside the internal environment of the bags. In addition, at the time, the CO₂ rate was far superior to the current (Morse and Mackenzie, 1998; Lichtenegger *et al.*, 2010; Sleep, 2010). The carbon dioxide was well suited as a source of carbon for the processes cited previously and is considered to occupy this role also in the work of Lane (2015; Sojo *et al.*, 2016).

Gradually, by trial and error, the roles of the various organic molecules present began to differentiate themselves. Thanks to its ability to form the double helix (Fig. 11, at the top, on the right and left), DNA was affirmed as the molecule responsible for the inheritance and control of the entire system. The proteins, thanks to the particular three-dimensional structure specific to each (Fig. 11, at the bottom of the centre), proved more functional, distinguishing themselves for their extreme specificity in carrying out enzymatic activity (see e.g. Petrounia and Arnold, 2000). Finally, RNA specialized as an intermediary between DNA and protein synthesis, becoming indispensable for this activity (a substantial part of ribosomes is composed of RNA; Nelson and Cox, 2021).

The phenomena of role selection described above may have gradually occurred over a hundred years according to a maximum and minimum fraction of 20 and 30%. The maximum time coincides with the observation time

Phase 8			
a_8	b_8	ΔT_8	ΔT_{08}
0.2	0.3	100	100

The ninth phase; the formation of the cell membrane

Following the last step, new organic molecules spread to the system, those concerning the synthesis processes and duplication of particular DNA chains being favoured and propagating.

However, new protein chains are gradually included in the double lipid thickness. Some are such as to maintain its stability and consistency. The bag in which this takes place will tend to no longer merge with the others to exchange its content. Gradually, the various metabolic processes begin to accumulate in individual bags that end up acting each on their own. Finally, at least one of these, with appropriate dimensions, will include all the processes and conquests listed in the previous stages, which can take place in a single protected micro environment (Fig. 12). It will then be the latter which will continue its evolution towards becoming a lifeform.

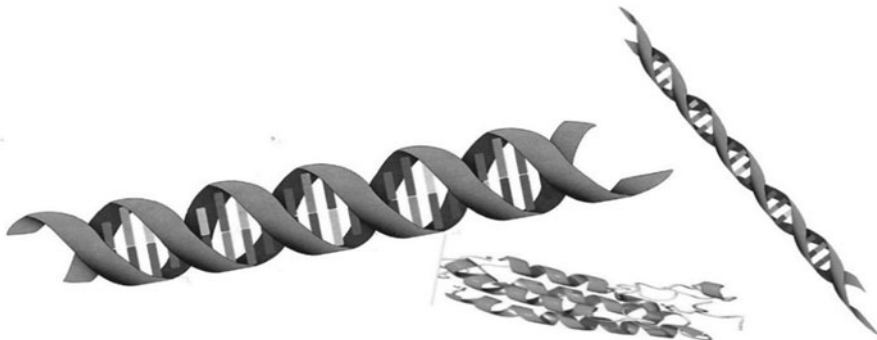


Figure 11. Fourth Drake: at the top, right and left, double propeller DNA molecules; 3D protein, at the centre, below (figure modified by Valli, 2020).



Figure 12. *Fourth Drake:* the metabolic processes of the previous stages now take place in a single bag, the surface of which no longer merges with the others.

We can assign minimum and maximum frequencies of 1 and 2% on a time of observation of a few days (time of inclusion of protein chains in the membrane), or 0.01 and 0.02 years and a time of 1 year (seasonal cycle).

Phase 9			
a_{10}	b_{10}	ΔT_{10}	ΔT_{010}
0.01	0.02	0.01	1

The tenth phase; the emergency of the genetic code

Once the processes described in the previous stages have occurred, a fundamental step still remains before obtaining a lifeform: the emergence of the genetic code, that is, the appropriate combinations of three nucleotides (Fig. 13) capable of specifically indicating the amino acids to be added to the protein chain (Watson *et al.*, 2013) in the protocell seen previously.

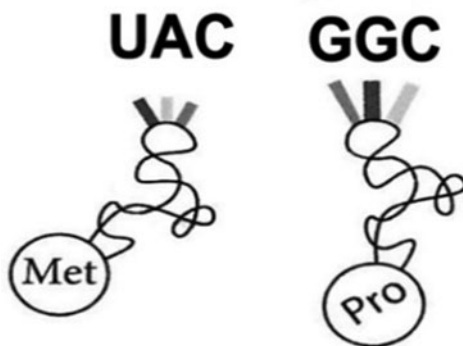


Figure 13. *Fourth Drake:* examples of ‘translation’ of the genetic code: on the left, the trio ‘uracil–adenine–cytosine’ (UAC) coding for the amino acid methionine (MET); on the right, the trio ‘guanine–guanine–cytosine’ (GGC) coding for the proline amino acid (Pro) (figure modified by Valli, 2020).

It is in this way that the main function of the DNA ‘programme’ (that says what to do and when) can do its job. It is also in this way that the consistency in the chemical processes of the system can be established.

How is this achieved? By trial and error (for a possible evolution, see Lei and Burton, 2020), the various nucleic filaments that favour the amino acid chains that intervene in the maintenance and generation of other copies of the filaments themselves, will be favoured and will be perpetuated (Ageno, 1991). So, gradually, in the protocell, one or some DNA chains will be able to produce all the molecules necessary for their duplication: these chains spread and any change capable of improving or speeding up the process is selected by evolution.

With the completion of the latter stage, we have reached a system that is now able to satisfy both the conditions of Ageno (1991) and the six needs indicated by Lane (2015), within a single compartment, now modified from the initial bags. We have finally obtained our lifeform.

In the latter case, as regards the estimation of the frequencies, we are faced with two obstacles to overcome: the formation of nucleotides (from a phosphate group, a pentose sugar and a nitrogen base) and their combination in filaments. While the second process seems very likely (Fraccia *et al.*, 2015), the first does not. By focusing on this, as in the previous case, we can assign minimal and maximum frequencies of 1 and 2%, this time, however, over an observation time of 5 years and a time limit of 20.

Phase 10			
a_9	b_9	ΔT_9	ΔT_{09}
0.01	0.02	5	20

Before concluding, it should be pointed out that this phase can be swapped with the previous one. In fact, the emergence of the genetic code, the final step in the creation of the lifeform, may have been produced when the system was still widespread within all the bags, or the majority of them.

What is the correct order? It is difficult to say precisely. By confining the last step to a single ‘bag’ and leaving to it the task of carrying out the transition between non-living and living, we ensure all the descendants will have the same genetic code, as is the case of all of the current organisms on Earth. We do not know if in the past there were more genetic codes nor what their impact on the evolution and interaction of living beings may have been.

We should point out, however, that the simple reversal of two or more phases, without any modification of the values attributed in the different stages, does not change the final value of the probability obtained by the Maccone algorithm, precisely because of the intrinsic mathematical properties of the algorithm itself.

Evaluation of the probability of passing each stage

We have thus obtained the 40 input values of pass 1 (Table 3).

By inserting these values into the calculation matrix shown in Tables 4–6, we obtain all the values of the following steps: we observe that the table values of μ_j and σ_j^2 of step 3 in Table 4 are the elements of the two sums of Fig. 5 which give rise to μ and σ^2 , or the average and variance of the logarithm of the variable X_0 in the medium period. ΔT_0 , as already stated, is the sum of the ΔT_{0j} and represents the medium term; while we have set the long period ΔT at about 100 000 000 years. To conclude, at the end of our analysis, we found, through the lognormal Φ , a probability of creating an entire cycle of the transition from non-living to the living, in the medium term $\Delta T_0 \sim 1\,000\,000$ years, equal to about 0.7%, (Table 6 and Fig. 14); while, in the long run $\Delta T \sim 100\,000\,000$ years (Table 6), we found an average probability of the onset of life on Earth equal to:

$$f_1 = 52\%$$

Table 3. Fourth Drake: the 40 values of the a_j and b_j frequencies minimum and maximum, of the time ΔT_j of observation and time ΔT_{0j} of micro-catastrophe, for each phase described in the previous paragraph

		a_j	b_j	ΔT_j	ΔT_{0j}
1	The abiological synthesis of biological molecules	0.9	1	1 000 000	1 000 000
2	The concentration of the primordial broth	0.05	0.15	100	10 000
3	The formation of lipid bags	0.9	1	0.10	10
4	The inclusion of chlorophyll in lipid membranes	0.1	0.2	1	10
5	The ‘photopump for protons’	0.1	0.2	0.01	10
6	The formation of nucleic acid filaments	0.02	0.03	0.01	1
7	The catalytic role of RNA	0.9	1	0.10	1
8	Determination of roles	0.2	0.3	100	100
9	Mobile membrane training	0.01	0.02	0.01	1
10	The emergency of the genetic code	0.01	0.02	5	20

Table 4. 4th Drake: evaluation of probability – the values in the box in darker grey are the entry data (pass 1); those in clearer grey the intermediate calculations (step 2 and 3)

	Step 1				Step 2			Step 3	
	Min in ΔT_j	Max in ΔT_j	ΔT_j	Time max	Intervals In ΔT_{0j} phase j	Min in ΔT_{0j}	Max in ΔT_{0j}	Comp. j aver. log	Comp. j var log
	a_j	b_j	ΔT_j	ΔT_{0j}	m_j	A_j	B_j	μ_j	σ_j^2
1	0.90	1.00	1 000 000	1 000 000	1	0.90	1.00	-0.0518	0.0009
2	0.05	0.15	100	10 000	100	0.99	1.00	-0.0030	0.0000
3	0.90	1.00	0.10	10	100	1.00	1.00	0.0000	0.0000
4	0.10	0.20	1	10	10	0.65	0.89	-0.2629	0.0082
5	0.10	0.20	0.01	10	1000	1.00	1.00	0.0000	0.0000
6	0.02	0.03	0.01	1	100	0.87	0.95	-0.0948	0.0007
7	0.90	1.00	0.10	1	10	1.00	1.00	0.0000	0.0000
8	0.20	0.30	100	100	1	0.20	0.30	-1.3930	0.0136
9	0.01	0.02	0.01	1	100	0.63	0.87	-0.2908	0.0081
10	0.01	0.02	5	20	4	0.04	0.08	-2.8568	0.0375

between the two minimum and maximum values

$$f_{IA} = 32\% \text{ and } f_{IB} = 66\%.$$

Drake 4	
f_{Imin} 3.2×10^{-1}	f_{Imax} 6.6×10^{-1}

Table 5. Fourth Drake: evaluation of probability – the values in the box in darker grey are the entry data (step 4); those in clearer grey the intermediate calculations (step 3 and 4)

Step 3					Step 4	
Max time total process (medium term) ΔT_0	Average logarithm μ	Variance logarithm σ^2	Average valour on the ΔT_0 period $\langle X_0 \rangle$	Standard deviation on the ΔT_0 period $\sigma(X_0)$	Max time tot process (long period) ΔT	Intervals number over time max tot process n
1 010 153	-4.95	0.07	7.31×10^{-3}	1.95×10^{-3}	100 000 000	99

Table 6. Fourth Drake: evaluation of the probability – data outgoing on time ΔT (long term): probability of development of life f_i and its values with standard deviation f_{IA} and f_{IB} (step 4)

Step 4		
Probability average tot process f_i	Probability minimum tot process f_{IA}	Probability maximum tot process f_{IB}
52%	32%	66%

4th Drake: lognormal distribution Φ of the fraction X_0 of the total process

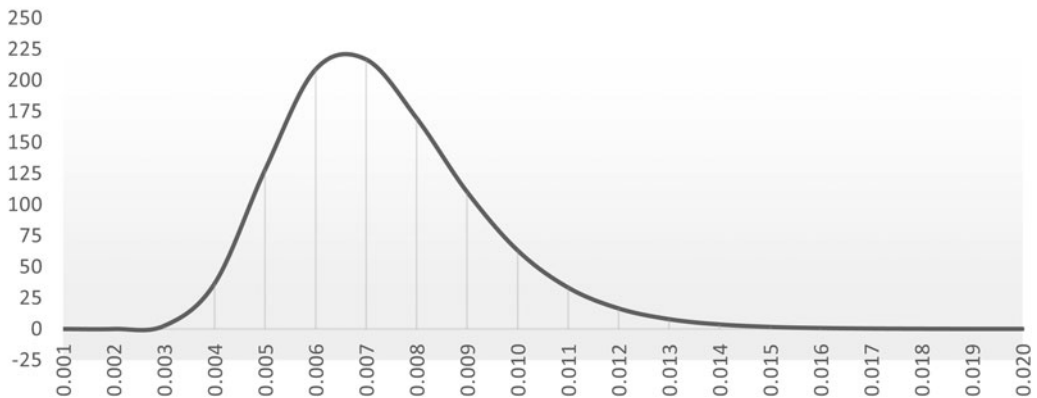


Figure 14. Fourth Drake: the lognormal distribution Φ of the process in the medium term ΔT_0 : the average value is 7.31×10^{-3} , the standard deviation is 1.95×10^{-3} .

Considerations on the fourth parameter

Although our work can only be considered preliminary and certainly contains elements and conditions that will need to be revised in the light of the scientific discoveries made in the coming years, we can already recognize some interesting results.

First of all, we found a value of the probability of the onset of life over 100 million years which, compared to what might be expected, is of the order of 0.5 – decidedly high (moreover equal to the value inserted by Maccone, in 2008, in his Drake statistical equation). So we do not need to invoke

an *anthropic principle* to justify our presence as observers of the phenomenon of life on Earth (a reasoning of the type: life in the universe is very rare, but since I exist and represent life, the probability is in any case not zero), but we can fall within the *principle of mediocrity* that asserts that the Earth, and us with it, is not a privileged point and we are not privileged *even as observers*. This conclusion was far from obvious even if, thanks to recent palaeontological observations, the suspicion that life on our planet had formed as soon as it had had the opportunity, a few tens of millions of years after the stabilizing of the planet, existed (see e.g. Dodd *et al.*, 2017).

Not only that, the Maccone method of dividing the problem into sub-problems dealt with individually from a mathematical–statistical point of view makes the phenomenon of the appearance of life less obscure or, at least, partially governable: it is obvious that the frequency values attributed to phases and the phases themselves can be improved and redefined (we hope that in the future they are), but what matters is that the algorithm gives an answer consistent with the data entered.

Finally, we want to emphasize that there is no reason not to use this approach not only for planets wholly similar to the Earth, but also in situations that deviate somewhat without precluding the possibility of the onset of life: for example, several situations close to us such as the sixth satellite of Saturn, Encelado, which could present favourable conditions for life under its frozen crust. But we are also thinking of more distant situations like the terrestrial exoplanets positioned in the habitability area of their star such as the Trappist-1 system at 40 ly from us; in such situations we could have planets with synchronous rotations (rotation equal to the revolution) or super-earths with masses more than ten times that of the Earth.

Finally, it is necessary to point out once again that for now we have dealt with the emergence of life in its most basic, unicellular and prokaryotic form. It is in this form that, with the appropriate initial conditions (suitable planet, etc.), the chances of life evolving are significant, however does not include animals, plants and all eukaryotic organisms – all those beings, that is, derived from a symbiotic association between several prokaryote cells (Margulis, 1998; Archibald, 2014). This process, which took place on Earth, will be the topic of the next section.

Fifth Drake: the probability of intelligent life

Given the complexity of the topic, in the fifth parameter (Mieli and Valli, 2023), we immediately find ourselves having to divide the process into at least three large macro-intervals:

Macro-interval A	The onset of the eukaryotic cell
Macro-interval B	The appearance of animals (metazoa)
Macro-interval C	The onset of intelligent civilization (ETC)

Each macro-interval will be divided into several phases, as for the fourth parameter. The substantial difference is on the temporal scale of the catastrophes: given that life, once formed, is decidedly more resistant than the biochemical environments that preceded it, the typical times of ΔT_j micro-catastrophes are now of the order of 100 million years, while those of ΔT_{0j} macro-catastrophes are of the order of half a billion years.

The phases that divide the three macro-intervals are as follows:

Macro-interval A

- the evolution of an aerobic bacterium
- the host–symbiont meeting
- the formation of the pores and the appearance of cytoplasmic extensions
- the ‘winding’ of the symbionts and the disappearance of the host’s cell wall
- the penetration of symbionts into the cytoplasm
- the migration of DNA from the genome of the symbiont to that of the host
- the acquisition of the eukaryotic cytoplasmic membrane
- incorporation into a single coating and phagocytosis

Macro-interval B

- the acquisition of a complex life cycle
- the aggregation of zoospores and the formation of the synzoospores
- the sedentary colony composed of differentiated cells
- the production of collagen

Macro-interval C

- increase in size of metazoa (nervous and vascular system)
- limb development
- colonization of dry land
- differentiation of land animals
- erect posture and manual skills
- change of diet and growth of brain
- organization of the brain on abstract thinking
- birth of articulated language and technique

The starting point; the stability conditions of a planet

For life as we know it to be sustained, it is necessary that water is present, especially in its liquid form. This substance can be broken down into its constituent elements of hydrogen and oxygen by ionizing radiations from the sun (Bolton *et al.*, 1985; Lane, 2002). To block them, the formation of a protective layer such as that of ozone (O₃) in the atmosphere is necessary. This molecular form is the product of common oxygen (O₂) reacting to the main solar electromagnetic rays which are thus shielded.

Paradoxically, the oxygen deriving from the decomposition of the water does not contribute to the formation of the ozone layer, because the phenomenon of hydrolysis is very slow and the freed gas is seized by the oxidation of the minerals present in the environment. In order to form O₃, oxygen molecules must be able to remain long enough in the atmosphere. For this to happen, their production must be regular and abundant. The only process that produces this gas in sufficient quantities is the photosynthesis carried out by chlorophyll plants and cyanobacteria (Lane, 2002). Not only that, but the mass of the planet must be large enough to retain oxygen molecules without them being dispersed into space. A sufficient planetary mass is one of the initial conditions evoked in the previous work (Valli and Mieli, 2022) and in the previous section of this work relating to the fourth parameter.

We will return to this question later, but let us remember that, if water vanished, no form of life would be possible and for this reason it is necessary to block its hydrolysis before it is too late.

However, if these conditions were sufficient for the onset of life, we will see that they are no longer enough for those conditions we wish to examine now. In fact, we must verify that the existence of the planet lasts long enough to ensure the level of biological evolution that interests us. As we saw for the third parameter, these times are measured in billions of years; the age of the Earth is in fact 4.54 ± 0.05 (Dalrymple, 2001). At the end of this work, we will compose together the information starting from the third parameter onwards to establish the number of planets sufficiently stable for the development of life in every stage, from the most primitive to the galactic civilizations.

Macro-interval A*The crucial passage; the onset of the eukaryotic cell*

The current prokaryotes include archaea and all bacteria. These are microscopic organisms, considerably smaller than the eukaryotes: despite the existence of 'giant' bacteria, eukaryotic cell organisms have an average volume 15 000 times greater than the prokaryotes (Lane, 2015) which, however, are present everywhere and represent the most consistent element of terrestrial biodiversity (DeLong and Pace, 2001; Ogunseitan, 2016; Selosse, 2017; Flemming and Wuertz, 2019).

The diversity of prokaryotes is not based on morphology, but on their metabolism. The set of metabolic differences that plants, animals, mushrooms and all other eukaryotic organisms present are nothing compared to the range of different processes presented by bacteria and archaea. The latter were once simply considered specialized prokaryotes in the colonization of extreme environments where living conditions are (according to our standards) if not impossible, at best very difficult (thermal springs at high temperatures, hypersea ecosystems, anoxic environments). In reality, the archaea would seem to be present in the majority of existing environments on our planet (DeLong and Pace, 2001; Robertson *et al.*, 2005; Forterre, 2007; Baker *et al.*, 2020).

Bacteria, on the other hand, are organisms that present the greatest metabolic diversity. Some are capable of living with hyperthermophile archaea while others perform the same type of photosynthesis carried out by chlorophyll plants, releasing O₂. Certain cannot stand this gas, while others grow very well in its presence (Stainer *et al.*, 1976; Aravind *et al.*, 1998; Fierer and Jackson, 2006; Lozupone and Knight, 2007). There are even bacteria capable of producing the energy they need thanks to the reduction of uranium (Lovley *et al.*, 1991). Finally, to underline the surprising skills of some representatives of this group, we need to only think of *Rubrobacter radiotolerans* (Yoshinaka *et al.*, 1973) one of the most resistant organisms to gamma radiation: it can tolerate doses thousands of times higher than those necessary to kill a man (Ferreira *et al.*, 1999). It also seems that there are various microbial strains belonging to both bacteria and archaea which present high tolerances to radiation (Egas *et al.*, 2014).

Eukaryotes cannot compete with prokaryotes on their own terrain, but thanks to their abilities and properties, these organisms occupy ecological niches precluded to bacteria and archaea. The eukaryotic cell differs from the prokaryote (Fig. 15) cell because of the presence of certain specific characteristics (Vellai and Vida, 1999; Lane, 2015; Webb, 2015):

- It has a double-wall nucleus, in which (almost all) the cellular DNA is contained, organized in the form of chromosomes;
- It contains cellular organelles possessing genetic material not present in the nucleus and internal membranes;

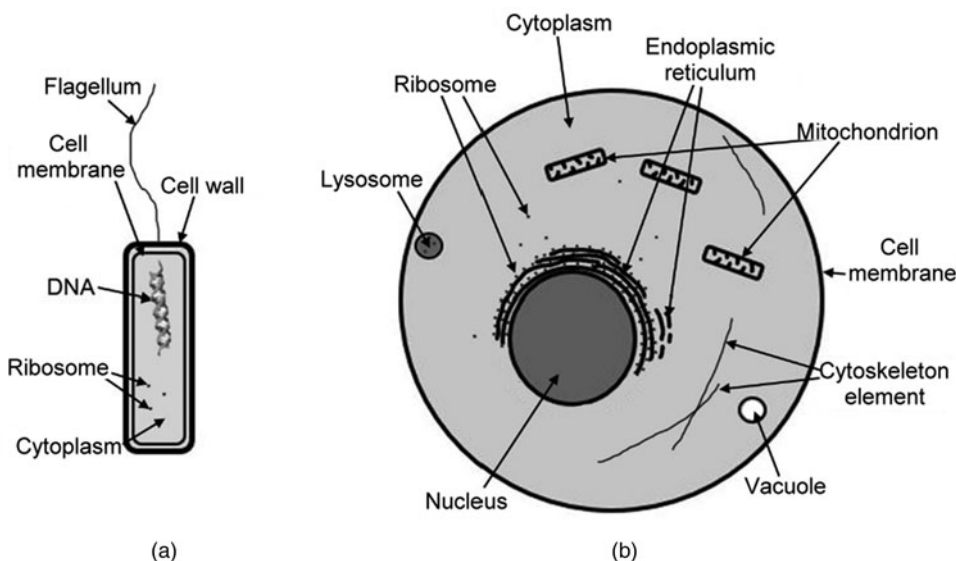


Figure 15. Fifth Drake: comparison between a prokaryote cell (a) and an animal eukaryotic cell (b), with the typical elements of the two cells indicated on the figure. The main differences between bacteria and archaea reside at the level of the cell membrane (see Fig. 5). The two cells are not in scale: the prokaryotic cell is about of size of the mitochondria of the eukaryotic cell.

- it is equipped with a dynamic cytoskeleton (cell skeleton) made up mainly of filaments consisting of the actin protein, which supports the membrane and which allows its deformation (eukaryotes did not originally have a cell wall, although certain lineages, like plants, did subsequently develop one);
- finally, a whole series of complex behaviours can develop, including among other things, phagocytosis (lost in eukaryotes with cell wall), sexuality and aggregation in multicellular organisms.

A eukaryotic cell normally possesses a much higher quantity of genes than a prokaryotic cell: the largest bacterial genome contains 12 megabases [Mbp] (a base [bp] is a pair of appeared nucleic acids; a megabase [Mbp] indicates one million bases) of DNA, while the human genome has 3000 Mbp – and certain eukaryotes reach up to 100 000 Mbp (Lane, 2015). It is precisely this ability to manage complex structures and processes, obtained thanks to a powerful collection of proteins that mediate the mass on site, that seems to be the main difference between the eukaryotes and the prokaryotes (Lane and Martin, 2010). In fact, theoretically, the various ‘eukaryotic’ characteristics all seem to have their prokaryote precursors (see e.g. Wujek, 1979; Lindsay *et al.*, 2001; Schulz and Jorgensen, 2001; Von Dohlen *et al.*, 2001; Simon and Zimmerly, 2008; Ettema *et al.*, 2011; Yutin and Koonin, 2012), but the latter never take the decisive step towards complexity.

To better understand what this complexity consists of, let us examine some typical examples. First, sexuality; in the fossil register, the oldest known testimony is *Bangiomorpha pubescens* (Butterfield, 2000), a red alga found in the sediments of the Canadian Arctic (Butterfield *et al.*, 1990) currently dated (Gibson *et al.*, 2018) to just over 1 billion years (Gy) ago. Even if we do not know exactly whether the first eukaryotic organism that appeared was able to reproduce sexually, it seems clear that the oldest ancestor of all the current eukaryotes was (Génermont, 2014). No prokaryotic organism, on the other hand, has a sexual cycle, although some are able to transmit genetic material for horizontal transfer of genes (Gogarten *et al.*, 2002; Watson *et al.*, 2013; Cabezón *et al.*, 2015).

With regard to the establishment of multicellular organisms, although some bacteria are known to aggregate (Castanier *et al.*, 1994; Bapteste, 2013), no prokaryote organism is able to form aggregates capable of behaving in such a coordinated way as to form a complete individual.

Finally, as indicated above, the unicellular eukaryotes are larger than the prokaryotes. There are, however, gigantic bacteria, but only a few forms in total are known. *Epulopiscium fishelsoni* (Montgomery and Pollak, 1988) and *Thiomargarita namibiensis* (Schulz *et al.*, 1999), for example, are genuine titans: their dimensions reach the tenths of a millimetre (they are practically visible to the naked eye), exceeding the size of many unicellular eukaryotic organisms. The peculiarity of these giants is that of having many copies (up to several thousand) of their genome relegated close to their cell wall, while most of their cytoplasm is metabolically inactive (Schulz, 2006; Mendell *et al.*, 2008; Miyake *et al.*, 2016). These precautions allow them to survive despite their excessive dimensions.

In any case, this strategy proves to be an evolutionary *cul-de-sac*, because it does not translate into any complex behaviour by these prokaryotes (Lane and Martin, 2010).

This said, how then to explain the differences between these two types of cells? How to justify the *performances* of eukaryotes compared to those of the prokaryotes? These last organisms are in no way lower or less advanced than the previous ones (as is shown by the fact that they present a range of metabolisms so diversified that they can be found absolutely everywhere). Put simply, the eukaryotes have evolved to occupy ecological niches precluded to bacteria and archaea. How did they manage it?

The eukaryotic cell as symbiosis between prokaryotes

The response lies in the genesis of eukaryote unity, deriving from a symbiotic association between prokaryotes (Margulis, 1998; Archibald, 2014) and, more particularly, between an archaeon and a bacterium (de Reviews, 2018). Certain specialists even think that viruses have been implicated in the formation of the nucleus of the new type of cell (Forterre and Gaïa, 2018). In any case, most authors now agree that eukaryotes are real ‘chimeras’, obtained from more than one living being.

All current eukaryotes have organelles, limited by a double membrane, which derive from symbiotic prokaryotes: mitochondria and plastids (the latter are present only in photosynthetic living being, as they are essential for such processes). The acquisition of these organs was accompanied by a transfer of genes from the genome of the symbiont to that of the guest, a phenomenon that is always produced in *all* endosymbiosis (de Reviers, 2018). The mitochondria in particular derive from a single form of bacterium belonging to the group of the *alphaproteobacteria* (Roger *et al.*, 2017), a fact that establishes the unique origin of this organelle. It was its acquisition that sanctioned the birth of the eukaryotic cell (Martin and Müller, 1998). In fact, all eukaryotes have mitochondria, even if some have transformed or have lost them, while preserving some characteristic genes in their nucleus (Tovar *et al.*, 2003; Zimorski *et al.*, 2019).

But what advantage does the mitochondrion confer? Is the fact of breathing O₂ sufficient to justify eukaryotic *performance*? Aerobic respiration (the oxidation of nutrition by O₂) is at least six times more advantageous than anaerobic respiration, but the costs of protein production are 13 times higher in its presence than in its absence (Zimorski *et al.*, 2019). In addition, in various bacteria, the aerobic metabolic processes develop much faster than in the mitochondrion (Lane and Martin, 2010). Therefore, the advantage does not seem to be linked only to the breathing of O₂. In reality, the benefit conferred by this organ lies in the ability to enormously increase the energy available for gene: the term ‘energy per gene’ indicates the cost necessary for *gene expression*: the cost of production of proteins and other cellular components (Lane and Martin, 2010). By increasing the energy per gene – and the presence of mitochondria allows the eukaryotic cell an increase between 4 and 6 orders of magnitude – the amount of energy that can be donated to gene expression is increased, meaning the number of genes that a cell can manage is also increased. The more genes there are, the more the cell becomes capable of ‘complex’ processes and behaviours, bearing in mind that the eukaryotic genome includes a much higher number of genes than the prokaryotic ones.

The details can be found in the works of Nick Lane (Lane and Martin, 2010; Lane, 2015) but we try to simplify this concept with an example. Let us imagine that you want to prepare tortellini with a particular filling of meat and a special sauce for 30 guests at a wedding reception. Who will be more efficient? A team of three specialized cooks (one for the tortellini pasta, another for the meat filling and the last for the sauce) or a single cook that prepares the dish in its entirety? It is clear that the team of three people, carrying out each phase of the work separately (decentralization), will produce more quickly and effectively, or with less waste, a large number of portions than if a single chef were asked to do all the work. The statement is even more valid in the case of ten or more cooks, each of whom must prepare the dish in its entirety.

This is precisely what the eukaryotic cell does: it decentralizes energy production in the various mitochondria which, in turn, transfer their genome to that of the nucleus except for the genes strictly necessary for the control of the functioning of the energy production chain (it is estimated that the mitochondria retain only about 1% of their estimated original genome; Gray *et al.*, 2004). In this way, the various components of the eukaryotic cell restart the tasks: the nucleus retains the genome and replicates it, the cytoplasm reserves the production of cellular material and the mitochondria, which must practically no longer deal with protein synthesis, handle energy production, making it more efficient and profitable for the whole organism. To recap: the eukaryotes derive from a symbiotic association between an archaeon and a bacterium (the latter will become the mitochondria). Currently, it is thought that the symbiont bacterium was an optional aerobe capable of breathing O₂, when present, but also equipped with anaerobic metabolism, in the absence of this gas (Zimorski *et al.*, 2019). The consumption of O₂, therefore, was present from the first steps of the onset of eukaryotes and this fact underlines the importance of this gas in the evolution of living beings. In this regard, what we said above about the ozone layer (O₃), which protects us from ionizing energy coming from space and allows us to live on the emerged lands, is worth remembering. Without free oxygen, not only would water be broken down into its basic elements (Lane, 2002) but the evolution of lifeforms beings would have been seriously upset. In fact, the level of O₂ affects the synthesis of cholesterol (Summons *et al.*, 2006), an indispensable molecule present in the cell membrane of all animals (Brown and Galea, 2010). It is no coincidence that the onset of the eukaryotic cell dates to after the *great oxidation event* (GOE), produced around 2.4 and 2.1 Gy (Lyons *et al.*, 2014). This event signals the presence of free O₂

in the environment, as evidenced by the geological formation of layers rich in iron oxides, the *Red Beds* (Knoll, 2015). In short, the importance of this gas for the first eukaryotes and their descendants has been amply demonstrated (Lane, 2002).

Although some rare cases of bacteria present within other prokaryotes are reported (Wujek, 1979; von Dohlen *et al.*, 2001, but for a correct interpretation of these cases, see also Yamaguchi *et al.*, 2020), the symbiotic association which allows the onset of eukaryotes is considered a unique event (although a recently discovered organism has raised questions; Yamaguchi *et al.*, 2012) or extremely unlikely (Lane, 2015). In fact, it should be noted that the onset of eukaryotes, placed between 2.1 and 1.6 Gy (Knoll *et al.*, 2006; Rasmussen *et al.*, 2008; El Albani *et al.*, 2019; Porter, 2020), occurs after more than 1.5 billion years after the appearance of the prokaryotes, which took place around 3.7 Gy (Nutman *et al.*, 2016), or even earlier (Pons *et al.*, 2011; Dodd *et al.*, 2017; Papineau *et al.*, 2022). During this long period of time, the eukaryotes were absent, while bacteria and archaea differed abundantly (see e.g. Nisbet, 2000; Schopf *et al.*, 2007, 2017; Javaux *et al.*, 2010).

Despite all this, in this article, we want to investigate the possibility that the time of onset of eukaryotes may have been influenced by parameters other than the alleged improbability of the symbiotic phenomenon. For example, one of the key factors could simply be the time necessary to achieve a certain content of O₂ in the environment, without which the association would not have occurred.

But in that case, why do all eukaryotes descend from a single ancestor but no other later symbioses of this type have been recorded, even though there is a relative abundance of O₂ in the environment? We have no definitive answer to this question. The only one that comes to mind is that, having worked perfectly the first time, the eukaryotes had gradually occupied all the niches available, limiting competition and preventing the phenomenon from repeating or strongly limiting it.

The inside-out model for the onset of the eukaryotic cell

Because of their wall, the prokaryotes (they being bacteria or archaea) lend themselves little to being ‘colonized’ by other microorganisms (Lane, 2015). So how to solve the problem of the association of an archaeon with endosymbiont bacteria?

A recent model called *inside-out* seems to be able to provide an interesting and original response to the problem of a symbiotic association between an archaeon and a bacterium and would allow a more detailed explanation of the onset of the eukaryotic cell. The authors (Baum and Baum, 2014, 2020) propose that it is not the bacteria which penetrate the wall of the archaeon, but that the latter is able to produce, through special pores homologous to those of the nuclear membrane of the eukaryotes, cytoplasmic outgrowths which over time can wrap around the associated and stationary microorganisms on its wall (Fig. 16(a)). According

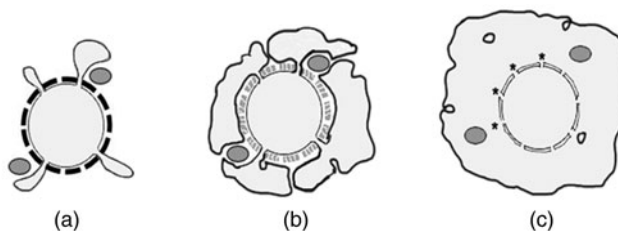


Figure 16. *Fifth Drake: simplified scheme of the inside-out model: (A) the outgrowth comes out from pores of the wall (thick black line) of the archaeon; (B) the outgrowth develops and begins to wrap the associated bacteria (the two grey ovals), while the wall begins to vanish; (C) the cytoplasm completely holds the archaeon and the bacteria have penetrated through the membrane, finding it inside: the original structure of the archaeon, covered with a double membrane equipped with pores (four of these are marked by asterisks), will become the nucleus of the new cell (figure modified by Baum and Baum, 2014).*

to this model, the outgrowths also cover the whole organism, enveloping the cell of the archaeon (Fig. 16 (b)), which in fact becomes the ‘nucleus’ of the new body, covered by a double-layer membrane, deriving from the original one plus the one added by the outgrowth lobes. Gradually, the wall of the archaeon disappears, becoming superfluous. Finally, associated bacteria penetrate through the extensions of the membrane to find themselves in the cytoplasm (Fig. 16(c)). In practical terms, the symbionts do not enter the guest or host, or at least, not initially, but the cytoplasm of the latter is evaginated to cover them.

Some archaea are perfectly capable of generating extracellular protrusions (Rachel *et al.*, 2002; Baker *et al.*, 2006; Marguet *et al.*, 2013). In addition, as we will see below, the *inside-out* model is perfectly compatible with the hypotheses made regarding the possible nature of the guest. For this reason, we will adopt it to describe the passages that lead to the onset of the eukaryotic cell.

The onset of the eukaryotic cell, phase by phase

The starting point; the liberation of oxygen and its diffusion in the environment

We have seen the importance of the concentration of O₂ for the onset of eukaryotic cells and evolution towards intelligent life forms. The only process that ensures the production of large quantities of this gas is photosynthesis, a purely biological phenomenon (Lane, 2002; Holland, 2006). But in this case, when do the first organisms able to free O₂ thanks to the photosynthesis process evolve? Let us not forget that only some photosynthetic organisms are able to release O₂ following this process (Gest, 2002): these are chlorophyll plants and cyanobacteria, which use water – H₂O – as an electron donor.

According to Ageno (1991), the first living organisms were not only capable of photosynthesis but even freed O₂. In fact, he claims that electrons must logically have been obtained from a substance which is very common in nature; H₂O, in fact. For this type of photosynthesis, particularly complex pigments – chlorophylls – are needed (Tomitani *et al.*, 1999; Eggink *et al.*, 2001). Ageno reports that laboratory experiments such as those carried out by Miller (1953) have shown that the habitual synthesis of these molecules is perfectly possible.

According to other specialists, however, the first lifeforms were chemoautotrophic. Although the GOE produced between 2.4 and 2.1 Gy, experts believe that prokaryotes capable of producing O₂ (cyanobacteria) were present, on our planet from at the latest 3 Gy (see e.g. Crowe *et al.*, 2013; Lyons *et al.*, 2014) or even earlier (Schopf and Packer, 1987; Javaux *et al.*, 2010).

However, there is no contradiction between these dates, as the process of accumulation of O₂ in the environment is considered a slow and one which is hindered by other phenomena (for the various models and the hypotheses that illustrate them, see e.g. Kasting, 2013; Olejarz *et al.*, 2021, and the bibliography mentioned in the two articles). In any case, the concentration of this gas in the environment became about 10⁻² times the current value only after 2.5 Gy, manifesting itself with an ability to produce the deposits called *red beds*. The appearance of eukaryotes is successive to this event.

The first phase; the evolution of an aerobic bacterium

The current theory of the onset of the eukaryotic cell provides for a symbiotic association between an archaeon, the host and various individuals of a bacterial strain, the symbionts (de Reviers, 2018). Martin and Müller (1998) formed the hypothesis that the guest archaeon was an anaerobic organism, rigorously dependent on H₂, while the symbiotic bacteria were able to breathe O₂ and produced H₂ as a metabolic waste product. These behaviours would have guaranteed complementarity between organisms.

But when exactly did the first aerobic bacteria appear? Research on the Precambrian layers has made a great deal of progress in recent years (Schopf, 2019) and has documented an extraordinary variety of organisms during the early billion years of our planet (Nisbet, 2000; Schopf *et al.*, 2007; Javaux *et al.*, 2010; Knoll, 2015). Not only that: a complex ecosystem has been documented at about 3.4 Gy, including microorganisms capable of producing sulphide acid (H₂S) plus other organisms, stromatolites

manufacturers, dependent on this substance they used as an electron donor to carry out photosynthesis (Schopf *et al.*, 2017).

As can be seen, already in this remote era, the prokaryotes had differentiated themselves and had constituted complex communities where several complementary ecological niches had been occupied. With such assumptions, given the metabolic versatility of the bacteria, it is legitimate to think that, once the O₂ had made itself available in the environment, some microbial strains became capable of exploiting this gas as a resource to produce energy in a few thousand years at most: *a probability of between 0.4 and 0.6 every 2000 years with a time of 100 000 years of micro-catastrophe*:

Phase 1			
a_1	b_1	ΔT_1	ΔT_{01}
0.4	0.6	2000	100 000

The second phase; the host–symbiont meeting

Let us now look at the host organism. Currently, thanks to a series of protein homologies, it is believed that the eukaryotes share a common ancestor with the set of archaeons called ‘Asgard Archaea’ or even that this ancestor was to be found within this group (Spang *et al.*, 2015; Zaremba-Niedzwiedzka *et al.*, 2017; Eme and Ettema, 2018; Liu *et al.*, 2021; but see also from Da Cunha *et al.*, 2017, and the response of Spang *et al.*, 2018).

The Archaea of Asgard constitute a super-phylum built mainly thanks to genetic material found in the environment. Despite this, they are very widespread organisms, the remains of which have been found in marine, lake and terrestrial sediments. They are mainly anaerobic and widespread in vent fields and/or in areas rich in methane (Macleod *et al.*, 2019). One strain is even anaerobic and dependent on H₂, the requirements required by Martin and Müller (1998) for the host of symbiotic association. They are therefore the ideal organisms in which to seek the protagonist archaeon of the onset of the eukaryotic cell.

Furthermore, a particular microorganism has recently been identified which is capable of surviving only thanks to symbiosis with other microbes, and which belongs to a phylum of the group of Archaea of Asgard, that is the *Lokiarchaeota*, considered close to eukaryotes (Spang *et al.*, 2015). The prokaryote described (not this time simply analyses of the gene sequences to be found in the environment, but of a true living being) has the ability to generate cytoplasmic outgrowths. According to the authors (IMACHI *et al.*, 2020) this ability allows it to facilitate exchanges of material with external symbiont. Therefore, in light of all these facts, this would appear to legitimize our use of *inside-out*.

Although the era of the origin of the Asgard Archaea is not known, judging from their supposed diversity (Macleod *et al.*, 2019) they should be sufficiently ancient. Let us consider, therefore, that the group already existed at the time of the appearance of aerobic bacteria, even if, being made up of majority anaerobic prokaryotes, probably, the two types of organisms lived, initially, in different environments. However, it is currently believed that the symbiont bacterium was an optional aerobic (Zimorski *et al.*, 2019), capable of populating the environments frequented by the anaerobic archaea.

We therefore consider that a 10 000-year interval is more than sufficient for the meeting to take place and for the association to form (associations between archaea and bacteria also take place currently, although the latter remain outside the former; Muller *et al.*, 2010): *a probability of between 0.01 and 0.02 every 10 000 years with a time limit of 100 000 years of micro-catastrophe*:

Phase 2			
A_2	B_2	ΔT_1	ΔT_{02}
0.01	0.02	10 000	100 000

The third phase; the formation of the pores on the membrane and the emergence of cytoplasmic extensions

In the previous stage, we have seen that the ability to produce cytoplasmic outgrowths is a characteristic of some groups of archaea. To allow them to protrude from the pores, it is necessary that particular structural proteins be produced, such as the molecules (COPII) that form the rings of the complex of the nuclear pores of the eukaryotes. Although prokaryotic equivalents of these molecules (Santarella-Mellwig *et al.*, 2010) were found, it would seem that these proteins are not homologous to those of the eukaryotes (Mcinerney *et al.*, 2011).

It is therefore preferable to imagine an evolution from scratch in the host's line rather than suppose a more ancient prokaryote inheritance. In any case, the pores being necessary for protrusions and this ability being spread across various groups of archaea (Baum and Baum, 2014), it is logical to suppose that a certain variety of support proteins were produced, including those homologous to the eukaryotic ones, from which the latter would have been derived.

Once the pore has been produced, the cytoplasm can escape forming an excrescence supported by cytoskeletal elements (Fig. 17). Proteins homologous to eukaryotic proteins were found in most phyla belonging to the *Asgard Archaea* (see e.g. Spang *et al.*, 2015; Zaremba-Niedzwiedzka *et al.*, 2017; Liu *et al.*, 2021). The formation of pores and outgrowths is treated as a single phase, due to the close link between the two processes (the first would not make sense without the second, whose probability can be set as equal to 1, once the previous one has occurred).

The time necessary for the production of molecules homologous to the eukaryotic ones to stabilize the pores and for the formation of those of the cytoskeleton is assessed at a few thousand years: *a probability of between 0.04 and 0.06 every 5000 years with a time of micro-catastrophe limit 100 000 years:*

Phase 3			
A_3	B_3	ΔT_3	ΔT_{03}
0.04	0.06	5000	100 000

The fourth phase; the 'winding' of the symbionts and the disappearance of the guest's cell wall

The next step consists of the development of the cytoplasmic excrescence that begins to approach and 'wrap' the bacteria (Fig. 16(b)). These protrusions would have evolved to facilitate the exchanges between the archaeon and the microorganisms in symbiosis with it (Baum and Baum, 2014), which were on its external surface, being unable to penetrate the wall of the host. The cytoplasmic expansions were supported by the cytoskeletal elements mentioned in the previous phase, which continue to

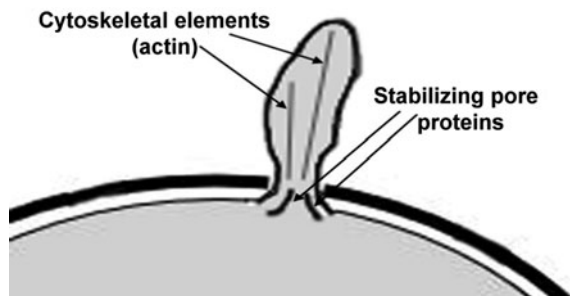


Figure 17. *Fifth Drake: scheme of the wall of the archaeon guest, with pore crossed by a cytoplasmic rise, according to the inside-out model (Baum and Baum, 2014, 2020).*

develop. At the same time, the wall of the archaeon begins to regress until it completely disappears, for two reasons:

- it becomes practically useless, as it is covered by cytoplasmic extensions, in contact with the internal environment of the archaeon;
- it is counterproductive because it forms an obstacle to a greater extrusion of the cytoplasm.

At this point, due to the disappearance of the cell wall, the membrane of extrusions covers the original membrane that covered the archaeon, folded towards the inside (Fig. 16(c)). Therefore, the future nucleus of the new cell, made up of the region occupied in ancient times by the archaeon and delimited by a double lipid membrane equipped with pores, begins to form.

The endoplasmic reticulum, a membrane with multiple folding located near the nucleus, where protein synthesis takes place, is supposed to derive from the folds of the membranes of the extrusions (Baum and Baum, 2014).

The duration of this phase is given by the enveloping of the host–symbionts complex by the excrescences protruding from the pores and by the complete disappearance of the wall of the archaeon; it can be evaluated at a few thousand years: *a probability between 0.01 and 0.02 every 2000 years with a micro-catastrophe time limit of 100 000 years:*

Phase 4			
a_4	b_4	ΔT_4	ΔT_{04}
0.01	0.02	2000	100 000

The fifth phase; the penetration of symbionts in the cytoplasm

The next phase involves the penetration of symbiotic bacteria into the cytoplasm of archaeon. Although it is difficult to establish the affinities of the mitochondria due to the tiny amount of genome they have preserved, recent studies indicate that the ancestors of these organs should be sought among the *alpha-proteobacteria* and, more specifically, among the bacteria similar to the group of *Rickettsia* (Ferla *et al.*, 2013; Han *et al.*, 2019). These compulsory endosymbionts parasitize the cells of the eukaryotes (especially in insects, but humans can also be attacked), penetrating them thanks to their ability of lysis of the lipid membranes (Emelyanov, 2001). If the ancestors of mitochondria were truly related to rickettsiae and possessed cell penetration capabilities, they could easily enter the cytoplasmic sacs of the expansions which were not defended by rigid walls.

It is important to note, as Baum and Baum (2014) do, that this process absolutely does not cause the intervention of phagocytosis (a phenomenon which, as we will see below, will be produced only in the final stages of the process). The bacteria were external symbionts and they penetrated the host thanks to the means available to them, taking advantage of the protrusions' failure to cover the wall.

Considering the biological affinities of the *proto-mitochondria* and the properties of the bacteria related to them, the time globally expected for the completion of this phase is rapid, estimated at no more than a few decades. However, we attribute only a low probability to the process to take into account the risk of compromise of the association following the penetration of the bacterium in the cytoplasm of the host: *a probability of between 0.01 and 0.02 every 50 years with a micro-catastrophe time limit of 100 000 years:*

Phase 5			
a_5	b_5	ΔT_5	ΔT_{05}
0.01	0.02	50	100 000

The sixth phase; the migration of DNA from the genome of the symbiont to that of the host

Once endosymbiosis has been established – the symbionts are now found within the host – a process begins that occurs every time this type of association occurs: the migration of the genes from the genome of the symbionts to that of the host (de Reviers, 2018). This process allows the association to increase its efficiency, as the host deals with protein synthesis, including that of various molecules of the symbionts, while the latter focus on their specific activities (energy production or specific biological compounds). The more ancient the endosymbiosis is, the larger the quantity of genetic material that has been transferred to the host DNA (Selosse, 2017) is. When we speak of ‘migration’ of genes from symbiont to the guest, we mean their ‘deletion’ from the genome of the first and their complete ‘transfer’ into that of the second (Fig. 18). In this way, the two partners are not only complementary but also dependent upon each other (especially the first). However, it is precisely this freeing of the mitochondrion from tasks related to protein synthesis, allowing it to focus only on energy production, which allows the future eukaryotic cell to increase the energy available per gene at higher levels for the prokaryotes (Lane, 2015).

It is thought that the mitochondria currently retain only approximately 1% of the genetic material possessed by their ancestor *alphaproteobacterium* (Gray *et al.*, 2004). We also know that more than 1.5 Gy separate us from the symbiotic association that sanctioned the onset of the eukaryotic cell.

How long is it necessary to wait for a sufficient migration of genetic material from the symbiont to the host to be carried out? Certainly in the first organisms with sexual reproduction (the oldest known is *Bangiomorpha pubescens*, whose fossils were found in sediments of just over 1 Gy; Gibson *et al.*, 2018), the percentage of reduction was already comparable to the current one. A sufficient level had however probably already been reached much earlier. We can therefore estimate a time period of an order of magnitude of about 10 000 years: a probability of between 0.1 and 0.2 every 10 000 years with a micro-catastrophe time limit of 100 000 years:

Phase 6			
a_6	b_6	ΔT_6	ΔT_{06}
0.1	0.2	10 000	100 000

The seventh phase; the acquisition of the eukaryotic cytoplasmic membrane

The cell membranes of archaea are made differently from those of bacteria and eukaryotes. Unlike archaea, these last two groups have coatings made up of the same types of lipids. We are dealing

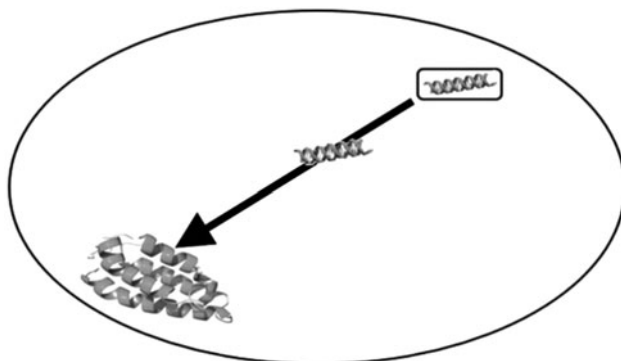


Figure 18. Fifth Drake – eukaryotes: migration (along the arrow) of the symbiont genome (top right rectangle) towards the host DNA (bottom, left); the genome thus transferred will be lost from the symbiont DNA but will be preserved in that of the host.

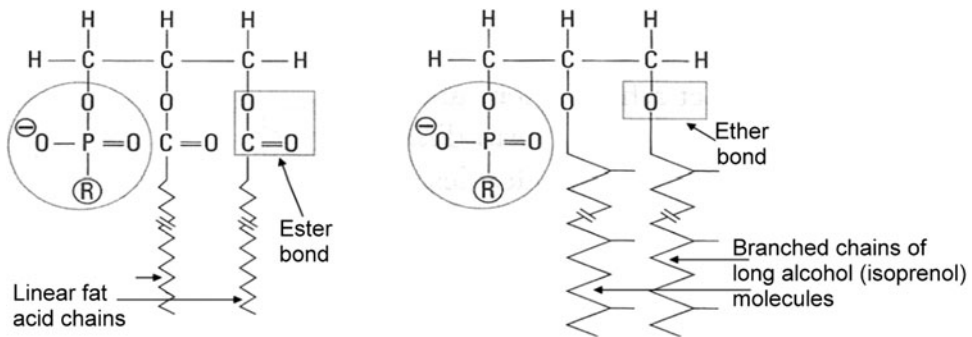


Figure 19. *Fifth Drake – eukaryotes: main differences between the constituents of the cell membranes of bacteria and eukaryotes (left) and those of archaea (right): the polar head of bacteria and eukaryotes binds to hydrophobic chains via an ester bond, while archaea use ether bonds; the hydrophobic chains of bacteria and eukaryotes are made up of linear fatty acids, while those of archaea are made up of long branched alcoholic molecules (the various elements are not to scale with each other; figure modified from Forterre, 2007).*

here with a very important structural diversity between archaea on the one hand and bacteria and eukaryotes on the other (Forterre, 2007; Koga and Morii, 2007).

In fact, eukaryotic and bacterial cells have membranes whose polar heads bind to lipid chains by means of *ester* bonds, while those of archaea use *ether* bonds. In addition, the chains of these organisms are made up of long *branched alcohol* molecules (isoprenol), while the chains of bacteria and archaea are *linear*, without any bifurcation (Fig. 19). These differences are explained by the fact that the membranes of the archaea are more resistant to the high temperatures where many of these organisms abound (and where the group's ancestors probably evolved; Forterre, 2007). But in that case, on the basis of the *inside-out* model, how can we explain the homologies between the bacterial and eukaryotic membranes if the host is archaea-like in nature and, therefore, possesses a different type of coating?

Once part of the genomic patrimony of the host, biological evolution will push to obtain an 'economical' situation: the simplest thing is to produce a single type of membrane for all the constituents of the symbiotic association. But which to choose? The original one of the archaeon or the one imported from the bacterium? The answer can only be the second. In fact, the symbiont's membrane has specialized for energy production thanks to the oxidation of organic molecules by O_2 and all the advantage conferred by these bodies to the association is, in fact, an efficient method of energy production (Lane and Martin, 2010; Lane, 2015).

It follows that the only membrane whose nature can be changed is the original one of the archaeon host. In this way, the future eukaryotic cell will be covered by a membrane whose nature is typical of bacteria. The bacterial genes that determine the assembly of the cell membrane will begin to be selected from the moment of their full integration into the guest genome.

Thanks to the selective pressure exerted by evolution, complete replacement can take place in relatively short times; at most, a few thousand years: *a probability of between 0.001 and 0.002 every 2000 years with a micro-catastrophe time limit of 100 000 years:*

Phase 7			
a_7	b_7	ΔT_7	ΔT_{07}
0.001	0.002	2000	100 000

The eighth phase; the incorporation of all the guest–symbiont into one coating (continuity of the cytoplasm) and phagocytosis

Finally, the expansion lobes begin to come into contact and merge together: the cytoplasm of the archaeon completely absorbs the guest and the symbionts, showing a relative continuity between all its parts.

Although the properties of the membrane's members (mostly lipid molecules) favour the merger in the contact areas (Houslay and Stanley, 1982; Lipowsky and Sackmann, 1995), something like what we have already seen in the third phase relating to the fourth Drake parameter (passage from non-living to living), other molecules are necessary for the completion of this process. The proteins of the dynamin family, for example, are able to mediate the fission and merger of biological membranes, allowing, among other things, the formation or merger of vesicles (Praefcke and McMahon, 2004). Many bacteria possess protein counterparts of these eukaryotic molecules (Low and Löwe, 2006). Eukaryotic proteins are therefore likely to be derived from bacterial precursors after the assimilation of the genome of the symbionts by the host. The new protein intake and the cytoplasmic skeleton, already discussed above (third phase), also allow the onset of phagocytosis, the process that allows the ingestion of solid particles of a certain size (including cells smaller than the one that engulfs them). It is precisely the development of a complex protein system of bacterial origin which explains why the formation of the external membrane and the appearance of phagocytosis were produced only in the terminal phases of the eukaryotic onset process.

With regard to other processes such as cellular division or the acquisition of cell cilia, these evolved in parallel to those already described (or immediately after), integrating perfectly with the *inside-out* model (for details see Baum and Baum, 2014). Further contributions to the nuclear genome may also have been obtained thanks to the action of viruses (Forterre and Gaïa, 2018), acting in parallel with the phenomena discussed above. However, such a scenario does not alter the picture that we have outlined.

The time scheduled for the definitive transformation into eukaryotic cell is estimated at a few thousand years: *a probability of between 0.01 and 0.02 every 5000 years with a micro-catastrophe time limit of 100 000 years:*

Phase 8			
a_8	b_8	ΔT_8	ΔT_{08}
0.01	0.02	5000	100 000

At the end of the process detailed above, we can observe the onset of a new type of cell consisting of the symbiotic association between an archaeon that forms the nucleus (but without forgetting the bacterial genetic contributions and, possibly, those transferred virally) also providing the organism's cytoplasm, with bacteria that have become the mitochondria. Subsequently, the new organism begins to diversify, occupying those niches precluded to the prokaryotes (of which we spoke in the paragraph outlining the onset of the eukaryotic cell) that involve the increase in the size or adoption of complex behaviours. From 1 Gy, but probably also from earlier, it is certain that the eukaryotes acquired the ability to reproduce sexually (Butterfield, 2000; Gibson *et al.*, 2018); this implies an acceleration in the biological evolution of the group and an increased capacity in the production of biological innovations, as we will see in the sections below.

Evaluation of the probability of passing each stage

We thus obtained the 32 input values to be included in step 1 of the algorithm for calculating Maccone's lognormal statistical distribution (Tables 7–10). Figure 20 shows the lognormal distribution of the macro-interval process A.

Table 7. Fifth Drake – eukaryotes: the 32 values of the minimum and maximum a_j and b_j frequencies, of the time ΔT_j of observation and time ΔT_{0j} of micro-catastrophe, for each phase described in the previous paragraph

	a_j	b_j	ΔT_j	ΔT_{0j}
1 The evolution of an aerobic bacterium	0.4	0.6	2000	100 000
2 The guest–symbiont meeting	0.02	0.03	10 000	100 000
3 The formation of the pores and the escape of cytoplasmic extensions	0.04	0.06	5000	100 000
4 The ‘winding’ of the symbionts and the disappearance of the guest’s cell wall	0.01	0.02	2000	100 000
5 The penetration of symbionts in the cytoplasm	0.1	0.2	5000	100 000
6 The migration of DNA from the genome of the symbiont to that of the guest	0.5	0.7	10 000	100 000
7 The acquisition of the eukaryotic cytoplasmic membrane	0.001	0.002	2000	100 000
8 Incorporation into a single coating and phagocytosis	0.01	0.02	5000	100 000

Table 8. Fifth Drake – eukaryotes: evaluation of probability; the values redeemed in darker grey are the entry data (step 1), those in clearer grey the intermediate calculations (step 2 and 3)

	Step 1				Step 2			Step 3	
	Min in ΔT_j	Max in ΔT_j	Max ΔT_j	Max time ΔT_{0j}	Intervals in ΔT_{0j}	Min in ΔT_{0j}	Max in ΔT_{0j}	Comp. j aver.log μ_j	Comp. j var.log σ^2_j
	a_j	b_j	ΔT_j	ΔT_{0j}	m_j	A_j	B_j	μ_j	σ^2_j
1	0.400	0.600	2000	100 000	50	1.00	1.00	0.0000	0.0000
2	0.020	0.030	10 000	100 000	10	0.18	0.26	-1.5071	0.0108
3	0.040	0.060	5000	100 000	20	0.56	0.71	-0.4582	0.0048
4	0.010	0.020	2000	100 000	50	0.39	0.64	-0.6720	0.0187
5	0.100	0.200	5000	100 000	20	0.88	0.99	-0.0695	0.0012
6	0.500	0.700	10 000	100 000	10	1.00	1.00	-0.0005	0.0000
7	0.001	0.002	2000	100 000	50	0.05	0.10	-2.6487	0.0365
8	0.010	0.020	5000	100 000	20	0.18	0.33	-1.3723	0.0296

Table 9. Fifth Drake – eukaryotes: evaluation of probability; the values redeemed in darker grey are the entry data (step 4), those in clearer grey the intermediate calculations (step 3 and 4)

Step 3					Step 4	
Max time total process ΔT_0	Sum average logarithm μ	Sum variance logarithm σ^2	Average fraction tot process $\langle X_0 \rangle$	Deviation fraction tot process $\sigma(X_0)$	Max time tot process ΔT	Intervals number over time max tot process n
800 000	-6.73	0.10	1.26×10^{-3}	4.12×10^{-4}	500 000 000	625

Table 10. *Fifth Drake – eukaryotes: evaluation of probability; output data on time ΔT (long term): probability of development of the eukaryotic fees and its values with standard deviation f_{eA} and f_{eB} (step 4)*

Step 4		
Average probability Tot process	Maximum probability Tot process	Minimum probability Tot process
f_e	f_{eA}	f_{eB}
54.49%	28.92%	70.88%

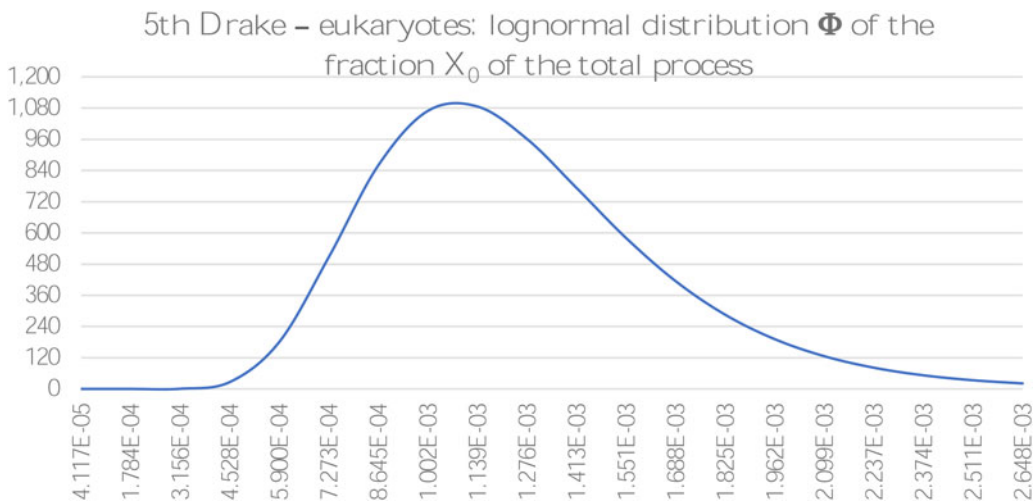


Figure 20. *Fifth Drake – eukaryotes: the lognormal distribution Φ of the process in the medium term ΔT_0 ; the average valour is 1.26×10^{-3} , the standard deviation is 4.12×10^{-4} .*

Macro-interval B

The second step; the birth of animals (the metazoa)

In the previous section, we described the onset of the eukaryotic cell as a symbiotic association between prokaryotes. The new body is no longer better or more advanced than the previous ones, but represents a higher level of complexity, obtained from the different distribution of activities in the different centres within the cell: for example, the mitochondrion is entrusted with energy production, since the organelle is free from other main tasks. So what will the next step be? It is possible to recognize the increase in complexity in the living kingdom by gradually considering the biological entities obtained from the sum of those of the previous level. To better explain this concept: we passed from level I, that of the prokaryotes, to level II (the eukaryotic cell), putting together elements of the previous level (prokaryote cells combined in symbiotic association). In the same way, it is possible to move on to a further level, the III, putting together various elements of the previous level, the II, and so on (Valli, 2020). This trend had already been strictly established by McShea (2001) and Rospars (2013). For us, therefore, the next step will be sought in the multicellular eukaryotes and, in particular, in the animal kingdom. In fact, in no other group or eukaryotic kingdom is it possible to meet ‘intelligent’ activities like those found in animals. The plants, evolutionarily speaking, although not at all lower than their cousins, have chosen different solutions, more suited to their existence as motionless beings, ‘rooted’ in the soil (Mancuso, 2017). The same applies to fungi and other groups of eukaryotes.

But how are animals characterized? When do their tracks appear among the fossils? The animals, better defined as metazoa, as we will call them later, have the following characteristics:

- (1) are multicellular eukaryotes, consisting of differentiated cells;
- (2) are heterotrophic (unable to make food, they must find it in the environment in which they live);
- (3) have a development that passes through very precise stages, including that of embryo;
- (4) are capable of moving, in at least one of their various stages of life;
- (5) finally, all the current animals, even the simplest, have collagen (Lecoitre and Le Guyader, 2017), a structural element that intervenes in numerous processes.

The oldest fossils of known metazoa date back to between 630 and 550 My (Xiao *et al.*, 1998; Porter, 2004; Hagadorn *et al.*, 2006). Meanwhile, between these dates and those of their first appearance (2.1 Gy), the eukaryotes differentiated (Javaux *et al.*, 2001) and had already made most of their evolutionary conquests: since just over 1 Gy multicellular organisms with sexuality exist (Butterfield *et al.*, 1990; Gibson *et al.*, 2018) and, shortly after, photosynthetic organisms appear which are the result of symbiotic associations between different eukaryotes (Butterfield, 2004). That is, the same process that led to the onset of the eukaryotic cell is repeated, but this time with eukaryotes as the protagonists. In more or less coeval layers (about 1 Gy about), fossils of multicellular organisms have been found with at least two different types. These eukaryotes, called *Bicellum brasieri* (Strother *et al.*, 2021) because of their morphological characteristics, are considered close to the group in which metazoan ancestors must be sought. The curious thing is that these are not marine organisms, but terrestrial ones.

But if multicellularity had already appeared before 1 Gy, why do metazoa manifest themselves only much later? First of all, multicellularity was achieved independently, and at different times, by at least 13 eukaryote lines (Rospars, 2013), if not more (Sebé-Pedrós *et al.*, 2017). This means that it is a property inherent in the condition of the eukaryotic cell.

But being multicellular does not suffice to make a lifeform an animal. Let us remember that one of the characteristics of modern metazoa is that of producing collagen. The formation of this molecule requires an appropriate content of O₂ in the environment (Saul, 2009). If we study the evolution of the rate of this gas, we discover new peaks and new *plateaux* for the values of O₂ greater than those relating to the GOE which we have already encountered in the previous paragraph. If there are values during the Paleozoic higher than those now (Krause *et al.*, 2018), in this context, we are interested in the interval including approximately between 0.8 and 0.5 Gy. In the indicated period, there is a further increase in O₂ compared to the values of the GOE (Lyons *et al.*, 2014). This event is indicated as the Neoproterozoic oxidation event (NOE): in correspondence there are values of O₂ comparable with today (Och and Shields-Zhou, 2012).

Among the periods in which the two different levels of O₂ occur, the eukaryotic cell emerged. Soon, eukaryotes become capable of carrying out photosynthesis thanks to the integration of a new endosymbiont, a cyanobacterium, which will turn into chloroplast (Cavalier-Smith, 2002). This new evolutionary step would be taken between 1.5 and 1.2 Gy (Yoon *et al.*, 2004; Gibson *et al.*, 2018). Subsequently, the new photosynthesizing organisms and those, in short, evolved from them (among these eukaryotes there are the distant precursors of land plants and their ancestors; Qiu, 2008) will contribute, together with the already present cyanobacteria, to the oxygenation of the environment and will be fundamental for reaching the new O₂ peak.

It is important to note the correspondence between the NOE (0.8–0.5 Gy) and the onset of metazoa (0.63–0.55 Gy) which makes us suppose that, in order to evolve, the animals needed high levels of O₂ in the environment. Why? Probably, because otherwise they would not have been able to synthesize collagen, which is necessary to give the extracellular matrix and future tissues the necessary mechanical resistance. The suspicion returns that the real deciding factor of the fifth Drake parameter is oxygen, whose net increase, first around 2.2 Gy and then 0.6 Gy, allowed further levels of complexity in living matter: the time constraint, linked to the oxygen rate, is (or seems to be) what imposes long times in the stabilization of a terrestrial planet.

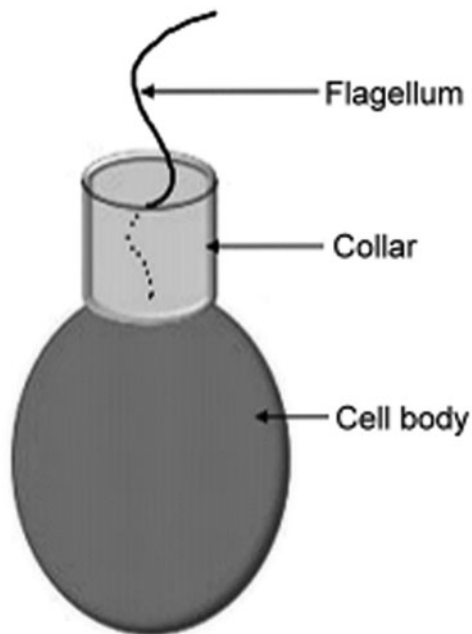


Figure 21. Fifth Drake – metazoa: choanoflagellate: the flagellum (dashed inside the collar), the collar and the cell body of the organism are indicated.

Let us now go in search of the ancestors of the metazoa and try to establish a model for their onset. The *Holozoa* constitute a clade of eukaryotes that includes metazoa (but which excludes mushrooms), in which various groups are made up of single-celled organisms (Lang *et al.*, 2002; Sebé-Pedrós *et al.*, 2017).

It is interesting to note that many animal proteins have homologues in eukaryotes of this group (Mikhailov *et al.*, 2009). However, the organisms closest to metazoa are those that make up the set of choanoflagellates (Lecoitre and Le Guyader, 2017), single-cell flagellates whose appendix is surrounded by a kind of collar (Fig. 21). These cells closely resemble choanocytes, cells with flagellum on the model of Porifera (i.e. sponges, simple sessile animals and filters, at the evolutionary base of the metazoa), which allows these organisms to convey nutritional particles to their oral cavities. No fossils of Choanoflagellata are known, but the experts, applying the molecular clock, think that the group may have appeared between 1.05 and 0.80 Gy, well before the onset of metazoa (Parfrey *et al.*, 2011).

Various models have been proposed to illustrate the onset of metazoa, but we will follow the *synzoospore theory*, initially proposed by Zakhvatkin (1949). Currently, the model is presented in the following form (Mikhailov *et al.*, 2009; Sebé-Pedrós *et al.*, 2017): an eukaryotic cell with a complex life cycle (including various morphological phases) produces zoospores which, instead of dispersing, unite to form the *synzoospore*. This, later, turns into a colony with differentiated cells, which reflect the different morphological phases of the initial eukaryotic cell.

The basic idea is that of starting from a cell that presents different morphologies according to its life cycle (a phenomenon that normally occurs in various single-celled eukaryotes, including the choanoflagellates; Mikhailov *et al.*, 2009), whose zoospores, cells derived from the zygote (Fig. 22(a)), come together to form the *synzoospore* (Fig. 22(b)). Subsequently, each cell develops following a ‘desynchronized’ growth with the others, in order to have a colony (‘proto-larva’) constituted of different cells (even if all have the same gene code, as they derive from the same zygote), which settles on the bottom for a sedentary trophic phase (Fig. 22(c)). Starting from this stage (and once the collagen that fills the cellular matrix and gives mechanical support to the whole has been produced) evolution

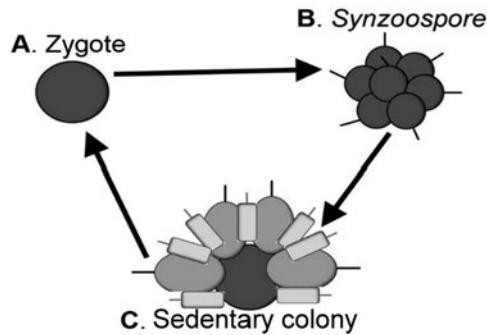


Figure 22. Fifth Drake – metazoa: synzoospore theory model: zygote (a) produces the zoospores that come together to form the synzoospore (b); the asynchronous development of the cells that compose it produces a colony consisting of different cells (although all with the same basic genetic code) that acquires sedentary costumes (c). To reproduce, the colony can generate a new zygote and the cycle starts again.

gets to work, allowing the differentiation of the embryonic states that follow *synzoospore*, in order to produce the first taxonomic divisions and differentiations within the group. Of course, in order to reproduce, the last stage generates a new zygote (Fig. 22: arrow between ‘C sedentary colony’ and ‘A zygote’) and the cycle can start again.

The onset of metazoa, phase by phase

The starting point; the choanoflagellates

These organisms constitute the group of eukaryotes closest to that of metazoa so it is therefore logical to seek there the progenitors of the animals. *Choanoflagellates* are all marine unicellular organisms that feed on bacteria (they are therefore heterotrophic). They reproduce asexually, but in at least one taxon several genes have been discovered to be referable to the process of meiosis, which is in turn linked to sexual reproduction (Carr *et al.*, 2010). It should also be remembered that the progenitor common to all current eukaryotes (LUCEA: *Last Universal Common Eukaryotic Ancestor*) is considered to be reproduced in a sexual way (Génermont, 2014).

Finally, we know that they share many genes with metazoa (Mikhailov *et al.*, 2009) and this allows us to consider them the best candidates in the search for the ancestors of this group.

The first phase; the acquisition of a complex life cycle

The base of the *synzoospore theory* is that morphological diversity was acquired before multicellularity, in the sense that the organism that unites to form the first animal already possessed a complex life cycle comprising various morphological phases, before associating and forming the ‘multicellular entity’. We know that this cycle exists in current *choanoflagellates* (Mikhailov *et al.*, 2009). But when did it evolve? Remembering that it is assumed that the group has existed since at least 800 My (Parfrey *et al.*, 2011) and that the first individual could probably reproduce sexually (in any case, their ancestors did), such a feature must have appeared relatively quickly. Among other things, the fact of having different morphological types available must be seen as an advantage, because it allows organisms to be able to cope with different environmental conditions.

Given these considerations, the complex life cycle in the group may have evolved over a few tens of thousands of years, with a high frequency in the medium term: *a probability of between 0.01 and 0.02 every 20 000 years with a micro-catastrophe time limit of 1 000 000 years:*

Phase 1			
a_1	b_1	ΔT_1	ΔT_{01}
0.01	0.02	20 000	1 000 000

The second phase; the aggregation of the zoospores and the formation of synzoospores

Why should zoospores aggregate rather than go their own way? At first glance, it would seem that the efficiency of the dispersion could be reduced, but in reality it is not so. In addition, the increase in size can serve to dissuade predators from attacking the colony (Mikhailov *et al.*, 2009). Not only that, but this also means being more competitive when initiating a sedentary phase. Such is, for example, the strategy used by many sponges (Ereskovsky, 2010). Let us not forget, then, that the colony (Fig. 22 (b)) is made up of cells that possess the same genetic heritage (as they derive from the same zygote) and this promotes intracellular communication and therefore the coordination of the whole (Mikhailov *et al.*, 2009), and that genes capable of producing cell membership substances are present within the Holozoa group (Sebé-Pedrós *et al.*, 2017). However, the aggregation of the zoospores produces the *synzoospore*, the mobile phase of the organism's life cycle. It (or its evolutionary development) can also represent the embryo of the future animal.

Knowing that there are *choanoflagellates* that can form colonies after cell division (Sebé-Pedrós *et al.*, 2017), this phase should also be able to be quickly completed (a thousand years): *a probability of between 0.02 and 0.03 every 15 000 years with a micro-catastrophe time limit of 1 000 000 years:*

Phase 2			
a_2	b_2	ΔT_2	ΔT_{02}
0.02	0.03	15 000	1 000 000

The third phase; the sedentary colony composed of differentiated cells

The asynchronous development of the various cells that make up the colony constitutes the third stage of the model. The cellular morphological diversification within the latter can be favoured by the division of tasks, which allows an increase in the efficiency of the organism (with what we have already seen regarding the onset of eukaryotes in mind).

Having started from a single cell characterized by a complex life cycle with different morphological stages, it should be possible to evolve a pool of genes that allows the asynchronous development of the cells, so that some present a morphology different from their neighbours (but which is however foreseen by the general development plan of the organism; Fig. 22(c)). It is not a question of 'inventing' anything except, perhaps, some regulation genes (Sebé-Pedrós *et al.*, 2017). Metazoa share with the most closest taxonomic groups not only structural genes but also others that regulate development (Mikhailov *et al.*, 2009), from which, possibly, those mentioned above may derive.

In this phase, the evolution of particular regulation genes is required, starting from the pool present in the ancestors of metazoa. Despite the apparent difficulty in its realization, the time necessary for its implementation cannot have been too long: *a probability of between 0.02 and 0.04 every 200 000 years with a micro-catastrophe time limit of 1 000 000 years:*

Phase 3			
a_3	b_3	ΔT_3	ΔT_{03}
0.02	0.04	200 000	1 000 000

The fourth phase; the production of collagen

From the previous phase, we already have a living being that we can define as a ‘metazoan’. It is a heterotrophic organism (the zygote feeds on bacteria and, possibly, other food particles, before dividing) whose zoospores come together to form the *synzoospore*, the mobile phase of the life cycle. We also have a sedentary phase with cell differentiation (but with cells that all possess the same genetic heritage). According to our definition, in order to achieve the complete transformation into a complex animal all that is required is collagen production. With regard to the onset of the embryo, the exact identification of this stage often depends on the animal group in question. We believe that the *synzoospore* or the first phases of existence of the sessile colony are a good representation. Finally, it should be pointed out that a phase relating to the production of collagen is not foreseen in the model discussed by Mikhailov *et al.* (2009) nor by that of Sebé-Pedrós *et al.* (2017). However, this synthesis is necessary to fill the spaces between one cell and another and to ensure mechanical resistance to the whole.

Apparently, collagen is absent in the unicellular eukaryotes (Saul, 2009), but this situation is not surprising, because in an organism consisting of a single cell, the cytoskeleton is sufficient to give rigidity to the whole. Alternatively, the single cell can choose other solutions, like that of having an exoskeleton (which appeared, however, only in more recent times). Collagen is therefore a substance that is produced *from scratch* by metazoa: there are no certain precursors among the unicellular ancestors.

However, for eukaryotic organisms that have a sexual reproduction and is made up of differentiated cells, it should not be a problem to devise a substance in a relatively short time that can fill the interstices between one cell and another and provide the desired mechanical resistance: *a probability of between 0.01 and 0.02 every 50 000 years with a micro-catastrophe time limit of 1 000 000 years:*

Phase 4			
a_4	b_4	ΔT_4	ΔT_{04}
0.01	0.02	50 000	1 000 000

Once all the basic characteristics, which contribute to the definition of metazoa, have been brought together, biological evolution can encourage the transformation of the cycle described above, developing some particular features which will lead to the differentiation of the main subgroups of the animals (Lecoitre and Le Guyader, 2017). Finally, let us remember the importance of the tenor of the O₂ in the environment: this and nothing else may have been the decisive factor that sanctioned the timing of the appearance of metazoa on our planet.

Evaluation of the probability of passing each stage

We thus obtained the 16 input values to be included in step 1 of the algorithm for calculating the Maccone lognormal statistical distribution (Tables 11–14). Figure 23 reports the lognormal distribution relating to the macro-interval B.

Macro-interval C

The ‘solution’ of the intelligence deduced by the definition of Kardašěv, centred on the energy or individual, and its birth within the metazoa (the case of Homo sapiens)

Biologists use various definitions of intelligence. For example, the one formulated by Pouydebat (2017) considers this faculty as an adaptive function that allows an individual to improve their behaviour according to the context; that is, like the ability to change behaviour in the face of new or complex situations. Clearly, though, if this definition is useful for describing the ‘intelligent’ behaviours of

Table 11. Fifth Drake metazoa: the 16 values of the minimum and maximum a_j and b_j frequencies, of the time ΔT_j of observation and time ΔT_{0j} of micro-catastrophe, for each phase described in the previous paragraph

	a_j	b_j	ΔT_j	ΔT_{0j}
1 The acquisition of a complex life cycle	0.01	0.02	20 000	100 000 000
2 The aggregation of the zoospores and the formation of the synzoospore	0.02	0.03	15 000	100 000 000
3 The sedentary colony composed of differentiated cells	0.02	0.04	200 000	100 000 000
4 The production of collagen	0.01	0.02	50 000	100 000 000

vertebrates and many other animals (the cephalopods, e.g.; Amodio *et al.*, 2019), a further element, inherent in the fifth paragraph of Drake, is required for our discussion of the phenomenon.

From a biological and social point of view, the definition of intelligence converges eventually on a single key concept: the onset of abstract thought, or the ability to put together different mental skills to build interpretative models of the environment and the actions to be carried out. This definition is wholly appropriate for any aspect taken into consideration except one: the extent of the energy that a species can manage through abstract thought itself. This is what we commonly call *technique* and that we can measure, in the very first instance, precisely in terms of energy, as power expressed for kilograms (kg) of body mass.

The new question we have to ask ourselves then is: what power, per kg of body mass, does a certain species express? From simple empirical calculations, we can derive that living beings, in particular animals, develop an average chemical-metabolic power of about 1 W kg^{-1} ; this power is sufficient to support the animal in its usual biological activities. However, for circa two centuries, the current human civilization, thanks to techniques including fossil fuels has had an estimated power of 10 W kg^{-1} which is a figure ten times larger. This energy surplus allows us to undertake previously impossible activities such as, for example, the construction of large structures like missiles or telescopes; in other words, it makes us one of the potential civilizations of the galaxy. If these techniques were not available to us, as they were not until two centuries ago, we could never hope to identify or be identified by other potential galactic civilizations if not by pure chance.

According to the Russian physicist Kardashev (1964), this parameter is essential for cataloguing the potentially communicating ETCs. For this purpose, he created a power scale on four main levels, later revised by Carl Sagan, according to the following recurring criterion (Sagan and Drake, 1975):

$W_1 = 10^{16} \text{ W}$ is all the solar power that an orbiting rocky planet receives in its habitability area (in Watts).

$W_2 = 10^{11} W_1$ is all the power radiated by the star.

$W_3 = 10^{11} W_2$ is all the power radiated by the galaxy.

$W_4 = 10^{11} W_3$ is all the power radiated by the observable universe.

As you can see, there is recurring growth between one level and the next equal to 10^{11} . This feature allows us to catalogue a civilization with the simple formula:

$$K = \frac{\log_{10}(W_{\text{ETC}}) - 5}{11},$$

where K is nothing more than the index at the base of the four levels W_1 , W_2 , W_3 and W_4 , while W_{ETC} is the power expressed by the civilization in its entirety.

On this scale, a K1 civilization is able to manage an amount of energy equal to that provided to the planet by its star, a K2 civilization manages all the energy of the star, a K3 civilization, all the energy of the galaxy and a civilization K4, all the energy of the universe. The current human civilization of about

Table 12. Fifth Drake metazoa: evaluation of probability; the values redeemed in darker grey are the entry data (step 1), those in clearer grey the intermediate calculations (step 2 and 3)

	Step 1				Step 2			Step 3	
	Probability min in ΔT_j	Probability max in ΔT_j	Observation time	Max time	Intervals in ΔT_{0j} phase j	Min in ΔT_{0j}	Max in ΔT_{0j}	Comp. j average log	Comp. j var log
	a_j	b_j	ΔT_j	ΔT_{0j}	m_j	A_j	B_j	μ_j	σ_j^2
1	0.01	0.02	20 000	1 000 000	50	0.39	0.64	-0.6720	0.0187
2	0.02	0.03	15 000	1 000 000	67	0.74	0.87	-0.2169	0.0021
3	0.02	0.04	200 000	1 000 000	5	0.10	0.18	-1.9807	0.0348
4	0.01	0.02	50 000	1 000 000	20	0.18	0.33	-1.3723	0.0296

Table 13. Fifth Drake metazoa: evaluation of probability; the values redeemed in darker grey are the entry data (step 4), those in clearer grey the intermediate calculations (step 3 and 4)

Step 3					Step 4	
Max time total process	Sum average logarithm	Sum variance logarithm	Average fraction tot process	Deviation fraction tot process	Max time tot process	Intervals number over time max tot process
ΔT_0	μ	σ^2	$\langle X_0 \rangle$	$\sigma(X_0)$	ΔT	n
4 000 000	-4.24	0.09	1.50×10^{-2}	4.48×10^{-3}	500 000 000	125

Table 14. Fifth Drake metazoa: evaluation of probability; output data on time ΔT (long term): probability of development of f_m metazoa and its values with standard deviation f_{mA} and f_{mB} (step 4)

Step 4		
Probability tot process	Maximum probability tot process	Minimum probability tot process
f_m	f_{mA}	f_{mB}
85%	60%	94%

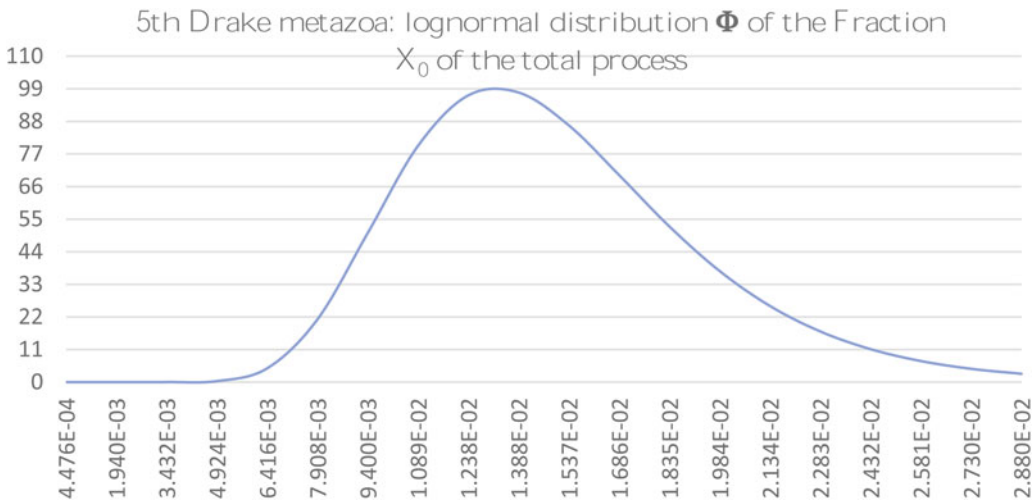


Figure 23. Fifth Drake metazoa: the lognormal distribution Φ of the process in the medium term ΔT_0 : the average valour is 1.50×10^{-2} , the standard deviation is 4.48×10^{-3} .

10 000 000 000 individuals of 100 kg each with a power of about 10 W kg^{-1} , has a total power of 10^{13} W which, in the Kardashev scale, is equivalent to a K_{humanity} equal to:

$$K_{\text{humanity}} = \frac{\log_{10}(10^{13}) - 5}{11} \cong 0.7.$$

Therefore, given our very basic technological level, an animal species must have a Kardašev level of at least $K = 0.7$ in order to be recognized as intelligent by other civilizations, and it will be this value of $K = 0.7$ that we will have to keep in mind later when we talk about ETC.

Given the characteristics indicated above, the intelligence objective that we will take as a reference is the one achieved by our species $K = 0.7$. Thus, rather than following a generic model, as in previous cases, below we will illustrate the main stages that lead to man's evolution.

We should also remind you that the various phases that characterized the evolution of land life have been 'cadenced' by mass extinctions, episodes in which a drastic and rapid (in geological terms) decrease in the biodiversity of our planet occurred. These extinctions followed each other more or less regular (in the last 250 My, extinction cycles – of varying intensity – would occur with a regularity of about 26 My; Raup, 1992). It should be emphasized, however, that extinctions do not have purely negative effects. By eliminating or reducing certain taxonomic groups, they allow others, which had remained in the shadow of dominant organisms, a chance and to realize new evolutionary solutions. If there had been no extinction at the end of the Triassic (at about 201 My), the dinosaurs would not have become the dominant life forms on land, nor would we enjoy birds today. Without the Cretaceous/Tertiary crisis (K/T crisis), which concluded the Mesozoic (approximately 66 My), mammals would have remained in the shadow of the dinosaurs and would not have reached their current sizes. And we would not exist!

The birth of intelligence, phase by phase

The starting point; the fauna of Ediacara

The term 'Ediacaran biota' indicates those associations of organisms found in the sedimentary states between 575 and 541 My. These faunas are made up of unusual animals, upon whose lifestyles rivers of ink have been and continue to be spilled (see e.g. Seilacher, 1984; McMenamin, 1998; Retallack, 2013; Xiao, 2013). However, alongside these, traces in the sediments suggest the existence of worms or other bilateral organisms (animals with bilateral symmetry and axis of antero-posterior polarity) or their ancestors. It is in this large group of metazoa that intelligent life forms evolve according to the definitions shown in the previous section.

The first phase; the increase in the size of metazoa and the acquisition of nervous and vascular systems

Although some exceptions can be found, one of the main laws found in the world of animals is that of the increase in body mass over time (Rospar, 2013). The Ediacara fauna was followed by the explosion of Cambrian life (a geological period between 541 and 485 My), a phenomenon that, in reality, lasted a few tens of millions of years and which continued in the following period, the Ordovician (485–444 My; Lefebvre, 2022). Practically, all current phyla (the different anatomical plans on which the metazoa are built) appeared, plus others which are today extinct. Mineral tissues begin to spread through the animal kingdom and the first predators evolve (Gould, 1989; Erwin and Valentine, 2013). Not only that, but during the Cambrian the dimensions of animals begin to increase dramatically: some exceed a half meter in length. Starting from the Lower Ordovician, there are even fossil cephalopods whose shells are over a meter in size (Klug *et al.*, 2015).

What produces this explosion of organisms with anatomical systems and complex organs, many but not all of which also have limestone exoskeletons that facilitate conservation in the sediments? Various solutions have been proposed: from the appearance of eyes (Parker, 1998) to other causes intrinsic in animal physiology or linked to environmental mutations (Marshall, 2006). Certainly, the cause of all these changes was not unique; various factors must have intervened. Among these factors, certainly, some appropriate geochemical conditions were produced in the oceans (Maloof *et al.*, 2010). Among other things, an increasing contribution of chemical elements, due to the alteration of the terrestrial rocks, was conveyed to the seas, favouring, in them the development of plant and animal life (Selosse, 2021).

The developments indicated in this section (increase in size, acquisition of nervous and vascular systems) are produced in different phyla animals at different times, including a few million years in each file line: *a probability of between 0.02 and 0.04 every 500 000 years with a micro-catastrophe time limit of 10 000 000 years:*

Phase 1			
a_1	b_1	ΔT_1	ΔT_{01}
0.02	0.04	500 000	10 000 000

The second phase; the development of limbs

In many different phyla, once they have reached a certain size and, above all, a certain complexity, various organisms developed ‘limbs’, that is, mobile appendices capable of performing various functions. Within the group of arthropods (whose name means ‘articulated legs’) which groups insects, arachnids, crustaceans and myriapodes, not only do the great majority of taxa have segmented limbs to move and perform other activities, but many, in particular insects, are particularly equipped with mandibular elements capable of articulating together (Lecoitre and Le Guyader, 2017), which make them suited to performing the most diverse functions.

Among the *chordates*, the large majority of vertebrates developed symmetrical appendages such as the rooted fins of fish or articulated members, increasingly complex and developed in the distal sector (the one farthest from the body), in the tetrapod group (vertebrates whose limbs are provided of an articulation with the bone belt – pelvic or scapular – corresponding) and in their ancestors. In the tetrapods, in fact, fingers evolved not from the spines of the fins of the actinopterygii fish, but were real evolutionary innovations (Steyer, 2009, and bibliography mentioned). It is thought that the oldest ancestors of the tetrapods (organisms still equipped with fins, although strengthened by an internal axial skeleton) had already made their appearance towards the beginning of the Devonian (Zhao *et al.*, 2021), towards 410 My, while the first symmetrical limbs had probably already appeared in the vertebrates, from the lower Silurian (Janvier, 1996), more than 430 My ago.

Finally, it should not be forgotten that, in the phylum of the molluscs, the cephalopods, starting from the front of the ‘foot’, developed tentacles – modified and prehensile lobes (Lecoitre and Le Guyader, 2017). These are ‘arms’ capable of performing even very complicated functions. The tentacles appeared with the first cephalopods, in the final part of the Cambrian (Staaf, 2020), more than 500 My ago.

As can be seen from the examples shown above, several groups of metazoa developed limbs mainly for locomotion but which, later, further evolved to adapt to the needs of the organisms that possess them. As in the previous phase, the various phyla developed their limbs at different times, however, within each group, they always did so after having acquired a certain complexity and nervous and vascular systems convenient: *a probability of between 0.01 and 0.02 every 500 000 years with a micro-catastrophe time limit of 10 000 000 years:*

Phase 2			
A_2	B_2	ΔT_1	ΔT_{02}
0.01	0.02	500 000	10 000 000

The third phase; the conquest of dry land

While not wishing to underplay the intelligence of the cetaceans and cephalopods, the only organisms that have developed a technological level like the one we seek evolved on dry land. We do not know if it would have been possible to obtain civilizations comparable to the current ones in an aquatic

environment, but we continue to follow the process that leads us to our species. The next step, therefore, is what we earned by moving onto dry land, the two previous phases being fully completed at sea.

The testimonies of terrestrial activities that are recorded during the first phase of the primary era (541–252 My) are rare if not unique. These are the footprints of arthropods that had moved onto dry land, though it is unknown whether they did this to go from one pool of water to another or for some other reason (Macnaughton *et al.*, 2002).

What prevented the animals from establishing themselves permanently on the emerged lands does not seem to have been, as was once believed, the lack of an adequate atmosphere capable of protecting organisms from UV rays. We saw in the previous section that, after the NOE, the level of O₂ in the atmosphere was more or less of the same order of magnitude as it is today (Och and Shields-Zhou, 2012). It would not have been difficult for an arthropod, protected by an exoskeleton, to walk on the mainland in the light of the sun. In reality, the problem seems to have been another: on the mainland, the environments were practically sterile and without vegetation. After all, it is always plants that initially occupy a new environment, creating the conditions for colonization by animals.

Although there are already traces of spores attributed to terrestrial plants in the middle Ordovician, since around 475 My (Wellman *et al.*, 2003), the first vegetable fossil remains of a certain dimension are only found much later, in the Silurian (444–416 My). In an extraordinary deposit uncovered near the village of Rhynie, in Scotland, and dated to 410 My approximately (Garwood *et al.*, 2020), there are clues that allow us to understand why the conquest of the emerged lands does not go back directly to the time of the NOE. In fact, among the exceptional remains in Rhynie, vegetable roots have been found that feature symbiont mushrooms, as occurs in the large majority of current terrestrial plants (Taylor *et al.*, 2009; Bidartondo *et al.*, 2011).

What determined the colonization time of the plants was not therefore the atmospheric conditions, but those required for the establishment of a plant–fungus symbiosis. This is in fact necessary to allow plants not only to develop a radical support system but above all to allow them to obtain (mainly thanks to fungal hyphae) water and mineral elements from the ground. That is, it was necessary to wait for the plants to meet the ‘good’ mushrooms to create the symbiosis capable of making them able to live on the emerged lands (Selosse, 2017).

Once the plants were established on the continents, the metazoa arrived. Fossil remains of various terrestrial arthropods (Garwood *et al.*, 2020) were found in Rhynie. In any case, at the end of the Devonian period (419–359 My), the plants were solidly in place on the continents: many stretches of coast were occupied by forests made up of real ‘trees’, even 30 m high (Steyer, 2009).

It is in this context that there was the appearance of the first, in which the limbs did not yet have the ability to support the animal during its movements outside the water. Rather, they served as specialized ‘paddles’ for movements in water between the florid aquatic vegetation of coastal environments (Steyer, 2009). However, even before the end of the Devonian, some traces testify to the existence of tetrapods capable of moving, at least temporarily, on dry land (Schoch, 2014).

Between the carboniferous (359–299 My) and the permian (299–252 My), the molluscs conquered the continents (Mordan and Wade, 2008; Stworzewicz *et al.*, 2009), even if, at least at the beginning, they were probably confined to humid environments. Note, however, that despite the fact that the species of terrestrial molluscs (freshwater or mainland) are currently more numerous than those living in the seas and oceans, the cephalopods (which group molluscs endowed with intelligence) constitute a whole that has always been *exclusively* marine. Having said that, strictly intelligent terrestrial animals are limited to vertebrates, so we will limit ourselves, in the following phases, to following the evolution of the tetrapods.

Although also in this case the various phyla conquer the continents independently, the colonization of each animal group must necessarily wait for that of the plants. Before the end of the primary era, various metazoa phyla had established themselves on dry land: *a probability of between 0.02 and 0.05 every 500 000 years with a micro-catastrophe time limit of 10 000 000 years:*

Phase 3			
A_3	i_3	ΔT_3	ΔT_{03}
0.02	0.05	500 000	10 000 000

The fourth phase; the differentiation of land animals

Knowing how to exploit the resources of the continents does not mean having completely left the liquid environment. In fact, most modern amphibians depend on the proximity of ponds and pools of water for reproduction. Furthermore, their skin needs a certain amount of humidity for them to survive: only rare forms have been able to colonize arid environments (even if some Australian frogs have succeeded, thanks to precautions to retain water, living underground and using the rare downpours for reproduction; Barker *et al.*, 1996).

Although the ancient terrestrial tetrapods have differentiated from a morphological and taxonomic point of view (in this regard, see Steyer, 2009; Schoch, 2014), the great diversification of the vertebrates on the continents is produced only when these organisms definitively abandon the liquid environment for reproduction. It is therefore necessary to wait for the onset of *amniotes*, a group that includes all reptiles, birds and modern and fossil mammals. What differentiates the amniotes from the other tetrapods? The key to their success is the amniotic egg (Fig. 24), an evolutionary innovation which means they no longer need a liquid environment for reproduction. Or better: they transfer this environment within the egg itself. The embryo, in fact, is immersed in the amniotic fluid, delimited by amnion which, being waterproof, recreates the aquatic environment necessary for development within it. The chorion, the outermost layer, is permeable to gases, allowing the embryo to breathe and gaseous exchange, assisted by the allantoid. As it is very difficult to recognize a fossil egg as amniotic, discrimination is made from the bone remains. The oldest known amniotes are *Hylonomys lyelli* (Dawson, 1860) and *Protoclepsydrops haplous* (Carroll, 1964), both found in Canadian carboniferous sediments from about 310 My ago (Van Tuinen and Hadly, 2004). Starting from these ‘precursors’, the amniotes became capable of colonizing all terrestrial environments, even the most arid. They could thus move away from the coasts and swampy areas to colonize even the most isolated parts of the continents. The

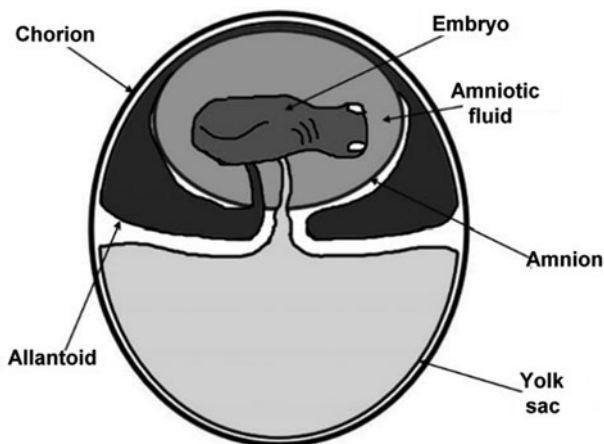


Figure 24. *Fifth Drake ETC: scheme of the amniotic egg: the embryo bathes in the amniotic fluid, delimited by the amnion, impermeable; the yolk sac contains the nutrients for the embryo; the allantois is the embryonic annex that contains waste and has a role in respiration; the chorion is the outermost layer of the egg (figure modified from Steyer, 2009).*

amniotes, therefore, quickly diversified (Benton, 2014): from the base of the Permian, we find ecosystems with ‘reptiles’ that occupied various ecological niches: herbivorous, carnivorous and intermediate. The dimensions increased further (but this also applied to amphibious tetrapods, which remained linked to the liquid environment, see e.g. Steyer, 2009).

Starting from the apparition of the amniotic egg, a few million years are necessary for the differentiation of the terrestrial vertebrates and the occupation of the niches present in the new environments: a probability of between 0.5 and 1 every 500 000 years with a micro-catastrophe time limit of 10 000 000 years:

Phase 4			
A_4	B_4	ΔT_4	ΔT_{04}
0.5	1	500 000	10 000 000

The fifth phase; the upright posture and manual skills

The next stage, in reality, consists of two phases that can be fulfilled independently: the acquisition of upright posture and that of manual skills. Only in our species they coexist.

The acquisition of upright posture among modern mammals is typical of man and also of kangaroos. However, among the current primates, we are the only ones to resort to the bipedal posture to walk (although gibbons know how to march erect, using open arms for balance; Fleagle, 2013). However, it seems that, in the past at least another primate walked in a bipedal posture, even if it was thought to be more similar to that of the gibbons than to ours (Rook *et al.*, 1999; Moyà-Solà *et al.*, 2005; Hammond *et al.*, 2020, but see also Susman, 2005). Despite this exception, the bipedal posture is the characteristic that allows you to place a fossil hominid in the restricted group from which our species has evolved (Fleagle, 2013).

In any case, even before the mammals achieved upright posture, it had been achieved by the dinosaurs. In fact, this peculiarity contributes to characterizing this group of peculiar reptiles (Benton, 2014) and has been inherited by their descendants, birds. All birds, regardless of their degree of intelligence, have a bipedal stature.

It is interesting to note that the American palaeontologist Dale A. Russell speculated on a possible descendant of the dinosaurs, if they had not become extinct during the K/T crisis (remembering that, without the extinction of the dinosaurs, the mammals would have remained confined to their niche). The scientist hypothesized that a representative of the Troodontidae family (=Stenonychosauridae) could have evolved into a ‘dinosauroid’ (Russell and Séguin, 1982; Naish and Tattersdill, 2021), an intelligent humanoid being derived from the great Mesozoic reptiles. Of course, its form, which would have been similar to ours, was guided by the anthropomorphism typical of our species. Nonetheless, the American palaeontologist proposed the evolution of a life form endowed with intelligence comparable to ours starting from a different group of tetrapods. What was special about this family of dinosaurs compared to the others that led to him choosing it as the cradle of the dinosauroid? Two characteristics above all: a relatively high encephalization coefficient compared to its contemporaries and a front limb whose fingers had a certain degree of opposability. We therefore find the two skills that are our characteristic prerogative: the upright posture station and manual dexterity.

The latter capacity is typical of animals that must grasp objects, such as arboreal mammals, the most characteristic of which are undoubtedly the primates. These are equipped with a series of adaptations to live in the trees (stereoscopic vision, opposable thumbs, etc.; Kemp, 2005; Benton, 2014). The oldest representative of the group, known by a partially preserved skeleton, was dated to about 55 My, about 10 years after the extinction of the dinosaurs.

The opposable thumb is a typical feature of the primates (Kemp, 2005), but no monkey is capable of touching the fingertip of the fingers of the same hand with its thumb. Although it is believed that at least some australopithecines (the ‘robust’ ones, of the genus *Paranthropus*, Broom, 1938) had an anatomical hand conformation capable of producing simple stone tools (Susman, 1991; McHenry and

Coffing, 2000), human manual skills were evolved well beyond the possibilities of the primitive hominids and our ancestors.

This phase brings us to the threshold of our kind, a jump of a few hundred millions of years compared to the previous phase. But this is justified by the occupation of two characters which, although they can develop independently, must contribute together (and achieve a relatively sophisticated evolutionary level) to give impulse to evolution towards an intelligence like that of humans: *a probability of between 0.005 and 0.01 every 500 000 years with a micro-catastrophe time limit of 10 000 000 years:*

Phase 5			
A_5	B_5	ΔT_5	ΔT_{05}
0.005	0.01	500 000	10 000 000

The sixth phase; the change of diet and the growth of the brain

The brain has a high energy cost and needs a large protein contribution (Rospars, 2013). Its development and increase required the contribution of precious resources to allow it to develop adequately. For this reason, the anthropologist Stanford (2001) hypothesized that for human evolution a change of diet from herbivorous/omnivorous, typical of the australopithecines, to a more purely carnivorous one was important.

The abundance of animal carcasses killed by the multiple African plio/pleistocenic carnivores and the herd habits (which would allow them to contend for and win prey from predatory mammals) would have allowed a population of hominids to undertake a carnivorous diet.

The large protein intake thus obtained would have favoured an increase in the size of the brain compared to that of the other primate populations. Stanford's proposal aroused various reactions but, apart from the correctness or otherwise of the hypothesis, if the first representatives of humankind are compared with their Australopithecian precursors, there are important morphological changes, such as a relative reduction of the chewing system (a shift from a diet containing more fibres to one poorer in these foods) as well as an increase in the cerebral volume (McHenry and Coffing, 2000).

Even without hypothesizing what the exact diet of our ancestors was, with the data in hand it is possible to find a correlation between a change of diet and the increase in the brain that occurred towards the beginning of the Pleistocene, between 2.5 and 1.5 My. The times in which it was achieved are relatively short, less than 1 My: *a probability of between 0.05 and 0.1 every 500 000 years with a micro-catastrophe limit time 10 000 000 years:*

Phase 6			
A_6	B_6	ΔT_6	ΔT_{06}
0.05	0.1	500 000	10 000 000

The seventh phase; the organization of the brain for abstract thinking

The next phase consists of the ability to conceive abstract thoughts. Although a number of animals possess an ability for abstraction, for example, the ability to manage different numbers and quantities of objects (Dehaene *et al.*, 1998), human possibilities go far beyond this. The skills related to cognitive functions, therefore to calculation, to abstract thought and also to language, are linked to the development of the frontal lobes (Fig. 25) and to the circumstances of these cerebral regions (Grimaud-Hervé, 1997). If, thanks to appropriate endocranial casts, one evaluates the evolution of the human brain, starting from our australopithecoid ancestors, it is observed that, starting from *Homo erectus* (Dubois, 1893) the organ significantly developed in the aforementioned regions. In particular, in modern man, cerebral

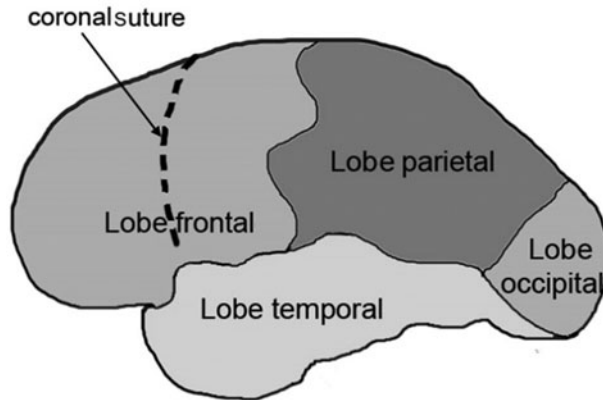


Figure 25. Fifth Drake ETC: simplified scheme showing the human brain, with the various brain lobes indicated.

evolution is manifested above all in the form of an enlargement in correspondence with the cranial coronal suture (Fig. 25).

The increase in endocranial capacity was obtained in a different way in Neanderthal man, *Homo neanderthalensis* (King, 1864), and in modern man, *Homo sapiens* (Linnaeus, 1758). If we compare the skulls of these two species, we note in fact that the skull of the Sapiens is more ‘round’ and taller than the other, which, in turn, is more elongated.

The brain proportions aside, what would have been the first manifestations of human abstract thought? It is difficult to answer this question. However, it is possible that they already manifested themselves in *H. erectus*. A particular artefact, found on the island of Java, is in fact attributed to this species: it is a mollusc shell decorated with a ‘zigzag’ pattern (Tattersall, 2016), made without any apparent practical purpose. No symbolic activity has yet been associated with Neanderthals, although, at a brain level, all the conditions necessary to achieve this would seem to have been brought together. Maybe it was just a matter of time.

Although current abstract abilities go far beyond the decorated shell mentioned above, it is very possible that, starting from the onset of *H. erectus*, certain human populations acquired the ability of abstract thought. In this case, a few tens of thousands of years would have been enough for his statement: *a probability of between 0.5 and 0.9 every 500 000 years with a micro-catastrophe time limit of 10 000 000 years:*

Phase 7			
A_7	B_7	ΔT_7	ΔT_{07}
0.5	0.9	500 000	10 000 000

The eighth phase; the birth of articulated language and technique

One of the characteristics that distinguishes us from all other animals is undoubtedly articulated language. In fact, although the great apes are capable of learning rudimentary sign language to communicate with their guardians (Tattersall, 2016), they are unable, due to their anatomy, to express themselves with the range of sound and articulations that we have.

The morphological characteristics that permit this are linked to the morphology of the larynx and to that of the hyoid bone, located at the base of the tongue, between jaw and thyroid cartilage of the larynx itself (Fig. 26).

It is not easy to reconstruct exactly the morphology of the anatomical region linked to human vocal capabilities starting from disarticulated bone remains. However, the hyoid bone of a fossil hominid can be

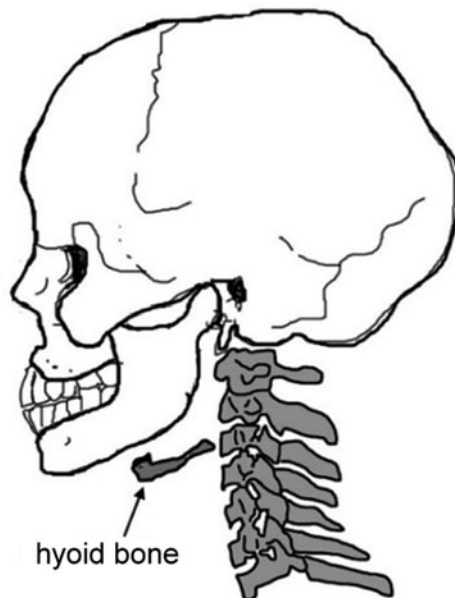


Figure 26. *Fifth Drake ETC: simplified scheme of the neck and human skull to represent the position of the hyoid bone; this bone has been coloured in grey, as well as the cervical vertebrae, in order to facilitate their identification.*

found, studied and compared with ours. In particular, one belonging to *H. erectus* (Capasso *et al.*, 2008) was found. Its morphology is very reminiscent of that of a modern bone, although some minor differences suggest a more limited modulation of the vocal tract which probably limited the use of articulated language. A hyoid bone of Neanderthal (Arensburg *et al.*, 1989) is also known, even more similar to that of a modern man than that of *H. erectus*. The fossil evidence therefore suggests that the ability to produce complex vocalizations existed at least from the common ancestor between Neanderthal and modern man (de Boer, 2017), even if this does not mean that they were already able to communicate like us. As regards the technique, we know that *H. neanderthalensis* was capable of refined stoneworking (Tattersall, 2016), not less skilled than that of contemporary *H. sapiens*, although the latter also expressed themselves in other ways, including rock painting. Of course, we are still very distant from modern technical skills.

However, articulated language was necessary to explain and transmit (first orally and then in writing) the technical instructions for the production of increasingly complicated objects and, therefore, to make technological progress from prehistoric to current levels. It was also necessary to be able to express abstract thought: *a probability of between 0.4 and 0.8 every 500 000 years with a micro-catastrophe time limit of 10 000 000 years:*

Phase 8			
A_8	B_8	ΔT_8	ΔT_{08}
0.4	0.8	500 000	10 000 000

At the end of these final eight phases, we have reached the onset of *H. sapiens*, the only species possessing the intelligence described at the end of the initial section of the macro-interval C. Thanks to its characteristics, our species has acquired a technical capacity such as to be able to send messages beyond our Solar System. Of course, this did not happen in one day; it took a couple of hundreds of thousands of years.

Table 15. Fifth Drake ETC: the 32 values of the minimum and maximum a_j and b_j frequencies, of the time ΔT_j of observation and time ΔT_{0j} of micro-catastrophe corporate, for each phase described in the previous paragraph

		a_j	b_j	ΔT_j	ΔT_{0j}
1	Increased metazoa size (nervous and vascular system)	0.02	0.04	500 000	10 000 000
2	Limb development	0.01	0.02	500 000	10 000 000
3	Conquers mainland	0.02	0.05	500 000	10 000 000
4	Differentiation of land animals	0.50	1.00	500 000	10 000 000
5	Station erected and manual skills	0.005	0.01	500 000	10 000 000
6	Diet and growth change	0.05	0.10	500 000	10 000 000
7	Organization of the brain on abstract thinking	0.50	0.90	500 000	10 000 000
8	Birth of articulated language and technique	0.40	0.80	500 000	10 000 000

Table 16. Fifth Drake ETC: evaluation of probability; the values requested in darker grey are the entry data (pass 1); those in clearer grey the intermediate calculations (step 2 and 3)

	Step 1				Step 2			Step 3	
	Min in	Max in			Intervals in	Min in	Max in	Comp. j	Comp. j
	ΔT_j	ΔT_j	ΔT_j	Max time	ΔT_{0j}	ΔT_{0j}	ΔT_{0j}	aver.log	var.log
	a_j	b_j	ΔT_j	ΔT_{0j}	m_j	A_j	B_j	μ_j	σ^2_j
1	0.02	0.04	500 000	10 000 000	20	0.33	0.56	-0.8202	0.0221
2	0.01	0.02	500 000	10 000 000	20	0.18	0.33	-1.3723	0.0296
3	0.02	0.05	500 000	10 000 000	20	0.33	0.64	-0.7369	0.0353
4	0.50	1.00	500 000	10 000 000	20	1.00	1.00	0.0000	0.0000
5	0.005	0.01	500 000	10 000 000	20	0.10	0.18	-1.9919	0.0341
6	0.05	0.10	500 000	10 000 000	20	0.64	0.88	-0.2786	0.0082
7	0.50	0.90	500 000	10 000 000	20	1.00	1.00	0.0000	0.0000
8	0.40	0.80	500 000	10 000 000	20	1.00	1.00	0.0000	0.0000

Table 17. Fifth Drake ETC: evaluation of probability; the values requested in darker grey are the entry data (step 4); those in clearer grey the intermediate calculations (step 3 and 4)

Step 3					Step 4	
Time total process	Sum med. log.	Sum var. log.	Average tot process	Deviation tot process	Max time tot process	Intervals number over time max
ΔT_0	μ	σ^2	$\langle X_0 \rangle$	$\sigma(X_0)$	ΔT	n
80 000 000	-5.20	0.13	5.89×10^{-3}	2.19×10^{-3}	500 000 000	6

Evaluation of the probability of passing each stage

We thus obtained the 32 input values to be included in step 1 of the algorithm of calculating the Maccone lognormal statistical distribution (Tables 15–18). Figure 27 shows the lognormal distribution relating to the macro-interval C.

Table 18. *Fifth Drake ETC: evaluation of probability; output data on time ΔT (long term): probability of Homo f_h development and its values with standard deviation f_{hA} and f_{hB} (step 4)*

Step 4		
Tot process probability f_h	Maximum probability tot process f_{hA}	Minimum probability tot process f_{hB}
3.5%	1.3%	5.7%

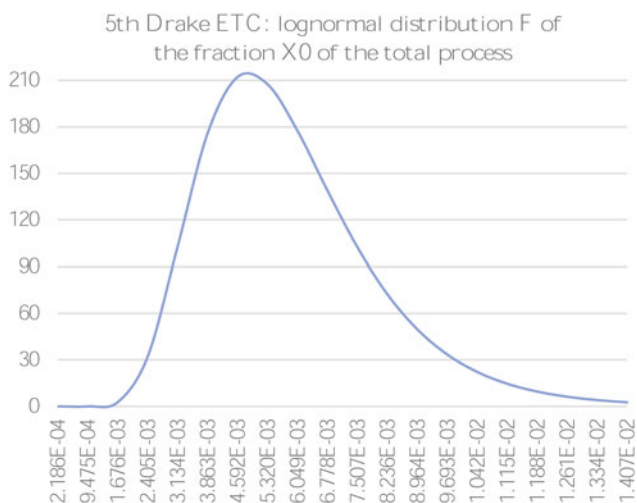


Figure 27. *Fifth Drake ETC: the lognormal distribution Φ of the process in the medium term ΔT_0 : the average valour is 5.89×10^{-3} , the standard deviation is 2.19×10^{-3} .*

Evaluation of the total probability: Drake’s fifth parameter

Having defined the chances of the three macro-intervals A, B and C necessary to describe more accurately the probability of intelligent life starting from bacteria, we now go to combine them in a new total lognormal which will represent the fifth parameter of Drake.

We should clarify that the application of the Maccone lognormal method for only three parameters cannot be rigorous because it does not respect the conditions of the central limit theorem which ensures that a sufficiently high number of random variables converge towards a *normal* (in our case *lognormal*) distribution; however, since in this context we are looking only for the order of magnitude of the Drake parameters, we consider this method amply justified.

We obtained six input values to be included in step 2 of the algorithm of calculating the lognormal statistical distribution of Maccone (Tables 19–22). Note that for the macro-intervals, step 1 is completely skipped because we have directly the final frequencies A_j and B_j of step 2. Furthermore, the period of reference for the realization of the entire process is the sum of the three macro-catastrophe times of the macro-intervals A, B and C:

$$0.5 \text{ Gy} \cdot 3 = 1.5 \text{ Gy.}$$

Figure 28 shows the lognormal distribution of the entire process A, B and C.

Table 19. Fifth Drake total: the six values of the A_j and B_j frequencies minimal and maximum for each phase

		A_j	B_j
A	Eukaryotes	0.29	0.71
B	Metazoa	0.60	0.94
C	Homo	0.01	0.06

Table 20. Fifth Drake total: evaluation of probability; the tabulated values are the intermediate calculations (step 2 and 3)

	Step 2		Step 3	
	Min in ΔT_{0j} A_j	Max in ΔT_{0j} B_j	Comp. j average log μ_j	Comp. j var log σ_j^2
1	0.29	0.71	-0.7264	0.0644
2	0.60	0.94	-0.2692	0.0172
3	0.01	0.06	-3.4425	0.1700

Table 21. Fifth Drake total: evaluation of probability; the tabulated values are the intermediate calculations (step 3)

Step 3			
Sum average logarithm μ	Sum variance logarithm σ^2	Average fraction tot process $\langle X_0 \rangle$	Deviation fraction tot process σX_0
-4.44	0.25	1.34×10^{-2}	7.17×10^{-3}

Table 22. Fifth Drake total: evaluation of probability; output data on time ΔT (long term): probability of development of intelligent life f_i and its values with standard deviation f_{iA} and f_{iB} (step 4)

Step 4		
Probability tot process f_i	Maximum probability f_{iA}	Minimum probability f_{iB}
1.3%	0.6%	2.1%

Drake 5	
f_i min 6.0×10^{-3}	f_i max 2.1×10^{-2}

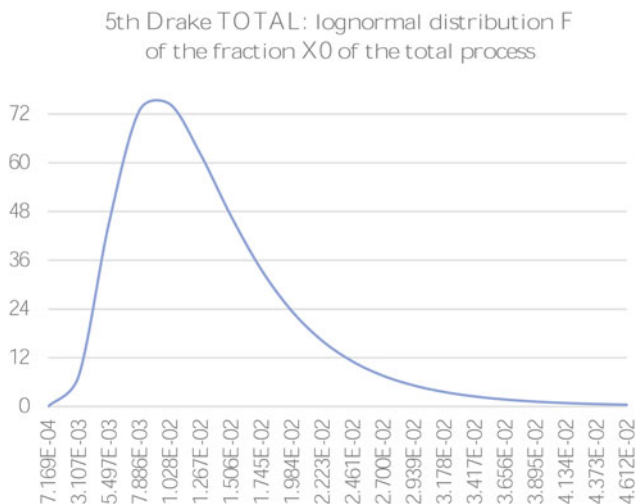


Figure 28. Fifth Drake total: the lognormal distribution Φ of the process in the medium term ΔT_0 : the average valour is 1.34×10^{-2} , the standard deviation is 7.17×10^{-3} .

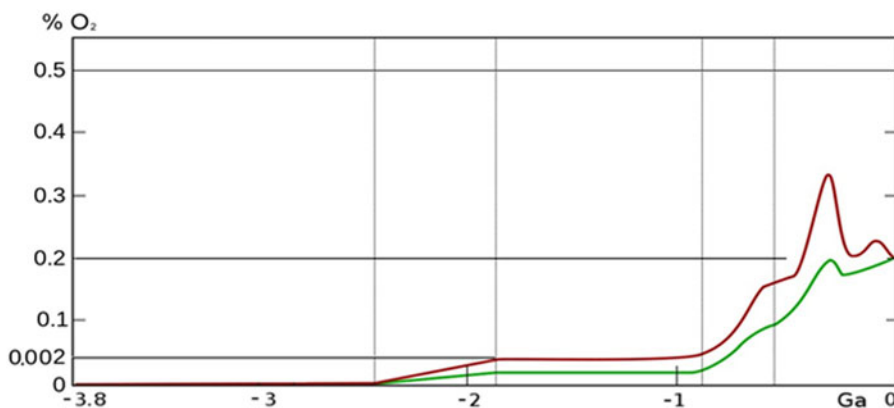


Figure 29. Fifth Drake: the curve depicted shows the climb of the concentration of oxygen in the atmosphere during the GOE from 0 to 0.2% between -2.4 and -1.9 Gy and, during the NOE, between -0.8 and -0.5 Gy. The green and red curve represents the minimum and maximum hypothesized value (figure modified by Holland, 2006).

The oxygen curve

At this point, it is possible to make some consideration on the well-known oxygen growth curve reported in Fig. 29. We found, in the calculation of the fourth parameter, a good probability of the development of the prokaryotes (50%) in 100 My, starting from at least -3.7 Gy. The positioning of the first photosynthetic prokaryotes is controversial, but in any case the first oxygen produced was reabsorbed by oxidative chemical phenomena. When these disappeared, the oxygen freed by the prokaryotes began to invade the planet bringing about a value of 1% of the current one to -2.1 Gy (GOE), triggering the first mass extinction of microorganisms, but favouring the development of *heterotrophic aerobic prokaryotes* and above all of the *heterotrophic eukaryotes*. We found the same probability of about 50% due to the onset of eukaryotes, but in 500 My starting from -2.1 Gy. Once the latter have also become photosynthetic (at about -1.5 Gy), the percentage of oxygen began to rise

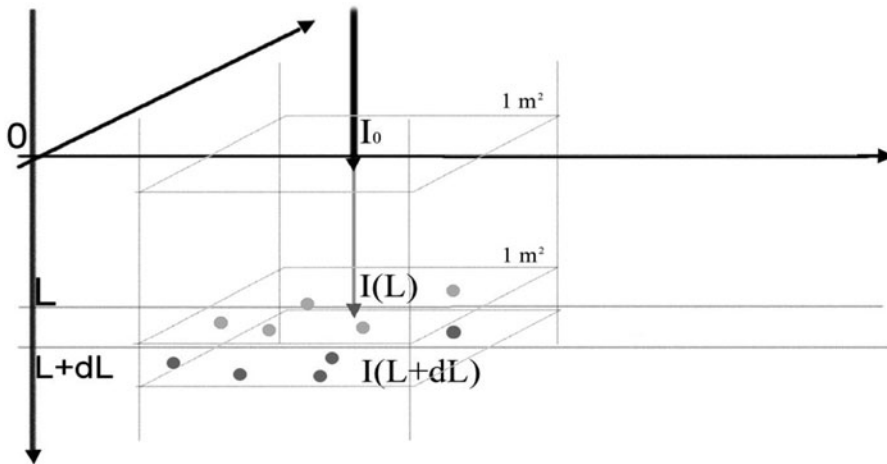


Figure 30. Fifth Drake: luminous penetration $I(L)$ between depth L and the depth $L + dL$ on an m^2 of marine surface. Little grey discs represent the suspension cells.

decidedly getting to the level of the current ones around -0.7 Gy (NOE). Let's now try to estimate the growth speed of oxygen in these two cardinal events, the GOE and the NOE. We take into consideration Fig. 30 which describes a marine environment from the shore 0 (sea level) towards the depth L . The light intensity I ($W m^{-2}$) will be equal to $I(L) = I(0) \equiv I_0$ on surface of the sea and equal to $I(L)$ to the depth L .

For each square meter of seabed, between depth L and $L + dL$, the number of photosynthetic cells in the volume element will be equal to:

$$N_f = 1 m^2 \times dL \times \rho,$$

where ρ is the density, or the number of cells for m^3 . Therefore, called r the linear size of the cells and ω their absorption coefficient (between 0 and 1; 0 for totally transparent cells and 1 for totally opaque cells), the effective impact section S_{eff} of the cells present in the direction of the light rays on $1 m^2$, will be:

$$S_{\text{eff}} = 1 m^2 \times \omega \times \rho \times r^2 \times dL.$$

Consequently, $(\omega \times \rho \times r^2 \times dL)$ is the percentage of *darkening*, due to the dL layer, of the light intensity $I(L)$ to depth L ; so the light intensity beyond this layer will be:

$$I(L + dL) = I(L) \times (1 - (\omega \times \rho \times r^2 \times dL))$$

$$I + dI = I - I \times \omega \times \rho \times r^2 \times dL$$

$$dI = -I \times \omega \times \rho \times r^2 \times dL$$

$$dI/I = -\omega \times \rho \times r^2 \times dL.$$

Integrating both members between 0 (sea level) and L , we have:

$$[\ln(I) - \ln(I_0)] = -\omega \times \rho \times r^2 \times L$$

$$\ln(I/I_0) = -\omega \times \rho \times r^2 \times L$$

and, finally, by extracting the exponential:

$$I/I_0 = \exp(-\omega\rho r^2 L)$$

$$I(L) = I_0 \exp(-\omega\rho r^2 L).$$

In this way, solving the differential equation for separation of the variables, the light intensity (W m^{-2}) is obtained which comes to depth L starting from intensity I_0 to sea level:

$$I(I_0, L, r, \rho, \omega) = I_0 e^{-\omega\rho r^2 L}.$$

Therefore, similarly to cells suspended in the liquid, the water molecules themselves also reduce the intensity according to a similar law, thus the complete equation of the reduction of light intensity caused by the water and the cells in suspension is written by adding, to the exponent, the factor due to the absorption of water molecules:

$$I(I_0, L, r, \rho, \omega, \varphi) = I_0 e^{-(\omega\rho r^2 + \varphi)L}.$$

We now estimate the world marine surface S interested in the phenomenon of photosynthesis: it is the coastal area of the planet whose waters do not exceed 20 m depth; that is:

$$S = C \times D \times \zeta = 10^9 \text{ m}^2.$$

Having place:

$C = 10^8 \text{ m}$	Extension of the continental coasts
$D = 10^2 \text{ m}$	Thickness of the continental coasts, where the depth does not exceed 20 m
$\zeta = 10^{-1}$	Fraction of the coasts not directly above the seabed

The dW light power, captured by photosynthetic cells with depth L on the entire surface S , will instead be:

$$dW = S \times dL \times \rho \times \alpha \times r^2 \times I_0 e^{-(\omega\rho r^2 + \varphi)L},$$

where α is the fraction of the cell surface interested in photosynthetic absorption. We observe that α must necessarily be less than the absorption coefficient ω which measures all luminous absorption, both photosynthetic and not.

If we add the contribution of all the layers of the seabed, we obtain the total power absorbed by the cells. To obtain this sum, we ideally integrate the latest formula obtained for dW between 0 and $+\infty$ compared to depth L (obviously the light absorption is practically zero beyond a certain depth). It is obtained for total power W :

$$W(\rho) = \frac{(S \times \alpha \times r^2 \times I_0) \times \rho}{(\omega \times r^2) \times \rho + \varphi}.$$

If we now make ρ tend to infinity, we obtain the *value of saturation* of the power captured for photosynthesis (turbid waters):

$$W_s = \frac{S \times \alpha \times I_0}{\omega}.$$

This is obviously valid for $\omega \neq 0$, which is the limit of totally transparent cells (moreover, if ω goes to 0, α , that is less than ω , must do the same, but their quotient does not). As we should have expected,

this value is independent of the size of the cells that carry out photosynthesis (saturation value), and of the water solution coefficient φ .

To get I_0 (effective photosynthetic power per m^2), we must multiply the three factors:

$W_{bs} = 10^3 \text{ (W m}^{-2}\text{)}$	Solar base power to the ground
$\eta = 0.154$	Average sun efficiency in the year
$\gamma = 0.3$	Visible light fraction used

Getting:

$I_0 = 46.2 \text{ (W/m}^2\text{)}$	Photosynthetic power for m^2 effective
-------------------------------------	--

Therefore:

$$W_s = \frac{\alpha}{\omega} \times W_{bf}$$

Having place:

$W_{bf} \equiv S \times I_0 = 4.62 \times 10^{10} \text{ W}$	Basic photosynthesis power
--	----------------------------

To obtain the energy necessary to produce an O_2 molecule, we must multiply the following factors:

$\nu_f = 5.45 \times 10^{14} \text{ (s}^{-1}\text{)}$	Medium light frequency in photosynthesis
$h = 6.63 \times 10^{-34} \text{ (J}\cdot\text{s)}$	Plank constant
$n = 10$	Number of photons for each O_2 molecule

Getting:

$\varepsilon = 3.62 \times 10^{-18} \text{ (J)}$	Energy for oxygen molecule produced
--	-------------------------------------

Let's now give an estimate of the oxygen molecules present after the GOE and after the NOE starting from the data of the current atmosphere.

$S_T = 5.3 - 10^{14} \text{ (m}^2\text{)}$	Earth surface
$M_a = 10^4 \text{ (kg m}^{-2}\text{)}$	Air mass for O_2
$p_{GOE} = 0.2\%$	GOE oxygen percentage
$p_{NOE} = 20\%$	NOE oxygen percentage
$M_{Oss} = 2 \times 10^{-26} \text{ (kg)}$	Mass molecule oxygen

There will be the following values:

$N_{GOE} = S_T \times M_a \times p_{GOE} / M_{Oss} = 5.3 \times 10^{41}$	Number of oxygen molecules GOE
$N_{NOE} = S_T \times M_a \times p_{NOE} / M_{Oss} = 5.3 \times 10^{43}$	Number of oxygen molecules NOE

We just have to try to evaluate the oxygen produced by a world cyanobacteria population and a similar population of photosynthetic eukaryotes. To do this, we must estimate the two optical-structural parameters for prokaryotes and eukaryotes, that is α (fraction of the photoactive surface of the cell) and ω (luminous absorption coefficient of the cell). We therefore place the following values (where the indices 'p' and 'e' indicate respectively 'prokaryotes' and 'eukaryotes'):

$$\begin{array}{l} \alpha_p = 1.0 \times 10^{-2} \\ \alpha_e = 4.0 \times 10^{-2} \\ \omega_p = 5.0 \times 10^{-1} \\ \omega_e = 1.0 \times 10^{-1} \end{array}$$

where we chose to attribute to the eukaryotes a fraction of photosynthetically active surface four times greater than the prokaryotes, given that the eukaryotes could probably be more efficient; in addition, it was chosen to attribute to the eukaryotes an absorption coefficient five times minor of the prokaryotes, given that the eukaryotes are without cell wall.

Finally, remembering that the calculated value of the total power (J/S) captured for photosynthesis is:

$$W_s = \frac{\alpha}{\omega} \times W_b \text{ (J/s)}$$

and energy, for oxygen molecule produced, is:

$$\varepsilon = 3.62 \times 10^{-18} \text{ (J)}.$$

The total number of oxygen molecules produced to the second is obtained for prokaryotes and eukaryotes:

$$N_{\text{Oss proc}} = \frac{\frac{\alpha_p}{\omega_p} \times W_b}{\varepsilon} = 2.56 \times 10^{26} \left(\frac{\text{molecules}}{\text{second}} \right),$$

$$N_{\text{Oss euc}} = \frac{\frac{\alpha_e}{\omega_e} \times W_b}{\varepsilon} = 5.11 \times 10^{27} \left(\frac{\text{molecules}}{\text{second}} \right).$$

Taking into account that in a million years, there are $1 \text{ My} = 3.15 \times 10^{13} \text{ (s)}$, the minimum formation of the GOE and NOE is respectively:

$$\begin{array}{l} T_{\text{GOE}} = N_{\text{GOE}} / (N_{\text{Oss proc}} \cdot 3.15 \times 10^{13}) = 66 \text{ My} \\ T_{\text{NOE}} = N_{\text{NOE}} / (N_{\text{Oss euc}} \cdot 3.15 \times 10^{13}) = 330 \text{ My} \end{array}$$

As you can see, even if photosynthetic eukaryotes are more efficient than their corresponding prokaryotes, the quantity of oxygen of the NOE is 100 times higher; therefore, the time of realization of the NOE remains higher than five times. Obviously, we did not consider the phenomena of reabsorption of oxygen (oxidation, breathing of the heterotrophic, etc.) that expands the estimated times.

Considerations on the fifth parameter

Unlike the fourth parameter of Drake which, in the previous section, we calculated around 0.5 (probability of 50%) in a span of 100 million years, the fifth Drake parameter is just above 0.01 (probability of 1%) in a period of 1500 million years (GOE and NOE excluded), therefore much lower. This does not surprise us because, after all, *H. sapiens* is the only attempt to be successful on an infinite number

of species that appeared on the planet. Moreover, the subdivision of the calculation in the three macro-intervals made us highlight two things:

- (a) the essential role that oxygen played in determining the time of realization of the evolutionary processes – see both the GOE and the NOE, the occurrence of which guided the times and gave a decisive push towards first the eukaryotes, and then the metazoa;
- (b) the bottleneck highlighted in the last step, or the onset of intelligence whose probability has been calculated at around 3% in 0.5 Gy, while neither the appearance of eukaryotes (probability of 50% in 0.5 Gy), nor that of metazoa (85% probability in 0.5 Gy) were particularly problematic from our calculations.

The Drake social parameters: f_c and f_L

The sixth and seventh parameters of Drake are rightly traditionally defined as *social parameters* and complete the descriptive framework of a potential galactic civilization.

Obviously, the approach to these topics is less robust than the previous ones because it rests on plausible hypotheses, but without any experimental feedback.

Sixth Drake: fraction of planets where life decides to communicate

As mentioned in the introduction, the sixth parameter of Drake, in this paper, represents only the fraction of civilizations that freely decide to communicate and not to hide.

While the sixth original parameter intended to count civilizations that become technological and communicating, we delegated this aspect to the fifth parameter through the definition of intelligence, derived from Kardašěv, of a K at least equal to 0.7 (just us).

In addition, we overturned onto the seventh parameter all those cases in which civilizations *are forced* or induced not to communicate and therefore cease to be visible.

What remains in the sixth parameter is the *deliberate* social choice of galactic civilization not to communicate from the beginning of their history. On such an elusive topic, we are not able to express scientific opinions and therefore *set* an average probability of 50%:

Drake 6	
f_c min	f_c max
4.0×10^{-1}	6.0×10^{-1}

Seventh Drake: temporal fraction of a civilization's duration

With the seventh parameter, we move to a slightly different context from the previous ones because we must no longer examine the probability of the manifestation of an event, but the duration of the same after having established an acceptable confidence interval for its occurrence. The lognormal $\Phi(X_0)$, a function of the probability composite X_0 , is transformed into another distribution function $F_p(\Delta T)$, a function of the time ΔT of duration of the galactic civilization and the confidence interval p that we will define immediately.

The mathematical issues end here, while those of the choice of entry data remain to be faced: in fact, it is a matter of hypothesizing which events, completely unrelated to the particular planetary context, can constitute *challenges*, or universal strands that jeopardize any galactic civilization; we must also set the probability of survival and the ΔT_0 duration of each *challenge* beyond which the danger is considered overcome. The result is the mathematical picture that we will describe in the following sections.

Finally, we reiterate that we have made small forays into the sixth parameter of Drake (percentage of civilizations they choose to communicate), as can be seen from the fourth and seventh challenge

(respectively, spontaneous involution and point Ω). This, however, is a false misunderstanding because in this context, we have analysed above all the causes that, in some way, lead the civilizations to no longer communicate *after a period of communication*, leaving out of the sixth parameter an analysis of the socio-cultural motivations that lead them to isolate voluntarily from the beginning of their history, always keeping themselves hidden from the others.

Is Gott's delta-T argument applicable to the duration of galactic civilizations?

In 1993, astrophysicist Richard Gott published an article entitled ‘*Implications of the Copernican Principle for our future prospects*’ in which he made the attempt to calculate the probable duration of the human race before its inevitable extinction (Gott, 1993). The genesis of the article began in 1969 when Gott passed through Berlin and, on the occasion, visited the notorious wall. Gott applied a mathematician’s reasoning to try to predict the duration of the life of the wall: he did not visit it in the year of its construction (which occurred in 1961) nor in the year of its demolition (which took place in 1989), but *in one random moment of its existence*; it was therefore reasonable to assume that his holiday in 1969 placed him within the two intermediate quarters of the life of the wall with 50% probability. If the visit was taking place right at the beginning of the second quarter (i.e. only the first quarter had passed) the wall had 3/4 of its life in front of it, that is, it would remain standing three times longer than the time since its construction. If the visit had placed itself at the end of the third quarter, instead, the wall had only 1/3 of life in front of it and it would remain standing for 1/3 of the time since its construction. At the time, the wall had been in existence for 8 years and Gott concluded that there was a 50% probability that the symbol of the Cold War still had a lifespan oscillating between 2.7 and 24 years. As we know, the wall was knocked down 20 years and a few months after Gott’s visit, perfectly inside his prediction range. According to Gott, this analysis can be applied in the forecast of any temporal event *as long as the observer is placed within it in a completely random way*.

We gave the classic example of a probability of reference $p = 1/2$, but we can extend the example to the general case of a probability of reference any p . In this case, the relationship between future and past life is expressed by:

$$\frac{\Delta T_{\text{future}}}{\Delta T_{\text{past}}} = \begin{cases} \frac{1+p}{1-p} \text{ max} \\ \frac{1-p}{1+p} \text{ min} \end{cases} .$$

In the case of the duration of human civilization with $p = 1/2$ and a duration to date of about 200 000 years, this would give a minimum future value of about 70 000 years and a maximum value of 600 000 years.

But is this way of proceeding correct? In our opinion, no, precisely because of the main prerequisite of Gott’s reasoning, or the supposed randomness of the moment chosen to make the calculation: while in the case of the Berlin Wall it is beyond any doubt that the visit of the astronomer to Berlin was unconnected to the history of the wall itself, in the case of the duration of a galactic civilization, the moment in which the question of Gott arises can only be immediately following the formulation of abstract mathematical thought, give or take a thousand years. Therefore, this is not a random moment of our civilization, but it is the era immediately following the birth of abstract mathematical thought; the era of the Galilei, Penrose and Gott. Delta-T reasoning cannot be applied and, as we will see in the conclusions, it is wrong by excess or by defect depending on whether we intend to analyse the duration of the entire species or only that of the technological civilization.

We will therefore not follow the Gott’s delta-T reasoning, but rather that of the reformulation of the Maccone distribution function applied to the duration ΔT .

The calculation of the distribution curve of the duration of a galactic civilization

As in the previous Drake parameters, let us define the mathematical quantities used in order:

- ΔT_{0j} is the time of the *bottleneck* or *challenge* phase, or the average time of permanence of the risk conditions of the j phase before it is definitively overcome.
- A_j, B_j are the minimum and maximum probability, of the X_j variable, of survival of the galactic civilization in the ΔT_{0j} period of the j phase.

$$\mu \equiv \sum_j \frac{B_j(\ln B_j - 1) - A_j(\ln A_j - 1)}{B_j - A_j}$$

is the so-called *logarithmic mean value* of the Maccone lognormal distribution.

$$\sigma^2 \equiv \sum_j \left(1 - \frac{A_j B_j (\ln B_j - \ln A_j)^2}{(B_j - A_j)^2} \right)$$

is the so-called *logarithmic variance* of the Maccone lognormal distribution.

$$\Phi(X_0) \equiv \frac{1}{X_0} \times \frac{1}{\sqrt{2\pi\sigma}} e^{-\frac{(\ln X_0 - \mu)^2}{2\sigma^2}}$$

is the lognormal distribution of Maccone function of the overall probability X_0 .

$$\Delta T_0 = \sum_j \Delta T_{0j}$$

is the total time of permanence of the risk conditions, sum of the individuals ΔT_{0j} .

At this point, from the three input values for each phase A_j, B_j and ΔT_{0j} , applying the formula of the lognormal, the average $\langle X_0 \rangle$ and the variance $\sigma(X_0)$ of the random variable X_0 would be obtained. However, these are the average and deviation of the probability of overcoming *all* the bottlenecks in the total time ΔT_0 , while now we want, given an appropriate confidence value of the probability of survival p (e.g. 50%), the average and the deviation of another random variable which is the survival time of civilization ΔT_p .

We then proceed as follows to obtain the distribution of the random variable ΔT_p function of X_0 ; let's set:

$$\frac{\Delta T_p}{\Delta T_0} \equiv \delta,$$

δ is the fraction of time compared to ΔT_0 for which to impose our probability of survival p . Obviously, the probability of survival in the ΔT_p time will be:

$$\langle X_0 \rangle^\delta = p.$$

By extracting the natural logarithm and isolating ΔT_p , we obtain:

$$\Delta T_p = \left(\sum_j \Delta T_{0j} \right) \times \frac{\ln p}{\ln \langle X_0 \rangle} = \Delta T_0 \times \frac{\ln p}{\ln \langle X_0 \rangle}.$$

Placing now for convenience:

$$\begin{cases} -\Delta T_0 \ln p = c > 0 \\ \Delta T_p = y > 0. \end{cases}$$

The previous equation can be written briefly as:

$$y = -c / \ln(X_0),$$

where, mind you, we passed from the average value $\langle X_0 \rangle$ to the complete X_0 random variable. By reversing the last expression, you have:

$$X_0 = e^{-\frac{c}{y}},$$

which is a growing monotonous function. Then, according to the distribution theorem of a function of a random variable, the new distribution for the $y = \Delta T_p$ variable is obtained from the lognormal distribution $\Phi(X_0)$ by replacing the value of X_0 just found according to y and multiplying everything by the X_0 derivative always according to y . That is to say:

$$F_p(y) = \Phi(e^{-\frac{c}{y}}) \times \left(e^{-\frac{c}{y}} \times \frac{c}{y^2} \right).$$

By replacing the well-known values of y and c , we have:

$$F_p(\Delta T_p) = \left(e^{\frac{\Delta T_0 \ln p}{\Delta T_p}} \right) \times e^{\frac{\Delta T_0 \ln p}{\Delta T_p}} \times \left(\frac{-\Delta T_0 \ln p}{\Delta T_p^2} \right),$$

and finally, in a more compact form:

$$F_p(\Delta T_p) = \Phi \left(p^{\frac{\Delta T_0}{\Delta T_p}} \right) \times p^{\frac{\Delta T_0}{\Delta T_p}} \times \left(\frac{\Delta T_0 \ln \frac{1}{p}}{\Delta T_p^2} \right).$$

This is our distribution function of the duration of galactic civilizations. Once the input values of all the phases/challenges A_j, B_j and ΔT_{0j} will have been inserted, we will calculate $\langle \Delta T_p \rangle$ and $\sigma(\Delta T_p)$, from the definitions of mean value and variance, with numerical methods. The curves in Fig. 31 show, by way of example, in the A box, the classic lognormal of Maccone with respect to the fixed temporal value of $\Delta T_0 = 450\,000$ years determined by the sum of all critical phases; box B, on the other hand, represents the distribution functions lasting ΔT_p of a galactic civilization, calculated starting from the lognormal function of Maccone, and imposing the probability of survival of civilization progressively from 40 to 60%: *the descent of the time ΔT_p is evident as the probability of survival, chosen as a reference, is growing.*

We verify this result by finding the locus of points of maximum shown in Fig. 31(b). Recall that the abscissa of these points is not exactly the average values of the curves because the latter are not perfectly symmetrical, but we can still make this approximation.

First of all, we calculate the derivative with respect to ΔT_p of our distribution function $F(\Delta T_p)$. The calculation is a little laborious, but after a few steps we will get (Appendix C):

$$\frac{d}{d\Delta T_p} F_p(\Delta T_p) = -\Phi \left(p^{\frac{\Delta T_0}{\Delta T_p}} \right) \times p^{\frac{\Delta T_0}{\Delta T_p}} \times \left(\frac{\Delta T_0 \ln \frac{1}{p}}{\sigma^2 \Delta T_p^4} \right) \times \left[\left(\ln \left(\frac{1}{p} \right) \frac{\Delta T_0}{\Delta T_p} + \mu \right) \ln \left(\frac{1}{p} \right) \Delta T_0 - 2\Delta T_p \sigma^2 \right].$$

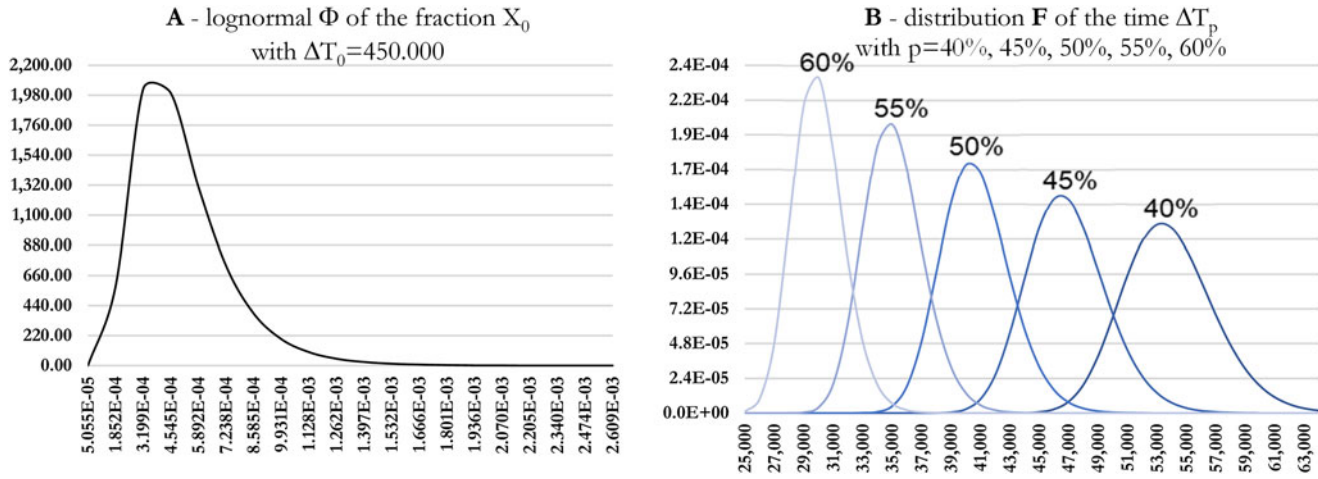


Figure 31. Seventh Drake: box A: classic lognormal function of Maccone; box B: distribution functions of duration ΔT_p .

By placing the steady point of the derivative (we do not report, for brevity the condition on the second derivative <0):

$$\frac{d}{d\Delta T_p} F_p(\Delta T_p) = 0,$$

we get the second-degree equation with $y = \Delta T_p$:

$$(-2\sigma^2)y^2 + \left(\mu y_0 \ln\left(\frac{1}{p}\right)\right)y + \left(y_0 \ln\left(\frac{1}{p}\right)\right)^2 = 0,$$

which has a single solution for positive values of ΔT_p .

The parametric coordinates, compared to parameter p , of points of maximum, are then:

$$\begin{cases} \Delta T_{p\text{MAX}} = C \times \ln\left(\frac{1}{p}\right) \Delta T_0 \\ F(\Delta T_{p\text{MAX}}) = D \times \frac{1}{\ln\left(\frac{1}{p}\right) \Delta T_0} \end{cases},$$

and, consequently, from the first of the two:

$$\begin{cases} p = e^{-\frac{\Delta T_{p\text{MAX}}}{\tau}} \\ \tau = C \times \Delta T_0 \end{cases},$$

having placed the positive constants:

$$\begin{cases} C = \left(\frac{\sqrt{\mu^2 + 8\sigma^2} + \mu}{4\sigma^2}\right) > 0 \\ D = \frac{\exp\left[-\frac{1}{2\sigma^2} \left(\frac{4\sigma^2}{\sqrt{\mu^2 + 8\sigma^2} + \mu}\right)^2\right]}{\sqrt{2\pi}\sigma \left(\frac{\sqrt{\mu^2 + 8\sigma^2} + \mu}{4\sigma^2}\right)^2} > 0 \end{cases}.$$

The product $C \times D = \cos t > 0$, therefore:

$$\Delta T_{p\text{MAX}} \times F(\Delta T_{p\text{MAX}}) = C \times D = \frac{\exp\left[-\frac{1}{2\sigma^2} \left(\frac{4\sigma^2}{\sqrt{\mu^2 + 8\sigma^2} + \mu}\right)^2\right]}{\sqrt{2\pi}\sigma \left(\frac{\sqrt{\mu^2 + 8\sigma^2} + \mu}{4\sigma^2}\right)} = \cos t > 0.$$

Then, the locus of points of the maximum of our temporal distributions will be a hyperbola branch equilateral as we had to expect (Fig. 32(a)).

This means that, by analysing the two trivial limit cases, the certainty of surviving ($p \rightarrow 1^-$) makes our temporal distribution function diverge in a Dirac delta at the origin of the axis of the times, which translated in poor words means that only the *today* is certain, while for infinitesimal probabilities

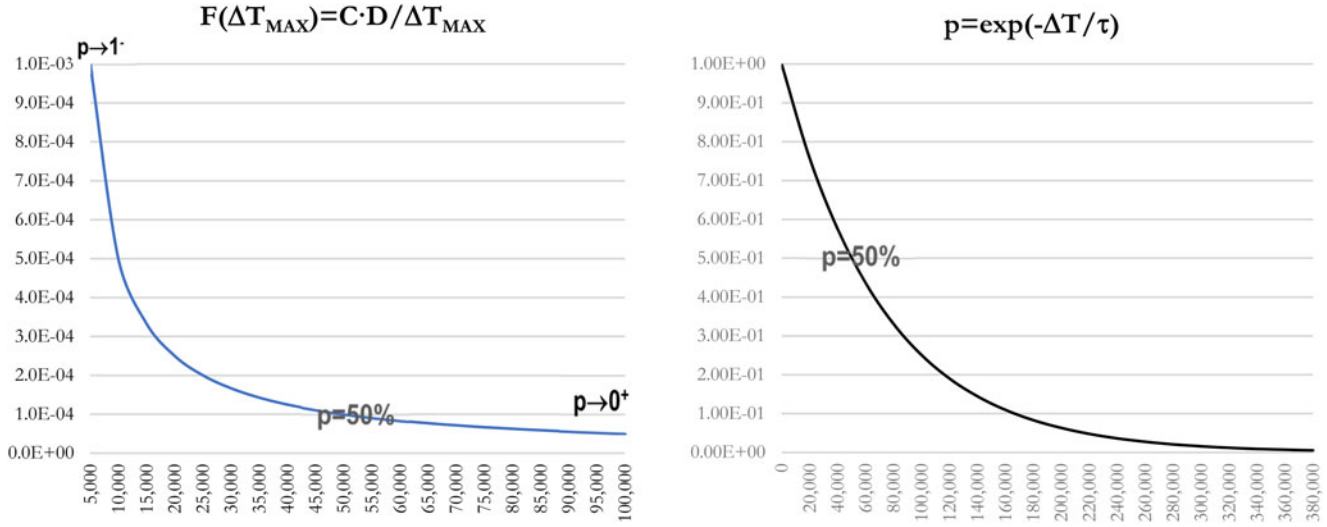


Figure 32. (a) Seventh Drake: the equilateral descent of the maximum distribution functions of the duration of civilization (equal to approximately $\langle \Delta T_p \rangle$); (b) seventh Drake: the exponential descent of the probability of survival at the time ΔT with about $\tau = 72\,300$ years; (b): seventh Drake: distribution of duration Δt for five reference probability values p : the one chosen by us is 50% which determines an average value of about 50 000 years.

($p \rightarrow 0^+$) diverges both the duration of civilization and its deviation, which means that civilization could last an arbitrary time. Only intermediate cases, for example ($p = 0.5$), give us useful information for our distribution of life times. Figure 32(b) is, trivially, the exponential descent of the probability of absence to the time ΔT with $\tau = 72.300$.

The seven challenges of galactic civilizations (and plan B)

The two difficulties we now have to solve are:

- (1) to imagine future scenarios, even ones which are remote in space and time
- (2) to free these scenarios from our planetary and cultural context

In other words: what could be the challenges that *any* galactic civilization would most likely face to persist over time? We hypothesized the following seven risk factors and a plan B for each:

- (1) self-destruction due to evolutionary failure
- (2) self-destruction due to a technological error
- (3) technological insufficiency to cope with planetary changes
- (4) spontaneous natural involution of civilization
- (5) artificial genetic involution of civilization
- (6) dead-end road after transition of artificial intelligence
- (7) reaching of point Ω and subsequent insolation of advanced intelligence

Plan B: interstellar journey in case of failure

We know the first three challenges well because they are typical of a technological civilization in its dawn like ours and therefore are today the subject of heated debate. The remaining four are scenarios that could arrive once the first three have been overcome; perhaps they appear less frightening to us because they are (or seem) not to be imminent, but thinking in terms of tens of thousands of years, they constitute pitfalls just as devastating as the first three.

The interstellar journey is the potential escape route from a hypothetical failure with the various challenges. Since the challenges occur in more or less early periods of civilization, the interstellar journey is or is not an effective method of escape depending on the challenge to which it is applied.

The first challenge: self-destruction due to evolutionary failure

It is inevitable that, at a certain point, an intelligent species equipped with the instinctual and cultural background that supported it in its evolutionary journey is faced with a sudden technological acceleration. The reason is obvious: science, but also nature often does not progress gradually, but proceeds in sudden and unexpected jumps, followed by periods of relative stasis. These accelerations are a risk (Menichella, 2005).

In our previous paragraph on the fifth Drake parameter, we followed the footsteps of Kardashev (1964) to catalogue the level of a galactic civilization on four levels:

$W_1 = 10^{16}$ W	is all the solar power that an orbiting rocky planet in its habitability area receives (in Watts)
$W_2 = 10^{11}$ W_1	is all the power radiated by the star
$W_3 = 10^{11}$ W_2	is all the power radiated by the galaxy
$W_4 = 10^{11}$ W_3	is all the power radiated by the observable universe

According to this scale, the level of a civilization, which develops a total W_{ETC} power, is expressed by the index $K = 1, 2, 3$ and 4 at the bottom of the powers W_K and is calculated:

$$K = \frac{\log_{10}(W_{\text{ETC}}) - 5}{11}.$$

For a common animal species (including ourselves, until two centuries ago) K does not exceed 0.6 , but for us today it already stands at 0.7 and is constantly growing. This means that our access to energy is increasing and, at the same time, the level of responsibility that we must have in the management of this energy level is growing. In a nutshell, a generic galactic civilization must try not to *burn itself with fire* once it has been discovered, especially if the levels of energy involved are of planetary dimensions, as is atomic energy in our current case.

However, a galactic civilization does not automatically have within its instinctual background such skills; and this is simply because technological changes belong only to the last phase of its development, that is to its culture. We can only hope that culture will be able to channel the behaviours from the natural base that forged the species in question in time. It is an arduous, perhaps desperate task, but the stakes are the highest possible: survival in the immediate future. This is what we must do in the control of nuclear armaments and beyond.

We think it is plausible that this step is universal for galactic civilizations and that it is very difficult to overcome (just about 10%). The challenge arises when, potentially, a civilization is able to express a technology and ends when the culture of the society has defused all that can lead to self-destruction, deriving from its natural past (about $100\,000$ years): *we assign a probability of surviving the challenge of between 0.05 and 0.15 on a challenge time limit of $100\,000$ years:*

Challenge 1		
A_1	i_1	Δi_{01}
0.05	0.15	$100\,000$

The second challenge: self-destruction due to a technological error

This second case resembles the first, but lacks *intent*, that is, while always dependent on the bad management of acquired technology, self-destruction is due to an error of evaluation where neither the nature nor the culture of a civilization have any responsibility.

It is a challenge that can temporally overlap even partially with the first but which tends to arrive later, when the technological power acquired is very high, the problems seem solved and the civilization lowers its level of control over the potential consequences of its actions.

This step is also inevitable for galactic civilizations and difficult enough to overcome (around 20%). The challenge presents itself since a civilization is in possession of a mature technology and ends when the technology itself provides sufficient tools such as interstellar travel to make the civilization safe (about $50\,000$ years): *probability of surviving the challenge between 0.1 and 0.3 on a challenge time limit of $50\,000$ years:*

Challenge 2		
A_2	i_2	ΔT_{02}
0.1	0.3	$50\,000$

The third challenge: technological failure to face emerging planetary changes

This phase depends strictly on the third Drake parameter which gives us the probability of terrestrial planets remaining permanently in their habitability area. Since the third parameter also has its own statistical distribution, we must also consider planets subjected to trauma, even if not definitive but in any case significant, of their stability during the existence of a civilization: known examples would be recurring meteor bombardment, severe shifts in the planet's rotation axis and severe climate change due to geological activity.

In this case, the only countermeasure that a civilization can adopt to face these events is an adequate technological level, let's say the achievement of a Kardashev parameter between 1 and 2, which is rather high.

This passage is less common than the previous for galactic civilizations (in fact it depends on the third parameter) and is easier to overcome (around 50%). In this case too, the challenge presents itself when a civilization enters into possession of a mature technology and ends when the technology itself provides the sufficient tools to ensure the safety of the civilization (about 20 000 years): *a probability of overcoming the challenge of between 0.4 and 0.6 on a challenge time limit of the 20 000 years:*

Challenge 3		
A_3	B_3	ΔT_{03}
0.4	0.6	20 000

The fourth challenge: spontaneous involution

With this parameter, we move away into the real future, that is, in those scenarios less familiar to science and more typical of by science fiction. The fact that a civilization must necessarily progress, in the technological sense of the term, is certainly our belief, dictated by the continuous presence of environmental pressure, often caused by ourselves, which favours a technologically advanced civilization over a less advanced one, whatever the price. Already in our small terrestrial civilization, we have learned that this is not always true, or rather, it is not possible to speak of technological progress without considering the price.

Obviously, we do not think that huge numbers of galactic civilizations suffer from *flower child* syndrome, but that in cases where external and internal dangers seem less impending, the choice not to progress, and therefore not to risk, is possible. In those cases, civilizations could deliberately choose to never become an evolved ETC with a high Kardashev parameter, but to live its life comfortably with a K of between 0.6 and 0.7 without too much trouble and with little probability of being identified.

There is also the case that this involutive phenomenon is determined by the progressive robotization of activities at the expense of the initiatives of the civilization that originally created these automatisms. In short, if the machines do everything, why change, evolve, explore and, above all, risk? A civilization could involuntarily wither away and find itself stuck (Gros, 2005).

We also consider this passage uncommon for galactic civilizations and easy to overcome (around 80%). The challenge presents itself when a civilization is in possession of a fairly mature technology advanced enough to make it feel safe and ends when it chooses to expand beyond its planet (about 30 000 years): *a probability of overcoming the challenge of between 0.7 and 0.9 on a challenge time limit of 30 000 years:*

Challenge 4		
A_4	B_4	ΔT_{04}
0.7	0.9	30 000

The fifth challenge: artificial genetic involution of civilization

A few years ago we might have treated this parameter as remote science fiction scenario, but instead must accept that the article ‘*The new frontier of genome engineering with CRISPR-Cas9*’, released in 2014 by Jennifer A. Doudna and Emmanuelle Charpentier, actually paves the way for precision genetic manipulation (Doudna and Charpentier, 2014). This implies that the assessment of this scenario overlaps with the first scenario which instead deals with the risk of self-destruction due to limits inherent in the species (less elegantly called *obtuseness*). Let us therefore leave out the part linked to the first parameter, because it has already been dealt with, and look only at the long-term consequences of a potential negative drift caused by genetic manipulation.

The negative consequences of genetic manipulation could be the following: unlike the natural selection that takes place over geological periods and gives the ecosystem time to always create a balance between all its parts, artificial genetic manipulation happens over very short timeframes, without the certainty that the ecosystem will once again find a balance.

This step is probably common for galactic civilizations and easy enough to overcome (around 70%). The challenge presents itself when a civilization is in possession of a sufficiently advanced technology (as we are today!) and ends when this technology is at high enough level that it can be corrected in the event of need (about 50 000 years): *a probability of exceeding the challenge of between 0.5 and 0.8 on a challenge time limit of 50 000 years:*

Challenge 5		
A_5	B_5	ΔT_{05}
0.5	0.8	50 000

The sixth challenge: dead-end road after transition of artificial intelligence

This parameter cannot be faced without defining what we mean by *artificial intelligence*. To this end, we will follow the steps of Roger Penrose whose monumental works ‘*The new mind of the emperor*’ (1990) and ‘*Shadows of the mind*’ (1994) are cornerstones on this topic (Penrose, 1990).

Artificial intelligence is not the mere automation of which we spoke in the fourth challenge but the actual birth of synthetic consciences. Penrose defines the simple automation, which includes the totality of machines built up to date, as weak artificial intelligence (WAI), while the possibility of creating conscious machines is defined as strong artificial intelligence (SAI). The power of Penrose’s reasoning lies in having demonstrated that the second *cannot* be a simple extension of the first, that is, machines, however complex, *based only on an algorithmic operation* cannot become conscious.

The demonstration is complex, but it is worth a brief mention: through Gödel’s incompleteness theorem (Gödel, 1931), Penrose points out that the possibility of formulating an unprovable but true theorem, such as the one constructed by Gödel, is the clear demonstration of the impossibility of a machine to do the same; the theorem, in fact, states that it is possible to build an infinite number of *true* but *not demonstrable* theorems through a formal starting system and a finite number of axioms; this system would actually work as an algorithm. How then does the human mind manage, if it works like an algorithm, however complex, to formulate a theorem like the one built in the Gödel test? The answer is that the human mind is conscious and consciousness is *not* based on an algorithm, but on something beyond that. For Penrose, this is an aspect of the still controversial quantum mechanics, namely the collapse of the quantum wave function (Paffuti, 2013); the latter phenomenon would not happen according to the subjective mechanism described by the classic interpretation of Copenhagen (i.e. the system analysed *decides* the result of the measure when it interacts with the observer), but according to a spontaneous mechanism, objective and unrelated to the observer and instead linked to the level of energy involved. The process is hypothesized to have happened inside the

cytoskeleton microtubules of the neurons (Penrose, 1994). In October 2022, further confirmation of this line of thought is provided by Christian Matthias Kerskens and David López Pérez (Kerskens and Pérez, 2022).

Without going further into this theme, what we are interested in pointing out now is that we are still a long way from building conscious machines; we can, at most, build excellent and fast automatisms, nothing more. To build truly conscious machines we would need to equip them with a mechanism as effective as that present in the brains of animals, with an objective collapse of the quantum wave function.

All this may seem somewhat abstract and naive, but Penrose formulated this hypothesis in 1990, when it was thought that the *Moore's law* on the exponential increase in calculating power would inevitably and in a few years lead us to artificial intelligence. After more than 30 years, we have machines which are very fast machines, but which are unable to make any real evaluation without having received adequate instructions on the matter. So what are we talking about when we discuss a transition to artificial intelligence? We certainly do not mean the control unit of the International Space Station, let alone the many voice response systems that are as stupid as a thermostat. We mean technological change that gives machines access to the true mechanisms of animal consciousness. If this leap occurred, then yes, a galactic civilization would have to face the problem of how to manage these new synthetic consciences in the same way as, in challenge number five, it had to face the problem of managing artificial genetic transition.

We therefore learn that, while the genetic transition here is already taking place after the discovery of CRISPR-Cas9, that of SAI is still far away. But, if it happened, what would be the challenges that a galactic civilization would face? The science fiction literature is packed with stories on the topic, which we can summarize in a single sentence: a civilization would find itself having to manage the onset of a new synthetic *species* that potentially would be in a position to all the levers to put it at risk. To overcome this danger, the newly formed synthetic consciousness (SAI) should be rigidly separated from the extraordinary technological tools that instead come from the automation (WAI). This is the challenge. In the case of failure, the galactic civilization could be destroyed by emerging synthetic civilization which might then not have the tools or motivations to survive itself (after all, what is a synthetic consciousness driven by?).

This passage has the same probabilistic and temporal characteristics as the previous one (it doesn't matter that the first is already underway and the other not): *a probability of overcoming the challenge of between 0.5 and 0.8 on a challenge time limit of 50 000 years:*

Challenge 6		
A_6	B_6	ΔT_{06}
0.5	0.8	50 000

The seventh challenge: achievement of point Ω

If the sixth challenge has been survived, would all the problems related to an SAI be solved? The writer and mathematician Vernor Steffen Vinge in 1993 hypothesized the occurrence of a phenomenon called *singularity* of civilization or point Ω (Vinge, 1993). This term means the explosion of an authentic intelligence due to the transfer of its principle of development from organic bases to synthetic bases with consequent acceleration of the trend to improvement; in short: a civilization designs and builds intelligent machines that in turn design and build smarter machines and so on. It is clear that, if the problem of the realization and the control of SAI were resolved, the point Ω could be the destiny of a civilization.

The characteristic of point Ω or a singularity is precisely that of going beyond our logical-scientific and moral understanding. As with a black hole, all we know about point Ω is that intelligence at this point expands and the decisions that will be made by such a civilization are inaccessible for us. One of

the possible decisions could be to definitively disappear from the sight of primitive *not* Ω civilizations and therefore to become completely invisible to others.

We cannot exclude the possibility of reaching such an exotic outcome for a galactic civilization, but, as we have already said in the sixth point, we still know too little about what the mechanisms of SAI are to be able to say whether a point Ω is inevitable. For this reason, we attribute to the overcoming of the risk of point Ω a high probability of success: *probability of overcoming the challenge of between 0.5 and 0.9 on a challenge time limit of 100 000 years:*

Challenge 7		
A_7	B_7	Δi_{07}
0.5	0.9	100 000

Plan B: escape to other planets and interstellar travel

It is reasonable to think that, in the event of failure seen in one or more of the previous challenges, galactic civilizations would attempt to move to other suitable solar systems considered. It must be emphasized that these would not be planned trips, but rather dictated by emergencies; therefore, their probability of success is low, especially if the galactic civilization is not mature enough (Mallove and Matloff, 1989). To take into account the maturity of the civilization at the time it could attempt interstellar travel, we have assigned a variable and gradually increasing probability π_j depending on the hypothetical technological background present at the time of presentation of the challenge in question (Zubrin, 1999).

The minimum and maximum A_j and B_j probabilities, previously defined, must then be corrected through the following formula:

$$A'_j = A_j + (1 - A_j)\pi_j$$

$$B'_j = B_j + (1 - B_j)\pi_j.$$

In this way the values A'_j and B'_j , which take into account the plan B of interstellar movement, are slightly increased compared to A_j and B_j . The probabilities assigned to π_j are as follows:

j	Challenge	π_j
1	Self-destruction due to evolutionary failure	1%
2	Involuntary technological error	3%
3	Technological insufficiency to face planetary changes	5%
4	Spontaneous involution	10%
5	Artificial genetic transition ended up on a dead track	20%
6	Transition of artificial intelligence ended up on a dead track	20%
7	Reaching point Ω	50%

The calculation of the seventh Drake parameter

At this point, we have all the elements necessary to calculate the duration of a galactic civilization. Tables 23–25 and Fig. 33(a) and (b) report the calculation carried out starting from the four input values for each challenge:

Min. prob. challenge j	Max. prob. challenge j	Span challenge j	Plan B probability j
A_j	B_j	ΔT_{0j}	π_j

Table 23. *Seventh Drake: input data in dark grey background and intermediate calculations of μ_j and σ^2_j in light grey*

Phase	Min. prob.	Max prob.	Max time phase j (anni)	Component j average log.	Component j variance log.	Plan B prob. escape
	over time ΔT_{0j}	over time ΔT_{0j}				
	A_j	B_j	ΔT_{0j}	μ_j	σ^2_j	π_j
1	0.05	0.15	100 000	-2.2531	0.0763	1%
2	0.10	0.30	50 000	-1.5293	0.0687	3%
3	0.40	0.60	20 000	-0.6499	0.0111	5%
4	0.70	0.90	30 000	-0.2005	0.0040	10%
5	0.50	0.80	50 000	-0.3332	0.0094	20%
6	0.50	0.80	50 000	-0.3332	0.0094	20%
7	0.50	0.90	100 000	-0.1648	0.0046	50%

Table 24. *Seventh Drake: input data ΔT_{MAX} on violet background; intermediate calculations of ΔT_0 , μ and σ^2 in light grey; lognormal mean values $\langle X_0 \rangle$, $\langle X_0 \rangle_A$ and $\langle X_0 \rangle_B$ in dark grey*

Max time process	Sum average log.	Sum variance log.	Average tot process	Min. prob. tot process	Max. prob. tot process	Lifetime planet
ΔT_0	μ	σ^2	$\langle X_0 \rangle$	$\langle X_0 \rangle_A$	$\langle X_0 \rangle_B$	ΔT_{MAX}
400 000	-5.46	0.18	0.46%	0.10%	0.83%	7.0×10^9

Table 25. *Seventh Drake: entry into p on the violet background of five probability values (that choice of 50% is reported with blue characters); in red and medium orange and standard deviation ΔT and its percentage value compared to ΔT_{MAX}*

Probability of survival	Duration (y) tot process	Min.	Max.	Fraction tot process	Minimum fraction	Maximum fraction
		duration tot process	duration tot process			
P	ΔT	ΔT_A	ΔT_B	f_d	f_{dA}	f_{dB}
40%	67 500	58 168	76 832	9.6×10^{-6}	8.3×10^{-6}	1.1×10^{-5}
45%	58 823	50 691	66 955	8.4×10^{-6}	7.2×10^{-6}	9.6×10^{-6}
50%	51 062	44 003	58 121	7.3×10^{-6}	6.3×10^{-6}	8.3×10^{-6}
55%	44 041	37 952	50 129	6.3×10^{-6}	5.4×10^{-6}	7.2×10^{-6}
60%	37 631	32 428	42 834	5.4×10^{-6}	4.6×10^{-6}	6.1×10^{-6}

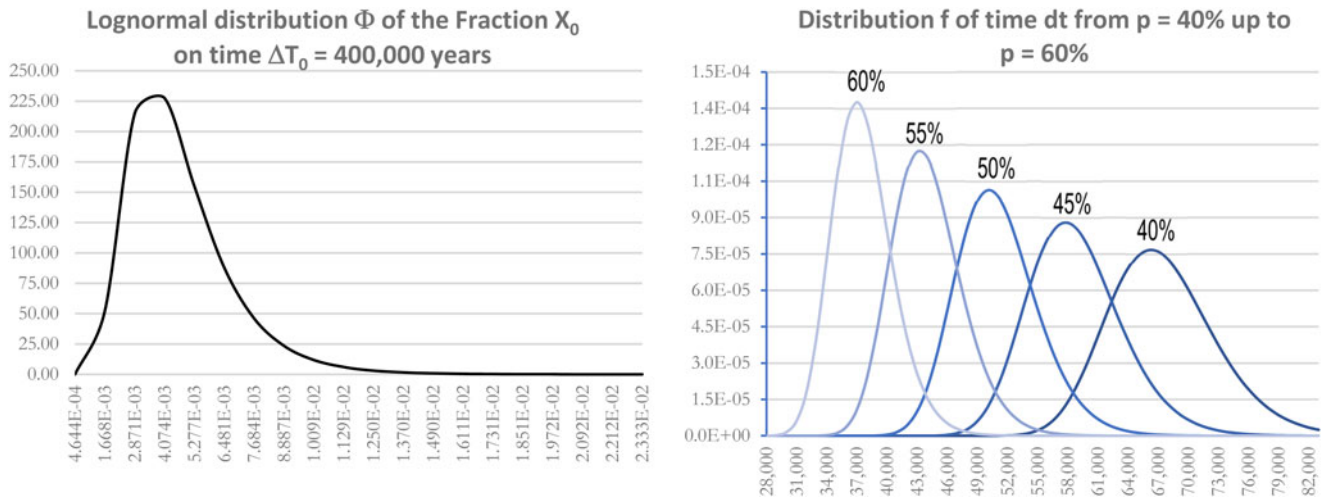


Figure 33. (a) Seventh Drake: Maccone lognormal for the entire process ΔT_0 ; (b) seventh Drake: distribution of duration Δt for five reference probability values p : the one chosen by us is 50% which determines an average value of about 50 000 years.

Drake 7 (static civilization)	
$f_L \text{ min}$	$f_L \text{ max}$
6.3×10^{-6}	8.3×10^{-6}

We should here admit that we have hypothesized here that the probability p_0 calculated with the lognormal on total time ΔT_0 was more or less independent of time and therefore its extrapolation at time ΔT , as we have seen, followed a simple exponential law of the type:

$$p = \exp(-\Delta T/\tau)$$

but this is actually *not true* because, especially for ΔT values lower than ΔT_0 , the probability is nothing more than the partial composition of the various probabilities of the individual seven challenges, which leads us to a curve of p and its derivative with changed sign (which is the distribution of the probability density of p on ΔT) a little more complex, as shown in Fig. 34(a) and (b).

However, the calculation of the seventh Drake parameter with this more laborious method would lead us to a result on the same order of magnitude as that we find by assuming a probability rigidly independent of time.

Considerations on the seventh parameter

As seen from Table 25 and Fig. 33(b), we found an average duration of galactic civilizations of about 50 000 years with a deviation of 7000. Assuming a reasonable duration of the life of the planet in the habitability region of about 7 Gy (remembering that the third parameter of Drake ensures this), the value of the temporal fraction of life of civilization is about 7×10^{-6} with a deviation of 10^{-6} . This means that our galactic civilization has a total timeframe of about 50 000 years during which it can recognize and be recognized by other civilizations.

Let's go back briefly to the delta- T reasoning which, as you will remember, we did not consider applicable: Gott had found a value of the duration of the human *species* of between 70 000 and 600 000 years with a probability of 50%. Now, however, we have found a value of the duration of the galactic *civilization* of between 44 000 and 58 000 years with a 50% probability; that is, we have more accurate data which, above all, refers to galactic technological civilizations rather than the intelligent galactic species. If we applied delta- T reasoning to human technological civilization, we should obtain worrying results, because we would obtain a value of the duration of human technological *civilization* of between 70 and 600 years.

At this point, one last consideration is necessary: so far we have considered only the case of a civilization forming and developing on its own planet of origin and moving *only to escape a potentially catastrophic danger* due to one of the seven challenges; that is, we have ignored the scenario analysed by Tipler (1980, 1994) and Brin (1983) of a civilization which, at a certain point in its development, freely decides to colonize the galaxy. How and when would such a scenario presents itself? First of all, it is conceivable that a civilization that wishes to and is in a position to colonize the galaxy is a K2 type civilization that has already survived *all* seven challenges after 400 000 years; but in this case, we would find ourselves facing an epochal passage of the whole process, that is: if this happened, then the civilization in question *would no longer become extinct*; therefore, the value that we should take into consideration in our formula is not that derived from temporal distribution with a probability of 50% of survival that leads us to an average duration of 50 000 years and a percentage fraction of 7×10^{-6} , but directly from the value provided by the Maccone formula to exceed all seven challenges in 400 000 years, which is far greater, namely 5×10^{-3} .

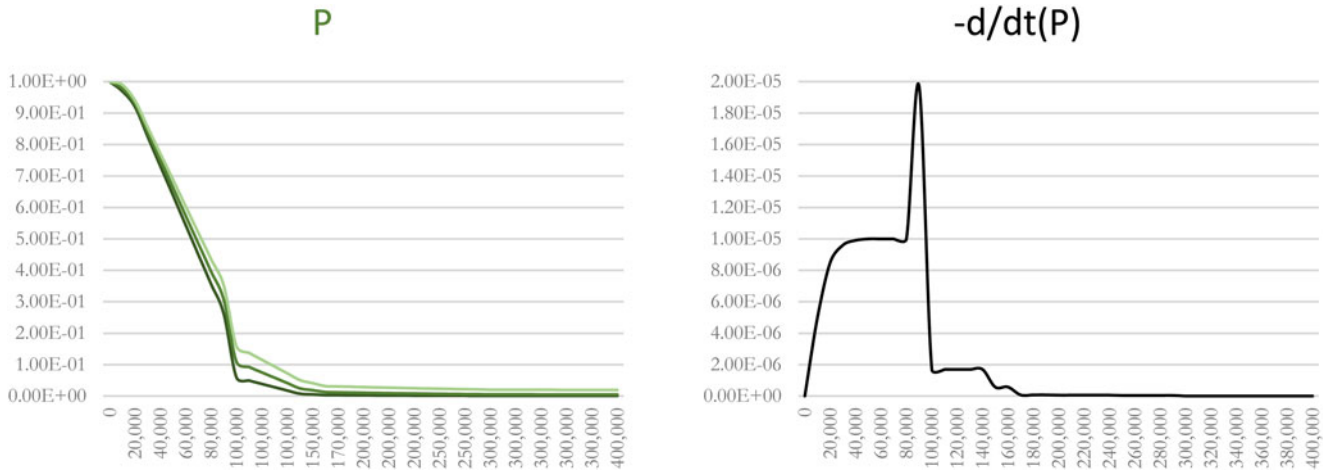


Figure 34. (a) Seventh Drake: the real descent of the probability of survival at the time Δt for the case of the seven challenges; (b) seventh Drake: the real distribution function of the probability of survival at the time Δt for the case of the seven challenges.

Drake 7 (dynamic civilization)	
f_L^{\min}	f_L^{\max}
1.03×10^{-3}	8.25×10^{-3}

All this leads to a predictable conclusion, namely that if we were to identify an ETC it would be much more probable that it would be an evolved K2 civilization moving through the galaxy rather than a static K1 (or lower) civilization like ours still grappling with challenges to overcome.

In conclusion, a potential transition from K1 to K2, as hypothesized by Kardašev (1964) is crucial and has a decisive impact on the calculation of the entire Drake equation.

The complete Drake equation

At this point, we have all seven Drake parameters to estimate the number of galactic civilizations. To be exact, the fifth parameter was explicit in its three components relating to eukaryotes, metazoa and intelligent technological civilization (ETC); as we have seen in the previous section, intelligent technological civilizations can be of two types: *static* (point 7A of Table 26 and Fig. 35) or *dynamic* (point 7B of Table 26 and Fig. 36); the first are those that did *not* make the jump beyond the level $K = 1.4$ and therefore almost certainly do not have the technological possibility to colonize other planets; the latter, on the other hand, made the jump beyond the level $K = 1.4$ and therefore spread beyond their

Table 26. Drake’s parameters defined with their minimum and maximum values

		Value minimum	Value maximum	Component j mean log	Component j variance log
		A_j	B_j	m_j	σ_j^2
1	Number of stars of the galaxy suitable for life (of spectral class F, G and K)	1.00×10^{10}	1.20×10^{10}	23.1198	0.0028
2	Number of planets suitable in the habitable area for stellar mass (spectral class F, G and K)	1.60×10^{-1}	2.00×10^{-1}	-1.7169	0.0041
3	Fraction of stable planets for 7 ga	3.65×10^{-2}	1.07×10^{-1}	-2.6762	0.0916
4	Hamlet of planets where life is born	3.22×10^{-1}	6.55×10^{-1}	-0.7359	0.0409
5	Eukaryotes	2.89×10^{-1}	7.09×10^{-1}	-0.7264	0.0644
	Metazoa	5.97×10^{-1}	9.44×10^{-1}	-0.2692	0.0172
	Intelligent technological civilization	1.25×10^{-2}	5.66×10^{-2}	-3.4425	0.1700
6	Fraction of planets where life decides to communicate	4.00×10^{-1}	6.00×10^{-1}	-0.6999	0.0136
7A	Temporal fraction lasting a static K1 type civilization	6.29×10^{-6}	8.30×10^{-6}	-11.8316	0.0064
7B	Fraction of planets where life gets dynamic K2 civilization	1.03×10^{-3}	8.25×10^{-3}	-5.4996	0.2935

The fifth parameter is explicit in its three components relating to eukaryotes, metazoa and intelligent technological civilization.

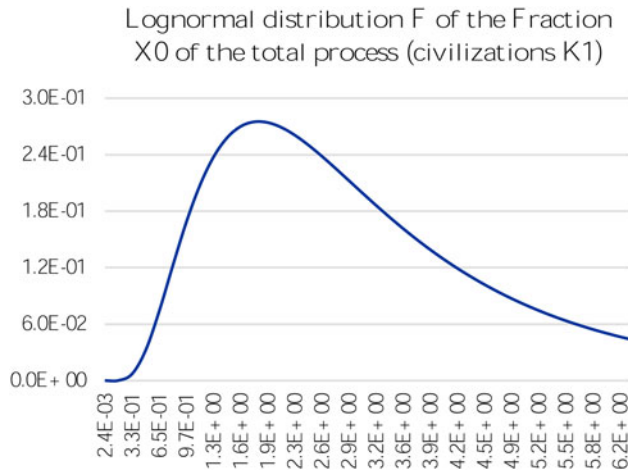


Figure 35. Lognormal of the distribution of static civilizations with $\langle N \rangle = 3.4194$ and $\sigma(N) = 2.43$.

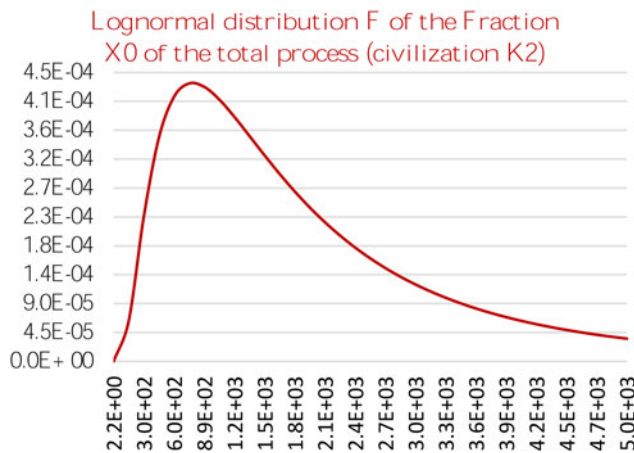


Figure 36. Lognormal of the distribution of dynamic civilizations with $\langle N \rangle = 2.214$ and $\sigma(N) = 2.224$.

planetary system of origin. We obtained the two results distinct from a reflection born from the conclusions taken from the seventh parameter. It is obvious, from simple energy calculations related to the cost in terms of the power of an interstellar space ship, why this limit value of $K = 1.4$ has been chosen: to accelerate a large space ship, say of 10^9 kg halfway to the speed of light (1.5×10^8 m s⁻¹) in about 3 months (about 10^7 s), a power of about 10^{18} W is required which, reasonably assuming that it represents 1% of the total power expressed by the civilization in question, leads us to a total power of $W_{\text{tot}} = 10^{20}$ W, which is to say:

$$K = \frac{\log_{10} 10^{20} - 5}{11} = 1.4.$$

Table 27. *The result of Drake's equation for static and dynamic civilizations*

Sum average log.	Sum variance log.	Average number ETC	Deviation number ETC	
μ	σ^2	$\langle N \rangle$	$\sigma(N)$	
1.02	0.41	3	2	Static civilizations $K < 1.4$
7.35	0.70	2.214	2.224	Dynamic civilizations $K > 1.4$

Table 28. *Temporal scale of the evolution of a galactic civilization (terrestrial model)*

Stage of life development	Duration	Chronology	
1 – ADEAN	0.80	0.80	Gy
2 – Prokaryote	0.10	0.90	Gy
3 – GOE	1.60	2.50	Gy
4 – Eukaryotes	0.50	3.00	Gy
5 – NOE	0.50	3.50	Gy
6 – Metazoa	0.50	4.00	Gy
7 – Past static ETC	0.50	4.50	Gy
8 – Present static ETC	0.05	4.55	Gy
9 – Dynamics ETC	0.40	4.95	Gy

Therefore, the result obtained for static and dynamic civilizations is that reported in Table 27, that is:

Average ETC number	Deviation ETC number	
$\langle N \rangle$	$\sigma(N)$	
3	2	Static civilizations
2214	2224	Dynamic civilizations

At this point, we leave aside for a moment the discussion of galactic civilizations to show the entire set of results that have been obtained using this method.

The third parameter, as we have seen, provided us with the number of stable planets as the function of the variable time ΔT . Now knowing the duration of all the processes of evolution of life, from the prokaryote level to the K2 civilization, we can count:

- (A) how many are the planets suitable for every level of development
- (B) how many of these hosted life
- (C) how many of these still host it

As we have seen, the dead times of the Hadean period (development of the planet), of the GOE (first increase of oxygen to 1% of the current value) and the NOE (according to the oxygen to the current value) must also be considered. By combining these times with the step-by-step calculation of the log-normal, the timescale shown in Table 28 is obtained, where we followed the terrestrial model of life:

Taking into account the results obtained, in the calculation of third parameter, for the percentage of past and present stable planets for ΔT years (Fig. 4(a) and (b)), Table 29 and Fig. 37 show the population of galactic life and its relative distances from us. In Appendix B, we show the complete calculation from which the data were obtained.

Table 29. The population of the galactic life and the relative distances from us of both suitable planets and planets suitable and populated in the past and in the present: an average volume of the galactic disk has been assumed of $1.53 \times 10^{13} \text{ al}^3$

	Age of Planet (Gy)	number of planets that hosted or host life	distance (ly)	total of suitable planets	distance (ly)
A	0.90	710,000,000 planets where prokaryotes were born in the past	28	1,500,000,000	22
B		92,000,000 planets where prokaryotes are present today	55	190,000,000	43
C	3.00	81,000,000 planets where eukaryotes were born in the past	57	330,000,000	36
D		35,000,000 planets where eukaryotes are present today	76	140,000,000	48
E	4.00	35,000,000 planets where metazoa were born in the past	76	190,000,000	43
F		20,000,000 planets where metazoa today are present	91	110,000,000	52
G	4.50	470,000 planets where static ETC K1 were born in the past	319	140,000,000	48
H		3 planets where static ETC K1 are present today	16.515	92,000,000	48
I	4.95	2,200 current planets with ETC K2 Dynamics (eternal)	1.909	92,000,000	48

See note in the [Appendix B](#) for the calculation of distances in the volume of the galactic disc.

The Fermi paradox and conclusions

We found, surprisingly enough that the number of current planets inhabited by galactic civilizations of type K1 (or with K lower), lasting an average of 50 000 years, is 3, that is, *us* and, perhaps, someone else at about 17 000 ly from us – therefore, very distant.

If we only considered static civilizations or civilizations that have not accomplished the jump beyond $K=1$ that would allow them to move between the stars, the Fermi paradox would, in fact, be resolved (Hart, 1975). Of course, to satisfy our desire for company in the galaxy, there would be a multitude of planets that host life in none-too advanced forms or that have hosted civilizations which are now extinct: this is bread and butter for astro-biologists or astro-archaeologists, but nothing more than that...but instead, there is more. Just as it is the case for life forms that arise in a certain niche and that, if conditions allow it, colonize the whole ecosystem, similarly, if a galactic civilization exceeded the seven challenges of the seventh parameter and reached the energy value of Kardašev $K=1.4$ then it would colonize the entire galaxy and become *eternal*: in this case, there would be over 2000 current civilizations, all highly evolved and travelling through the galaxy.

The Fermi paradox therefore reappears in another form: it is not civilizations like ours that are missing from the role call and which are residual, but the super-civilizations hypothesized by Kardašev. The point would be that we must not necessarily look for them on a specific planet because these civilizations also move between one star and another and it would be much easier for them to find us rather than the reverse. So, the question we should ask ourselves is another: if we were a super-civilization capable of moving around the galaxy, where would we choose to go? Would solar systems like ours (and ourselves who, as we have seen, in addition to being alone, as a K1 civilization, we have only a 0.4% probability of becoming K2 civilization) be *attractive* for these civilizations? Red dwarf stars, much longer-lasting than the sun, or even the dead stars, such as black holes and neutron stars, perhaps exploitable as hypothetical sources of energy would probably be more attractive (Sweeney *et al.*, 2022).

The journey we have taken has brought us, therefore, to the following conclusions:

- (a) In the galaxy, as a *primitive* K1 (actually lower than K1) civilization, we are almost alone, there being at the moment around three ETCs including us; a civilization like ours forms for every 20 000 years and has a probability of not extinguishing itself of just above 0.4% (1 out of 250).

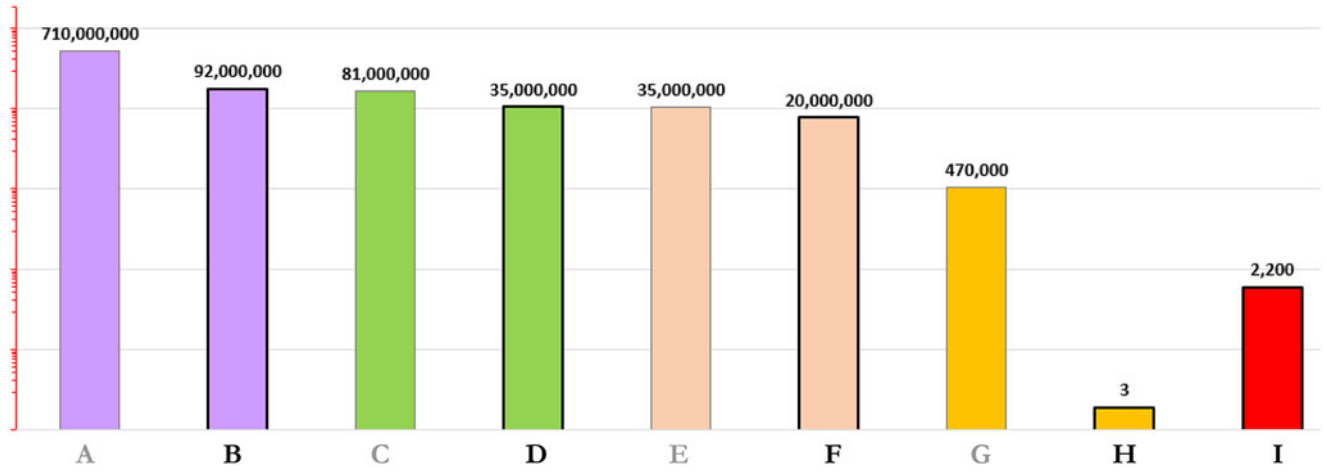


Figure 37. The data of [Table 29](#) (number planets who hosted or host the life) are reported in logarithmic graphics.

- (b) There are already almost half a million extinct civilizations like these in the galaxy.
- (c) On the contrary, if they exceeded the seven challenges of the seventh parameter, about 2000 super-civilizations, of level K2, or almost, could exist in the galaxy, one forming every 5 My.
- (d) In this case, these super-civilizations would now be free to move between one planetary system and the other and would probably be within 50 light years of us (that is, the distance of the nearest habitable planets and usable as transit stations). The possible organization and intentions of these super-civilizations are at the moment obscure to us and could be examined in our future research.
- (e) The rest of the galaxy is a jungle of life forms at various levels of development (tens of millions of planets inhabited by living forms).

While statements *d* and *e* on super-civilizations are based on the correct understanding of the seventh Drake parameter and therefore concern futurology, all the other statements, thanks to the mathematical discussion inspired by Maccone, are firmly anchored to their reference parameters and no longer range, as we have too often seen them do, between dozens and dozens of orders of magnitude between the maximum and minimum values of uncertainty. A statement, for example, on the probability of the onset of prokaryotic life must now be strictly compared with the mathematical process that we have shown: if we have to re-discuss or review it, we must also review the process that guides its parameter (in this case the fourth Drake parameter). This is the greatest advantage obtained from this type of discussion and by the method inaugurated by Claudio Maccone in 2008 with his lognormal.

We do one last socio-political observation. One of the consequences of this analysis is that we have understood, at least in principle, where the real *bottlenecks* in the evolution of a galactic civilization are:

- (A) a first intensive selection skimming of life forms that become ETC (about 1/70 of the planets that host animal life forms)
- (B) a second dramatic reduction due to the technological challenges of the seventh parameter (about 1/250 of the ETCs who developed)

While we have no control over point A, point B tells us that the *great silence* consequent to the Fermi paradox warns us about the scarce possibilities a civilization has of surviving – above all of surviving itself. That is to say, we should understand that we must do everything possible to raise that intimidatingly low percentage of 0.4% of surviving our own technology to less severe values that give us a minimum of stimulus to carry on as a species and as a planet ... despite everything

Acknowledgements. We thank Professor Stephen Webb for the inspiration on many of the topics covered and for the encouragement he has given us to complete this work. Dr Richard McKenna is thanked for the fundamental help in translation of the manuscript. We also want to thank Dr Manuela Miggiano for her useful suggestions on nucleic acids.

Author contributions. C. Maccone, with his main works Mathematical SETI and EVOSETI, indicated the method that was followed in the entire article. He supervised the drafting of work and suggested precious changes. A.M.F. Valli took care of all the chemical, biological and palaeontological part relating to the fourth and fifth Drake parameter. E. Mieli has formulated the mathematical models used in all Drake parameters and developed the analysis relating to the astronomical parameters (first, second and third) and to the social ones (sixth and seventh).

Financial support. This research received no specific grant from any funding agency, commercial or not-for-profit sectors.

Conflict of interest. None.

References

- Agno M (1991) *Dal Non Vivente al Vivente*. Rome–Naples, Italy: Theoria.
- Agno M (1992a) *Punti Cardinali*. Milan, Italy: Sperling and Kupfer.
- Agno M (1992b) *La Macchina Batterica*. Rome, Italy: Lombardo Editore.
- Altamura E, Milano F, Tangorra RR, Trotta M, Omar OH, Stano P and Mavelli F (2017) Highly oriented photosynthetic reaction centers generate a proton gradient in synthetic protocells. *Proceedings of the National Academy of Sciences* **114**, 3837–3842.
- Altamura E, Albanese P, Marotta R, Milano F, Fiore M, Trotta M, Stano P and Mavelli F (2020) Light-driven ATP production promotes mRNA biosynthesis inside hybrid multi-compartment artificial protocells. *bioRxiv*, <https://doi.org/10.1101/2020.02.05.933846>.

- Amodio P, Boeckle M, Schnell AK, Ostojic L, Fiorito G and Clayton NS (2019) Grow smart and die young: why did cephalopods evolve intelligence? *Trends in Ecology and Evolution* **34**, 45–56.
- Anders E (1989) Pre-biotic organic matter from comets and asteroids. *Nature* **342**, 255–257.
- Andrade-Ines E, Beaugé C, Michtchenko T and Robutel P (2016) Secular dynamics of S-type planetary orbits in binary star systems: applicability domains of first- and second-order theories. *Celestial Mechanics and Dynamical Astronomy* **124**, 405–432.
- Aravind L, Tatusov RL, Wolf YI, Walker DR and Koonin EV (1998) Evidence for massive gene exchange between archaeal and bacterial hyperthermophiles. *Trends in Genetics* **14**, 442–444.
- Archibald J (2014) *One Plus One Equals One – Symbiosis and the Evolution of Complex Life*. Oxford, UK: Oxford University Press.
- Arensburg B, Tillier AM, Vandermeersch B, Duday H, Schepartz LA and Rak Y (1989) A middle palaeolithic human hyoid bone. *Nature* **338**, 758–760.
- Baker BJ, Tyson GW, Webb RI, Flanagan J, Hugenholtz P, Allen EE and Banfield JF (2006) Lineages of acidophilic archaea revealed by community genomic analysis. *Science* **314**, 1933–1935.
- Baker BJ, De Anda V, Seitz KW, Dombrowski N, Santoro AE and Lloyd KG (2020) Diversity, ecology and evolution of archaea. *Nature Microbiology* **5**, 887–900.
- Ball P (2017) Water is an active matrix of life for cell and molecular biology. *Proceedings of the National Academy of Sciences* **114**, 13327–13335.
- Bapteste E (2013) *Les gènes voyageurs – L'odyssée de l'évolution*. Paris, F: Belin.
- Barge LM, Doloboff IJ, Russell MJ, Vandervelde D, White LM, Stucky GD, Baum MM, Zeytounian J, Kidd R and Kanik I (2014) Pyrophosphate synthesis in iron mineral films and membranes simulating prebiotic submarine hydrothermal precipitates. *Geochimica et Cosmochimica Acta* **128**, 1–12.
- Barker J, Grigg GC and Tyler JM (1996) *A Field Guide to Australian Frogs*. Sidney, AU: Surrey Beatty and Sons.
- Bartel DP and Unrau PJ (1999) Constructing an RNA world. *Trends in Cell Biology* **9**, M9–M13.
- Baum DA and Baum B (2014) An *inside-out* origin for the eukaryotic cell. *BMC Biology* **12**, 1–22.
- Baum B and Baum DA (2020) The merger that made us. *BMC Biology* **18**, 1–4.
- Benton MJ (2014) *Vertebrate Palaeontology*, 4th Edn. New York, NY: John Wiley and Sons.
- Berkeley University (2022) Introduction to the Hadean. <https://ucmp.berkeley.edu/precambrian/hadean.html>.
- Bidartondo MI, Read DJ, Trappe JM, Merckx V, Ligrone R and Duckett JG (2011) The dawn of symbiosis between plants and fungi. *Biology Letters* **7**, 574–577.
- Bolton JR, Strickler SJ and Connolly JS (1985) Limiting and realizable efficiencies of solar photolysis of water. *Nature* **316**, 495–500.
- Bonomo AS, Desidera S, Benatti S, Borsa F, Crespi S, Damasso M, Lanza AF, Sozzetti A, Lodato G, Marzari F, Boccato C, Claudi RU, Cosentino R, Covino E, Gratton R, Maggio A, Micela G, Molinari E, Pagano I, Piotto G, Poretti E, Smareglia R, Affer L, Biazio K, Bignamini A, Esposito M, Giacobbe P, Hébrard G, Malavolta L, Maldonado J, Mancini L, Martinez Fiorenzano A, Masiero R, Nascimbeni V, Pedani M, Rainer M and Scandariato G (2017) The GAPS programme with HARPS-N at TNG-XIV. Investigating giant planet migration history via improved eccentricity and mass determination for 231 transiting planets. *Astronomy and Astrophysics* **602**, A107.
- Brin GD (1983) The 'great silence': the controversy concerning extraterrestrial intelligent life. *QJR Astronomical Society* **24**, 283–309.
- Broom R (1938) The Pleistocene anthropoid apes of South Africa. *Nature* **142**, 377–379.
- Brown AJ and Galea AM (2010) Cholesterol as an evolutionary response to living with oxygen. *Evolution: International Journal of Organic Evolution* **64**, 2179–2183.
- Burcar BT, Barge LM, Trail D, Watson EB, Russell MJ and McGown LB (2015) RNA oligomerization in laboratory analogues of alkaline hydrothermal vent systems. *Astrobiology* **15**, 509–522.
- Butterfield NJ (2000) *Bangiomorpha pubescens* n. gen., n. sp.: implications for the evolution of sex multicellularity, and the Mesoproterozoic/Neoproterozoic radiation of eukaryotes. *Paleobiology* **26**, 387–404.
- Butterfield NJ (2004) A vaucheriacean alga from the middle Neoproterozoic of Spitsbergen: implications for the evolution of Proterozoic eukaryotes and the Cambrian explosion. *Paleobiology* **30**, 231–252.
- Butterfield NJ, Knoll AH and Sweet K (1990) A bangiophyte red alga from the Proterozoic of Arctic Canada. *Science* **250**, 104–107.
- Cabezón E, Ripoll-Rozada J, Peña A, De La Cruz F and Arechaga I (2015) Towards an integrated model of bacterial conjugation. *FEMS Microbiology Reviews* **39**, 81–95.
- Cafferty BJ and Hud NV (2014) Abiotic synthesis of RNA in water: a common goal of prebiotic chemistry and bottom-up synthetic biology. *Current Opinion in Chemical Biology* **22**, 146–157.
- Camprubí A, González-Partida E, Torró L, Pura A, Canet C, Miranda-Gasca MA, Martini M and González-Sánchez F (2017) Mesozoic volcanogenic massive sulfide (VMS) deposits in Mexico. *Ore Geology Reviews* **81**, 1066–1083.
- Capasso L, Michetti E and D'Anastasio R (2008) A *Homo erectus* hyoid bone: possible implications for the origin of the human capability for speech. *Collegium Antropologicum* **32**, 1007–1011.
- Carr M, Leadbeater BS and Baldauf SL (2010) Conserved meiotic genes point to sex in the choanoflagellates. *Journal of Eukaryotic Microbiology* **57**, 56–62.
- Carroll RL (1964) The earliest reptiles. *Journal of the Linnean Society of London, Zoology* **45**, 61–83.

- Castanier S, Perthuisot J-P, Maurin A, Gèze V and Camoin G (1994) Colonies bactériennes organisées actuelles. Quelques réflexions sur l'évolution des procaryotes. *Géobios* **27**, 645–657.
- Cavalier-Smith T (2002) Chloroplast evolution: secondary symbiogenesis and multiple losses. *Current Biology* **12**, 62–64.
- Chambers JE (2006) Planet formation with migration. *The Astrophysical Journal* **652**, L133.
- Chaplin MF (2001) Water: its importance to life. *Biochemistry and Molecular Biology Education* **29**, 54–59.
- Chavanis P-H, Denet B, Le Berre M and Pomeau Y (2019) Supernova implosion–explosion in the light of catastrophe theory. *The European Physical Journal B* **92**, 1–36.
- Chivers DJ, Anandam MV, Groves CP, Molur S, Rawson BM, Richardson MC, Roos C, Whittaker DM, Heredia A, Cordero G, Camprubí A, Negrón-Mendoza A, Ortega-Gutiérrez F, Beraldi H and Ramos-Bernal S (2016) Hydrothermal vents and prebiotic chemistry: a review. *Boletín de la Sociedad Geológica Mexicana* **68**, 599–620.
- Colín-García M, Heredia A, Cordero G, Camprubí A, Negrón-Mendoza A, Ortega-Gutiérrez F, Beraldi H and Ramos-Bernal S (2016) Hydrothermal vents and prebiotic chemistry: a review. *Boletín de la Sociedad Geológica Mexicana* **68**, 599–620.
- Crossfield IJ, Malik M, Hill ML, Kane SR, Foley B, Alex SAS, Coria D, Brande J, Zhang Y, Wienke K, Kreidberg L, Cowan NB, Dragomir D, Gorjian V, Mikal-Evans T, Benneke B, Christiansen JL, Deming D and Morales FY (2022) GJ 1252b: a hot terrestrial super-earth with no atmosphere. *The Astrophysical Journal Letters* **937**, L17.
- Crowe SA, Døssing LN, Beukes NJ, Bau M, Kruger SJ, Frei R and Canfield DE (2013) Atmospheric oxygenation three billion years ago. *Nature* **501**, 535–538.
- Da Cunha V, Gaia M, Gadelle D, Nasir A and Forterre P (2017) Lokiarchaea are close relatives of Euryarchaeota, not bridging the gap between prokaryotes and eukaryotes. *PLoS Genetics* **13**, 1–24.
- Dalrymple GB (2001) The age of the Earth in the twentieth century: a problem (mostly) solved. *Geological Society Special Publications* **190**, 205–221.
- Dasgupta R (2013) Ingassing, storage, and outgassing of terrestrial carbon through geologic time. *Reviews in Mineralogy and Geochemistry* **75**, 183–229.
- DasGupta S (2020) Molecular crowding and RNA catalysis. *Organic and Biomolecular Chemistry* **18**, 7724–7739.
- Dawson JW (1860) On a terrestrial mollusk, a *Chilognathous* myriapod, and some new species of reptiles, from the coal-formation of Nova Scotia. *Quarterly Journal of the Geological Society of London* **16**, 268–277.
- Dawson RI and Johnson JA (2018) Origins of hot Jupiters. *Annual Review of Astronomy and Astrophysics* **56**, 175–221.
- de Boer B (2017) Evolution of speech and evolution of language. *Psychonomic Bulletin and Review* **24**, 158–162.
- Dehaene S, Dehaene-Lambertz G and Cohen L (1998) Abstract representations of numbers in the animal and human brain. *Trends in Neuroscience* **21**, 355–361.
- DeLong EF and Pace NR (2001) Environmental diversity of bacteria and archaea. *Systematic Biology* **50**, 470–478.
- de Reviers B (2018) Les associations dans l'évolution du vivant. In Palka L (ed). *Microbiodiversité – Un Nouveau Regard*. Paris: Éditions Matériologiques, pp. 51–103.
- Dodd MS, Papineau D, Grenne T, Slack JF, Rittner M, Pirajno F, O'Neil J and Little CT (2017) Evidence for early life in Earth's oldest hydrothermal vent precipitates. *Nature* **543**, 60–64.
- Dole SH (1964) *Habitable Planets for Man*. Santa Monica, CA: Rand Corporation.
- Doudna JA and Charpentier E (2014) The new frontier of genome engineering with CRISPR-Cas9. *Science* **346**, 1258096.
- Doyle L, Ramsay G and Doyle JG (2020) Superflares and variability in solar-type stars with TESS in the Southern hemisphere. *Monthly Notices of the Royal Astronomical Society* **494**, 3596–3610.
- Drake FD (1961) *US Academy of Sciences Conference on Extraterrestrial Intelligent Life*. Green Bank: West Virginia.
- Dubois E (1893) Palaeontologische onderzoekingen op Java. *Verslag Mijlwezen* **10**, 10–14.
- Egas C, Barroso C, Froufe HJC, Pacheco J, Albuquerque L and da Costa MS (2014) Complete genome sequence of the radiation-resistant bacterium *Rubrobacter radiotolerans* RSPS-4. *Standards in Genomic Sciences* **9**, 1062–1075.
- Eggink LL, Park H and Hooper JK (2001) The role of chlorophyll b in photosynthesis: hypothesis. *BMC Plant Biology* **1**, 1–7.
- El Albani A, Mangano MG, Buatois LA, Bengtson S, Riboulleau A, Bekker A, Konhauser K, Lyons T, Rollion-Bard C, Bankole O, Lekele Baghekema SG, Meunier A, Trentesaux A, Mazurier A, Aubineau J, Laforest C, Fontaine C, Recourt P, Chi Fru E, Macchiarelli E, Reynaud JY, Gauthier-Lafaye F and Canfield DE (2019) Organism motility in an oxygenated shallow-marine environment 2.1 billion years ago. *Proceedings of the National Academy of Sciences* **116**, 3431–3436.
- Eme L and Ettema TJG (2018) The eukaryotic ancestor shapes up. *Nature* **562**, 352–353.
- Emelyanov VV (2001) Evolutionary relationship of Rickettsiae and mitochondria. *FEBS Letters* **501**, 11–18.
- Ereskovsky AV (2010) *The Comparative Embryology of Sponges*. New York, NY: Springer.
- Erik G (2009) *The Milky Way and Beyond Stars*. Britannica Educational Publishing, pp. 35–38.
- Erwin DH and Valentine JW (2013) *The Cambrian Explosion – The Construction of Animal Biodiversity*. Greenwood Village, CO: Roberts and Company.
- Ettema TJ, Lindås AC and Bernander R (2011) An actin-based cytoskeleton in archaea. *Molecular Microbiology* **80**, 1052–1061.
- Fei Y, Seagle CT, Townsend JP, McCoy CA, Boujibar A, Driscoll P, Shulenburg L and Furnish MD (2021) Melting and density of MgSiO₃ determined by shock compression of bridgmanite to 1254 GPa. *Nature Communications* **12**, 1–9.
- Ferla MP, Thrash JC, Giovannoni SJ and Patrick WM (2013) New rRNA gene-based phylogenies of the Alphaproteobacteria provide perspective on major groups, mitochondrial ancestry and phylogenetic instability. *PLoS ONE* **8**, 1–14.
- Ferreira AC, Nobre MF, Moore E, Rainey FA, Battista JR and da Costa MS (1999) Characterization and radiation resistance of new isolates of *Rubrobacter radiotolerans* and *Rubrobacter xylanophilus*. *Extremophiles* **3**, 235–238.

- Fierer N and Jackson RB (2006) The diversity and biogeography of soil bacterial communities. *Proceedings of the National Academy of Sciences* **103**, 626–631.
- Fleagle JG (2013) *Primate Adaptation and Evolution*, 3d Edn. London, UK: Academic Press.
- Flemming HC and Wuertz S (2019) Bacteria and archaea on Earth and their abundance in biofilms. *Nature Reviews Microbiology* **17**, 247–260.
- Foley SF and Fischer TP (2017) An essential role for continental rifts and lithosphere in the deep carbon cycle. *Nature Geoscience* **10**, 897–902.
- Forterre P (2007) *Microbes de l'enfer*. Paris, France: Belin pour la Science.
- Forterre P and Gaïa M (2018) *Microbiodiversité, Un nouveau regard. Éditions Matériologiques*. Paris, pp. 23–49.
- Forterre P, Gribaldo S and Brochier C (2005) Luca: à la recherche du plus proche ancêtre commun universel. *Médecine Sciences* **21**, 860–865.
- Fracchia TP, Smith GP, Zanchetta G, Paraboschi E, Yi Y, Walba DM, Dieci G, Clark NA and Bellini T (2015) Abiotic ligation of DNA oligomers templated by their liquid crystal ordering. *Nature Communications* **6**, 1–8.
- Fry I (2000) *The Emergency of Life on Earth – A Historical and Scientific Overview*. New Brunswick, NJ: Rutgers University Press.
- Garwood RJ, Oliver H and Spencer AR (2020) An introduction to the Rhynie chert. *Geological Magazine* **157**, 47–64.
- Génémont J (2014) *Une histoire naturelle de la sexualité – Plus d'un milliard d'années d'évolution*. Paris, France: Éditions Matériologiques.
- Gest H (2002) History of the word photosynthesis and evolution of its definition. *Photosynthesis Research* **73**, 7–10.
- Gibson TM, Shih PM, Cumming VM, Fischer WW, Crockford PW, Hodgskiss MS, Würndle S, Creaser RA, Rainbird RH, Skulski TM and Halverson GP (2018) Precise age of *Bangiomorpha pubescens* dates the origin of eukaryotic photosynthesis. *Geology* **46**, 135–138.
- Goëdel K (1931) Über formal unentscheidbare Sätze der Principia Mathematica und verwandter Systeme, I. *Monatshefte für Mathematik und Physik* **38**, 173–198.
- Gogarten JP, Doolittle WF and Lawrence JG (2002) Prokaryotic evolution in light of gene transfer. *Molecular Biology and Evolution* **19**, 2226–2238.
- Gomes R, Levison HF, Tsiganis K and Morbidelli A (2005) Origin of the cataclysmic Late Heavy Bombardment period of the terrestrial planets. *Nature* **435**, 466–469.
- Gonzalez G (2005) The galactic habitable zone. *Astrophysics of Life* **16**, 89–97.
- Gonzalez G, Brownlee D and Ward P (2001) The galactic habitable zone: galactic chemical evolution. *Icarus* **152**, 185–200.
- Gott JR (1993) Implications of the Copernican principle for our future prospects. *Nature* **363**, 315–319.
- Gould SJ (1989) *Wonderful Life: The Burgess Shale and the Nature of History*. New York, NY: W. W. Norton and Co.
- Gray MW, Lang BF and Burger G (2004) Mitochondria of protists. *Annual Review of Genetics* **38**, 477–524.
- Green NJ, Xu J and Sutherland JD (2021) Illuminating life's origins: UV photochemistry in abiotic synthesis of biomolecules. *Journal of the American Chemical Society* **143**, 7219–7236.
- Grimaud-Hervé D (1997) *L'évolution de l'encéphale chez Homo erectus et Homo sapiens: exemples de l'Asie et de l'Europe*. Cahiers de paléanthropologie. France: CNRS Editions.
- Gros C (2005) Expanding advanced civilizations in the universe. *JBIS* **58**, 1–3.
- Hagadorn JW, Xiao S, Donoghue PC, Bengtson S, Gostling NJ, Pawlowska M, Raff EC, Raff RA, Turner FR, Chongyu Y, Zhou C, Yuan X, McFeely MB, Stambanoni M and Neelson KH (2006) Cellular and subcellular structure of Neoproterozoic animal embryos. *Science* **314**, 291–294.
- Hammond AS, Rook L, Anaya AD, Cioppi E, Costeur L, Moyà-Solà S and Almécija S (2020) Insights into the lower torso in late Miocene hominoid *Oreopithecus bambolii*. *Proceedings of the National Academy of Sciences* **117**, 278–284.
- Han B, Lin CCJ, Hu G and Wang MC (2019) 'Inside out' – a dialogue between mitochondria and bacteria. *The FEBS Journal* **286**, 630–641.
- Harrington JD, Morcene J and Watzke M (2008) Discovery of most recent supernova in our galaxy. https://chandra.harvard.edu/press/08_releases/press_051408.html.
- Hart MH (1975) An explanation for the absence of extraterrestrials on earth. *Quarterly Journal of the Royal Astronomical Society* **16**, 128–135.
- Higgs PG and Lehman N (2015) The RNA world: molecular cooperation at the origins of life. *Nature Reviews Genetics* **16**, 7–17.
- Holland HD (2006) The oxygenation of the atmosphere and oceans. *Philosophical Transactions of the Royal Society B: Biological Sciences* **361**, 903–915.
- Houslay MD and Stanley KK (1982) *Dynamics of Biological Membranes*. Chichester, UK: Wiley.
- HyperPhysics (2014) Populations I and II stars. <http://hyperphysics.phy-astr.gsu.edu/hbase/Starlog/pop12.html>.
- Imachi H, Nobu MK, Nakahara N, Morono Y, Ogawara M, Takaki Y, Takano Y, Uematsu K, Ikuta T, Ito M, Matsui Y, Miyazaki M, Murata K, Saito Y, Sakai S, Song C, Tasumi E, Yamanaka Y, Yamaguchi T, Kamagata Y, Tamaki H and Takai K (2020) Isolation of an archaeon at the prokaryote–eukaryote interface. *Nature* **577**, 519–525.
- Izidoro A (2022) The exoplanet radius valley from gas-driven planet migration and breaking of resonant chains. *The Astrophysical Journal Letters* **939**, L19.
- Janvier P (1996) *Early Vertebrates*. Oxford, UK: Clarendon Press.

- Javaux EJ, Knoll AH and Walter MR (2001) Morphological and ecological complexity in early eukaryotic ecosystems. *Nature* **412**, 66–69.
- Javaux EJ, Marshall CP and Bekker A (2010) Organic-walled microfossils in 3.2-billion year-old shallow-marine siliciclastic deposits. *Nature* **463**, 934–938.
- Johansen A, Ida S and Brasser R (2019) How planetary growth outperforms migration. *Astronomy and Astrophysics* **622**, A202.
- Kardašev NS (1964) *Transmission of Information by Extraterrestrial Civilizations*. Soviet Astronomy, pp. 217–221.
- Kasting JF (2013) What caused the rise of atmospheric O₂? *Chemical Geology* **362**, 13–25.
- Kauffman SA (2011) Approaches to the origin of life on earth. *Life* **1**, 34–48.
- Kemp TS (2005) *The Origin and Evolution of Mammals*. New York: Oxford University Press, pp. 90–135.
- Kenyon SJ, Najita JR and Bromley BC (2016) Rocky planet formation: quick and neat. *The Astrophysical Journal* **831**, 8.
- Kerskens CM and Pérez DL (2022) Experimental indications of non-classical brain functions. *Journal of Physics Communications* **6**, 105001.
- Kiang NY, Siefert J and Blankenship RE (2007) Spectral signatures of photosynthesis. I. Review of Earth organisms. *Astrobiology* **7**, 222–251.
- King W (1864) On the Neanderthal skull, or reasons for believing it to belong to the Clyidian Period and to a species different from that represented by man. *British Association for the Advancement of Science, Notices and Abstracts for 1863* 82.
- King GW, Wheatley PJ, Salz M, Bourrier V, Czesla S, Ehrenreich D, Kirk J, Lecavelier des Etangs A, Louden T, Schmitt J and Schneider PC (2018) The XUV environments of exoplanets from Jupiter-size to super-Earth. *Monthly Notices of the Royal Astronomical Society* **478**, 1193–1208.
- Klug C, De Baets K, Kröger B, Bell MA, Korn D and Payne JL (2015) Normal giants? Temporal and latitudinal shifts of Palaeozoic marine invertebrate gigantism and global change. *Lethaia* **48**, 267–288.
- Knoll AH (2015) *Life in a Young Planet – The First Three Billion Years of Evolution on the Earth*. Princeton, NJ: Princeton University Press.
- Knoll AH, Javaux EJ, Hewitt D and Cohen P (2006) Eukaryotic organisms in Proterozoic oceans. *Philosophical Transactions of the Royal Society B: Biological Sciences* **361**, 1023–1038.
- Koga Y and Morii H (2007) Biosynthesis of ether-type polar lipids in archaea and evolutionary considerations. *Microbiology and Molecular Biology Reviews* **71**, 97–120.
- Koonin EV (2003) Comparative genomics, minimal gene-sets and the last universal common ancestor. *Nature Reviews Microbiology* **1**, 127–136.
- Krause AJ, Mills BJ, Zhang S, Planavsky NJ, Lenton TM and Poulton SW (2018) Stepwise oxygenation of the Paleozoic atmosphere. *Nature Communications* **9**, 1–10.
- Krissansen-Totton J and Catling DC (2020) A coupled carbon–silicon cycle model over Earth history: reverse weathering as a possible explanation of a warm mid-Proterozoic climate. *Earth and Planetary Science Letters* **537**, 116181.
- Krissansen-Totton J, Arney GN and Catling DC (2018) Constraining the climate and ocean pH of the early Earth with a geological carbon cycle model. *Proceedings of the National Academy of Sciences* **115**, 4105–4110.
- Kulikov YN, Lammer H, Lichtenegger HIM, Terada N, Ribas I, Kolb C, Langmayr D, Lundin R, Guinan EF, Barabash S and Biernat HK (2006) Atmospheric and water loss from early Venus. *Planetary and Space Science* **54**, 1425–1444.
- Kunimoto M and Matthews JM (2020) Searching the entirety of Kepler data. II. Occurrence rate estimates for FGK stars. *The Astronomical Journal* **159**, 248.
- Kwok S (2007) *Physics and Chemistry of the Interstellar Medium*. Melville, NY: University Science Books.
- Kwok S (2017) Abiotic synthesis of complex organics in the universe. *Nature Astronomy* **1**, 642–643.
- Lada CJ (2006) Stellar multiplicity and the IMF: most stars are single. *The Astrophysical Journal Letters* **640**, L63–L66. doi: 10.1086/503158
- Lane N (2002) *Oxygen: The Molecule That Made the World*. Oxford, UK: Oxford University Press.
- Lane N (2015) *The Vital Question – Energy, Evolution, and the Origin of the Complex Life*. New York, NY: W. W. Norton and Company.
- Lane N and Martin W (2010) The energetics of genome complexity. *Nature* **467**, 929–934.
- Lang BF, O’kelly C, Nerad T, Gray MW and Burger G (2002) The closest unicellular relatives of animals. *Current Biology* **12**, 1773–1778.
- Lazcano A and Miller SL (1996) The origin and early evolution of life: prebiotic chemistry, the pre-RNA world, and time. *Cell* **85**, 793–798.
- Lecoitre G and Le Guyader H (2017) *Classification Phylogénétique du Vivant*, 4th Edn. Paris, France: Belin.
- Ledrew G (2001) The real starry sky. *Journal of the Royal Astronomical Society of Canada* **95**, 32.
- Lefebvre B (2022) *La diversification des échinodermes au Paléozoïque inférieur: l’apport des gisements à préservation exceptionnelle*. Lyons, France: Dédale Éditions.
- Lei L and Burton ZF (2020) Evolution of life on Earth: tRNA, aminoacyl-tRNA synthetases and the genetic code. *Life* **10**, 1–22.
- Lichtenegger HIM, Lammer H, Griesbeier JM, Kulikov YN, von Paris P, Hausleitner W, Krauss S and Rauer H (2010) Aeronomical evidence for higher CO₂ levels during Earth’s Hadean epoch. *Icarus* **210**, 1–7.
- Lindsay MR, Webb RI, Strous M, Jetten MS, Butler MK, Forde RJ and Fuerst JA (2001) Cell compartmentalisation in planctomycetes: novel types of structural organisation for the bacterial cell. *Archives of Microbiology* **175**, 413–429.

- Linnaeus C (1758) *Systema naturae*. Stockholm, SW: Holmiae (Laurentii Salvii).
- Lipowsky R and Sackmann E (eds) (1995) *Structure and Dynamics of Membranes (Handbook of Biological Physics vol 1)*. Amsterdam, HO: Elsevier.
- Liu Y, Makarova KS, Huang WC, Wolf YI, Nikolskaya AN, Zhang X, Cai M, Zhang C-J, Xu W, Luo Z, Cheng L, Koonin EV and Li M (2021) Expanded diversity of Asgard archaea and their relationships with eukaryotes. *Nature* **593**, 553–557.
- Lovley DR, Phillips EJP, Borby YA and Landa ER (1991) Microbial reduction of uranium. *Nature* **350**, 413–416.
- Low HH and Löwe J (2006) A bacterial dynamin-like protein. *Nature* **444**, 766–769.
- Lozupone CA and Knight R (2007) Global patterns in bacterial diversity. *Proceedings of the National Academy of Sciences* **104**, 11436–11440.
- Lynden-Bell RM, Morris SC, Barrow JD, Finney JL and Harper C (eds) (2010) *Water and Life: The Unique Properties of H₂O*. Boca Raton, FL: CRC Press.
- Lyons TW, Reinhard CT and Planavsky NJ (2014) The rise of oxygen in Earth's early ocean and atmosphere. *Nature* **506**, 307–315.
- Maccone C (2010) The statistical Drake equation. *Acta Astronautica* **67**, 1366–1383.
- Maccone C (2015) Statistical Drake–Seager equation for exoplanet and SETI searches. *Acta Astronautica* **115**, 277–285.
- MacLeod F, Kindler GS, Wong HL, Chen R and Burns BP (2019) Asgard archaea: diversity, function, and evolutionary implications in a range of microbiomes. *AIMS Microbiology* **5**, 48–61.
- MacNaughton RB, Cole JM, Darlympe RW, Braddy SJ, Briggs DEG and Lukie TD (2002) First steps on land: arthropod trackways in Cambrian–Ordovician eolian sandstone, southeastern Ontario, Canada. *Geology* **30**, 391–394.
- Maehara H, Shibayama T, Notsu S, Notsu Y, Nagao T, Kusaba S, Honda S, Nogami D and Shibata K (2012) Superflares on solar-type stars. *Nature* **485**, 478–481.
- Mallove E and Matloff G (1989) *The Starflight Handbook: A Pioneer's Guide to Interstellar Travel*. Hoboken, NJ: John Wiley and Sons, Inc.
- Maloof AC, Porter SM, Moore JL, Dudás FÖ, Bowring SA, Higgins JA, Fike DA and Eddy MP (2010) The earliest Cambrian record of animals and ocean geochemical change. *GSA Bulletin* **122**, 1731–1774.
- Mancuso S (2017) *Plant Revolution – Le piante hanno già inventato il nostro futuro*. Firenze–Milano: Giunti.
- Margalef-Bentabol B, Conselice CJ, Mortlock A, Hartley W, Duncan K, Kennedy R, Kocevski DD and Hasinger G (2018) Stellar populations, stellar masses and the formation of galaxy bulges and discs at *z*. *Monthly Notices of the Royal Astronomical Society* **473**, 5370–5384.
- Marguet E, Gaudin M, Gauliard E, Fourquaux I, Plouy S, Matsui I and Forterre P (2013) Membrane vesicles, nanopods and/or nanotubes produced by hyperthermophilic archaea of the genus *Thermococcus*. *Biochemical Society Transactions* **41**, 436–442.
- Margulis L (1998) *Symbiotic Planet – A New Look at Evolution*. New York, NY: Basic Books.
- Marshall CR (2006) Explaining the Cambrian 'explosion' of animals. *Annual Review of Earth and Planets Sciences* **34**, 355–384.
- Martin W and Müller M (1998) The hydrogen hypothesis for the first eukaryote. *Nature* **392**, 37–41.
- McCormick TM and Seewald JS (2007) Abiotic synthesis of organic compounds in deep-sea hydrothermal environments. *Chemical Reviews* **107**, 382–401.
- McHenry HM and Coffing K (2000) Australopithecus to Homo: transformations in body and mind. *Annual Review of Anthropology* **29**, 125–146.
- McInerney JO, Martin WF, Koonin EV, Allen JF, Galperin MY, Lane N, Archibald JM and Embley TM (2011) Planctomycetes and eukaryotes: a case of analogy not homology. *Bioessays* **33**, 810–817.
- McMenamin MAS (1998) *The Garden of Ediacara – Discovering the First Complex Life*. New York, NY: Columbia University Press.
- McMillan PJ (2011) Mass models of the Milky Way. *Monthly Notices of the Royal Astronomical Society* **414**, 2446–2457.
- McShea DW (2001) The hierarchical structure of organisms: a scale and documentation of a trend in the maximum. *Paleobiology* **27**, 405–423.
- Meinesz A (2008) *Comment la vie a commencé – Les trois genèses du vivant*. Paris, France: Belin.
- Melott AL, Lieberman BS, Laird CM, Martin LD, Medvedev MV, Thomas BC, Cannizzo JK, Gehrels N and Jackman CH (2004) Did a gamma-ray burst initiate the late Ordovician mass extinction? *International Journal of Astrobiology* **3**, 55–61.
- Mendell JE, Clements KD, Choat JH and Angert ER (2008) Extreme polyploidy in a large bacterium. *Proceedings of the National Academy of Sciences* **105**, 6730–6734.
- Ménez B, Pisapia C, Andreani M, Jamme F, Vanbelligen QP, Brunelle A, Richard L, Dumas P and Réfrégiers M (2018) Abiotic synthesis of amino acids in the recesses of the oceanic lithosphere. *Nature* **564**, 59–63.
- Menichella M (2005) *Mondi futuri: viaggio tra i possibili scenari*. Pisa, Italy: Scibooks.
- Menichella M and Hack M (2002) *A Caccia di ET*. Rome, Italy: Avverbi.
- Mieli E and Valli AMF (2023) Le cinquième paramètre de Drake et la probabilité de vie intelligente. *Revue scientifique du Bourbonnais et du centre de la France, année 2022*, 25–79.
- Mikhailov KV, Konstantinova AV, Nikitin MA, Troshin PV, Rusin LY, Lyubetsky VA, Panchin YV, Mylnikov AP, Moroz LL, Kumar S and Aleoshin VV (2009) The origin of Metazoa: a transition from temporal to spatial cell differentiation. *Bioessays* **31**, 758–768.
- Miller S (1953) A production of amino acids under possible primitive Earth conditions. *Science* **117**, 528–529.
- Miyake S, Ngugi DK and Stingl U (2016) Phylogenetic diversity, distribution, and cophylogeny of giant bacteria (*Epulopiscium*) with their surgeonfish hosts in the Red Sea. *Frontiers in Microbiology* **7**, 1–15.

- Modjaz M, Liu YQ, Bianco FB and Graur O (2016) The spectral SN-GRB connection: systematic spectral comparisons between type Ic supernovae and broad-lined type Ic supernovae with and without gamma-ray bursts. *The Astrophysical Journal* **832**, 108.
- Montgomery WL and Pollak PE (1988) *Epulopiscium fishelsoni* NG, N. Sp., a protist of uncertain taxonomic affinities from the gut of an herbivorous reef fish. *The Journal of Protozoology* **35**, 565–569.
- Mordan P and Wade C (2008) Heterobranchia II – the Pulmonata. In Ponder WF and Lindeberg DR (eds). *Phylogeny and Evolution of the Molluscan*. Berkeley, CA: University of California Press, pp. 409–426.
- Morse JW and Mackenzie FT (1998) Hadean ocean carbonate geochemistry. *Aquatic Geochemistry* **4**, 301–319.
- Moyà-Solà S, Köhler M and Rook L (2005) The Oreopithecus thumb: a strange case in hominoid evolution. *Journal of Human Evolution* **49**, 395–404.
- Muller F, Brissac T, Le Bris N, Felbeck H and Gros O (2010) First description of giant archaea (Thaumarchaeota) associated with putative bacterial ectosymbionts in a sulfidic marine habitat. *Environmental Microbiology* **12**, 2371–2383.
- Naish D and Tattersdill W (2021) Art, anatomy, and the stars: Russell and Séguin’s dinosaur. *Canadian Journal of Earth Sciences* **58**, 968–979.
- Nelson DL and Cox MM (2021) *Lehninger Principles of Biochemistry*, 4th Edn. W H Freeman and Co., pp. 369–420.
- Neveu M, Kim HJ and Benner SA (2013) The ‘strong’ RNA world hypothesis: fifty years old. *Astrobiology* **13**, 391–403.
- Nisbet E (2000) The realms of Archaean life. *Nature* **405**, 625–626.
- Nutman AP, Bennett VC, Friend CR, Van Kranendonk MJ and Chivas AR (2016) Rapid emergence of life shown by discovery of 3,700-million year-old microbial structures. *Nature* **537**, 535–538.
- Och LM and Shields-Zhou GA (2012) The Neoproterozoic oxygenation event: environmental perturbations and biogeochemical cycling. *Earth – Science Reviews* **110**, 26–57.
- Ogunseitan OA (2016) Introduction to bacterial diversity. In Kliman RM (ed). *Encyclopedia of Evolutionary Biology*, 1. Oxford, UK: Academic Press, pp. 114–118.
- Olejarz J, Iwasa Y, Knoll AH and Nowak MA (2021) The great oxygenation event as a consequence of ecological dynamics modulated by planetary change. *Nature Communications* **12**, 1–9.
- Oosterloo M, Höning D, Kamp IEE and Van Der Tak FFS (2021) The role of planetary interior in the long-term evolution of atmospheric CO₂ on Earth-like exoplanets. *Astronomy and Astrophysics* **649**, A15.
- Paffuti G (2013) *Note Sulla Nascita Della Meccanica Quantistica*. Pisa, Italy: Pisa University Press.
- Papineau D, She Z, Dodd MS, Iacoviello F, Slack JF, Hauri E, Shearing P and Little CTS (2022) Metabolically diverse primordial microbial communities in Earth’s oldest seafloor-hydrothermal jasper. *Science Advances* **8**, 1–16.
- Parfrey LW, Lahr DJG, Knoll AH and Katz LA (2011) Estimating the timing of early eukaryotic diversification with multigene molecular clocks. *Proceedings of the National Academy of Sciences* **108**, 13624–13629.
- Parker AR (1998) Colour in Burgess Shale animals and the effect of light on evolution in the Cambrian. *Proceedings of the Royal Society Biological Sciences, Series B: Biological Sciences* **265**, 967–972.
- Penny D and Poole A (1999) The nature of the last universal common ancestor. *Current Opinion in Genetics and Development* **9**, 672–677.
- Penrose R (1990) *The Emperor’s New Mind: Concerning Computers, Minds, and the Laws of Physics*. Oxford, UK: Oxford University Press.
- Penrose R (1994) *Shadows of the Mind: A Search for the Missing Science of Consciousness*. Oxford, UK: Oxford University Press.
- Petronia IP and Arnold FH (2000) Designed evolution of enzymatic properties. *Current Opinion in Biotechnology* **11**, 325–330.
- Picaud S and Robin AC (2004) 3D outer bulge structure from near infrared star counts. *Astronomy and Astrophysics* **428**, 891–903.
- Pollack JB, Hubickyj O, Bodenheimer P, Lissauer JP, Podolak M and Greenzweig Y (2009) Formation of the giant planets by concurrent accretion of solids and gas. *Icarus* **124**, 62–85.
- Pons ML, Quitté G, Fujii T, Rosing MT, Reynard B, Moynier F, Douche C and Albarède F (2011) Early Archean serpentine mud volcanoes at Isua, Greenland, as a niche for early life. *Proceedings of the National Academy of Sciences* **108**, 17639–17643.
- Porter SM (2004) The fossil record of early eukaryotic diversification. *The Paleontological Society Papers* **10**, 35–50.
- Porter SM (2020) Insights into eukaryogenesis from the fossil record. *Interface Focus* **10**, 1–9.
- Pouydebat E (2017) *L’intelligence animale – Cerveille d’oiseaux et mémoire d’éléphant*. Paris, F: Odile Jacob.
- Praefcke GJ and McMahon HT (2004) The dynamin superfamily: universal membrane tubulation and fission molecules? *Nature Reviews Molecular Cell Biology* **5**, 133–147.
- Qiu Y-L (2008) Phylogeny and evolution of charophytic algae and land plants. *Journal of Systematics and Evolution* **46**, 287–306.
- Rachel R, Wyszchony I, Riehl S and Huber H (2002) The ultrastructure of *Ignicoccus*: evidence for a novel outer membrane and for intracellular vesicle budding in an archaeon. *Archaea* **1**, 9–18.
- Rasmussen B, Fletcher IR, Brocks JJ and Kilburn MR (2008) Reassessing the first appearance of eukaryotes and cyanobacteria. *Nature* **455**, 1101–1104.
- Raup DM (1992) *Extinction – Bad Genes or Bad Luck?* New York, NY: WW Norton and Company.
- Retallack GJ (2013) Ediacaran life on land. *Nature* **493**, 89–92.
- Ritson D and Sutherland JD (2012) Prebiotic synthesis of simple sugars by photoredox systems chemistry. *Nature Chemistry* **4**, 895–899.

- Robertson CE, Harris JK, Spear JR and Pace NR (2005) Phylogenetic diversity and ecology of environmental archaea. *Current Opinion in Microbiology* **8**, 638–642.
- Roger AJ, Muñoz-Gómez SA and Kamikawa R (2017) The origin and diversification of mitochondria. *Current Biology* **27**, 1177–1192.
- Rook L, Bondioli L, Köhler M, Moyà-Solà S and Macchiarelli R (1999) Oreopithecus was a bipedal ape after all: evidence from the iliac cancellous architecture. *Proceedings of the National Academy of Sciences* **96**, 8795–8799.
- Rospars J-P (2013) Trends in the evolution of life, brains and intelligence. *International Journal of Astrobiology* **12**, 186–207.
- Rubenstein EP and Schaefer BE (2000) Are superflares on solar analogues caused by extrasolar planets? *The Astrophysical Journal* **529**, 1031–1033.
- Russell DA and Séguin R (1982) Reconstruction of the small Cretaceous theropod *Stenonychosaurus inequalis* and a hypothetical dinosaurid. *Syllogeus* **37**, 1–43.
- Sagan C and Drake F (1975) The search for extraterrestrial intelligence. *Scientific American* **232**, 80–89.
- Salpeter EE (1954) The luminosity function and stellar evolution. *American Astronomical Society* **121**, 161.
- Sanders RH (2014) *Revealing the Heart of the Galaxy: The Milky Way and its Black Hole*. Cambridge, UK: Cambridge University Press.
- Santarella-Mellwig R, Franke J, Jaedicke A, Gorjánác M, Bauer U, Budd A, Mattaj IW and Devos DP (2010) The compartmentalized bacteria of the Planctomycetes–Verrucomicrobia–Chlamydiae superphylum have membrane coat-like proteins. *PLoS Biology* **8**, 1–11.
- Saul JM (2009) Did detoxification processes cause complex life to emerge? *Lethaia* **42**, 179–184.
- Schoch RR (2014) *Amphibian Evolution – The Life of Early Land Vertebrate*. Oxford, UK: WILEY Blackwell.
- Schopf JW (2019) *Life in Deep Time – Darwin’s ‘Missing’ Fossil Record*. Boca Raton, FL: CRC Press.
- Schopf JM and Packer BM (1987) Early Archean (3.3 billion to 3.5 billion year old) microfossils from Warrawoona Group, Australia. *Science* **237**, 70–73.
- Schopf JW, Kudryavtsev AB, Czaja AD and Tripathi AB (2007) Evidence of Archean life: stromatolites and microfossils. *Precambrian Research* **158**, 141–155.
- Schopf JW, Kudryavtsev AB, Osterhout JT, Williford KH, Kitajima K, Valley JW and Sugitani K (2017) An anaerobic ~3400 Ma shallow-water microbial consortium: presumptive evidence of Earth’s Paleoarchean anoxic atmosphere. *Precambrian Research* **299**, 309–318.
- Schulz HN (2006) The genus *Thiomargarita*. *Prokaryotes* **6**, 1156–1163.
- Schulz HN and Jørgensen BB (2001) Big bacteria. *Annual Review of Microbiology* **55**, 105–137.
- Schulz HN, Brinkhoff T, Ferdelman TG, Mariné MH, Teske A and Jørgensen BB (1999) Dense populations of a giant sulfur bacterium in Namibian shelf sediments. *Science* **284**, 493–495.
- Schulze-Makuch D, Heller R and Guinan E (2020) In search for a planet better than Earth: top contenders for a superhabitable world. *Astrobiology* **20**, 1394–1404.
- Sebé-Pedrós A, Degnan BM and Ruiz-Trillo I (2017) The origin of Metazoa: a unicellular perspective. *Nature Reviews Genetics* **18**, 498–512.
- Seilacher A (1984) Late Precambrian Metazoa: preservational or real extinctions? In Holland DH and Trendall AF (eds). *Patterns of Change in Earth Evolution*. Berlin, GE: Springer-Verlag, pp. 159–168.
- Selosse M-A (2017) *Jamais seul – Ces microbes qui construisent les plantes, les animaux et les civilisations*. Arles, France: Actes Sud.
- Selosse M-A (2021) *L’origine du monde – Une histoire naturelle du sol à l’intention de ceux qui le piétinent*. Arles, France: Actes Sud.
- Shevchenko II, Melnikov AV, Popova EA, Bobylev VV and Karelin GM (2019) Circumbinary planetary systems in the solar neighborhood: stability and habitability. *Astronomy Letters* **45**, 620–626.
- Simon D and Zimmerly S (2008) A diversity of uncharacterized retroelements in bacteria. *Nucleic Acids Research* **36**, 7219–7229.
- Simon JL, Bretagnon P, Chapront J, Chapront-Touzé M, Francou G and Laskar J (1994) Numerical expressions for precession formulae and mean elements for the moon and planets. *Astronomy and Astrophysics* **282**, 663–683.
- Sleep NH (2010) The Hadean–Archaean environment. *Cold Spring Harbor Perspectives in Biology* **2**, 1–14.
- Smulsky JJ (2011) The influence of the planets, sun and moon on the evolution of the Earth’s axis. *International Journal of Astronomy and Astrophysics* **1**, 117.
- Sojo V, Herschy B, Whicher A, Camprubí E and Lane N (2016) The origin of life in alkaline hydrothermal vents. *Astrobiology* **16**, 181–200.
- Southam G, Rothschild LJ and Westall F (2007) The geology and habitability of terrestrial planets: fundamental requirements for life. *Space Science Reviews* **129**, 7–34.
- Spang A, Saw JH, Jørgensen SL, Zaremba-Niedzwiedzka K, Martijn J, Lind AE, van Eijk R, Schleper C, Guy L and Ettema TJG (2015) Complex archaea that bridge the gap between prokaryotes and eukaryotes. *Nature* **521**, 173–179.
- Spang A, Eme L, Saw JH, Caceres EF, Zaremba-Niedzwiedzka K, Jonathan Lombard J, Guy L and Ettema TJG (2018) Asgard archaea are the closest prokaryotic relatives of eukaryotes. *PLoS Genetics* **14**, 1–4.
- Staaf D (2020) *Monarchs of the Sea – The Extraordinary 500–Millionyear History of Cephalopods*. New York, NY: The Experiment LLC.
- Stainer RY, Adelberg EA and Ingraham J (1976) *The Microbial World*, 4th Edn. Englewood Cliffs, NJ: Prentice Hall.

- Stanford CB (2001) *The Hunting Apes: Meat Eating and the Origins of Human Behavior*. Princeton, NJ: Princeton University Press.
- Steyer S (2009) *La terre avant les dinosaures*. Paris, France: Belin.
- Strother PK, Brasier MD, Wacey D, Timpe L, Saunders M and Wellman CH (2021) A possible billion year-old holozoan with differentiated multicellularity. *Current Biology* **31**, 2658–2665.
- Stworzewicz E, Szulc J and Pokryszko BM (2009) Late Paleozoic continental gastropods from Poland: systematic, evolutionary and paleoecological approach. *Journal of Paleontology* **83**, 938–945.
- Summons RE, Bradley AS, Jahnke LL and Waldbauer JR (2006) Steroids, triterpenoids and molecular oxygen. *Philosophical Transactions of the Royal Society B: Biological Sciences* **361**, 951–968.
- Susman RL (1991) Who made the Oldowan tools? Fossil evidence for tool behavior in Plio–Pleistocene hominids. *Journal of Anthropological Research* **47**, 129–151.
- Susman RL (2005) *Oreopithecus*: still apelike after all these years. *Journal of Human Evolution* **49**, 405–411.
- Sweeney D, Tuthill P, Sharma S and Hirai R (2022) The galactic underworld: the spatial distribution of compact remnants. *Monthly Notices of the Royal Astronomical Society* **516**, 4971–4979.
- Tajima H (2009) Fermi observations of high-energy gamma-ray emissions from GRB 080916C. *arXiv preprint arXiv:0907.0714*.
- Takeuchi Y, Furukawa Y, Kobayashi T, Sekine T, Terada N and Kakegawa T (2020) Impact-induced amino acid formation on Hadean Earth and Noachian Mars. *Scientific Reports* **10**, 1–7.
- Tattersall I (2016) A tentative framework for the acquisition of language and modern human cognition. *Journal of Anthropological Sciences* **94**, 157–166.
- Taylor TN, Taylor EL and Krings M (2009) *Paleobotany: The Biology and Evolution of Fossil Plants*, 2nd Edn. Amsterdam, HO: Academic Press.
- Theobald DL (2010) A formal test of the theory of universal common ancestry. *Nature* **465**, 219–222.
- Tipler FJ (1980) Extraterrestrial intelligent beings do not exist. *Journal of the Royal Astronomical Society* **21**, 267–281.
- Tipler FJ (1994) *The Physics of Immortality*. New York, NK: Anchor.
- Tokovinin AA (1997) MSC, a catalogue of physical multiple stars. *Astronomy and Astrophysics Supplement Series* **124**, 75–84.
- Tomitani A, Okada K, Miyashida H, Matthijs HCP, Ohno T and Tanaka A (1999) Chlorophyll b and phycobilins in the common ancestor of cyanobacteria and chloroplasts. *Nature* **400**, 159–162.
- Tovar J, León-Avila G, Sánchez LB, Sutak R, Tachezy J, Van Der Giezen M, Hernández M, Müller M and Lucocq JM (2003) Mitochondrial remnant organelles of Giardia function in iron–sulphur protein maturation. *Nature* **426**, 172–176.
- Trail D, Watson EB and Taibly ND (2011) The oxidation state of Hadean magmas and implications for early Earth's atmosphere. *Nature* **480**, 79–82.
- Trail D, Watson EB, Taibly NDZ-L, Yang M, Zhang ZJ and Wang FY (2020) Superflares on solar-type stars from the first year observation of TESS. *The Astrophysical Journal* **890**, 46.
- Valli AMF (2020) *Bactéries, Dinosaures et Kangourous – Brève Histoire de la Biodiversité*. Lyons, F: Dédale Éditions.
- Valli AMF and Mieli E (2022) Un modèle mathématique pour le passage du non vivant au vivant. *Revue scientifique du Bourbonnais et du centre de la France* **2021**, 9–35.
- van Tuinen M and Hadly EA (2004) Error in estimation of rate and time inferred from the early amniote fossil record and avian molecular clocks. *Journal of Molecular Evolution* **59**, 267–276.
- Vellai T and Vida G (1999) The origin of eukaryotes: the difference between prokaryotic and eukaryotic cells. *Proceedings of the Royal Society of London. Series B: Biological Sciences* **266**, 1571–1577.
- Vinge VS (1993) Technological singularity. In VISION-21 symposium sponsored by NASA Lewis Research Center and the Ohio Aerospace Institute. Verner Vinge Magazine: Whole Earth Review, pp. 30–31.
- von Dohlen CD, Kohler S, Alsop ST and McManus WR (2001) Mealybug β -proteobacterial endosymbionts contain γ -proteobacterial symbionts. *Nature* **412**, 433–436.
- Watson JD, Baker TA, Bell SP, Gann A, Levine M and Losick R (2013) *Molecular Biology of the Gene*, 8th Edn. London, UK: Pearson PLC.
- Webb S (2015) *If the Universe is Teeming with Aliens ... Where is Everybody? – Seventy-Five Solutions to the Fermi Paradox and the Problem of Extraterrestrial Life*, 2th Edn. Berlin, GE: Springer International Publishing.
- Wellman CH, Osterloff PL and Mohiuddin U (2003) Fragments of the earliest land plants. *Nature* **425**, 282–285.
- Wujek DE (1979) Intracellular bacteria in the blue-green alga *Pleurocapsa minor*. *Transactions of the American Microscopical Society* **98**, 143–145.
- Xiao S (2013) Muddying the waters. *Nature* **493**, 28–29.
- Xiao S, Zhang Y and Knoll AH (1998) Three-dimensional preservation of algae and animal embryos in a Neoproterozoic phosphorite. *Nature* **391**, 553–558.
- Yadav M, Kumar R and Krishnamurthy R (2020) Chemistry of abiotic nucleotide synthesis. *Chemical Reviews* **120**, 4766–4805.
- Yamaguchi M, Mori Y, Kozuka Y, Okada H, Uematsu K, Tame A, Furukawa H, Maruyama T, O'Driscoll Worman C and Yokoyama K (2012) Prokaryote or eukaryote? A unique microorganism from the deep sea. *Journal of Electron Microscopy* **61**, 423–431.
- Yamaguchi M, Yamada H and Chibana H (2020) Deep-sea bacteria harboring bacterial endosymbionts in a cytoplasm?: 3D electron microscopy by serial ultrathin sectioning of freeze-substituted specimen. *Cytologia* **85**, 209–211.

- Yoon HS, Hackett JD, Ciniglia C, Pinto G and Bhattacharya D (2004) A molecular timeline for the origin of photosynthetic eukaryotes. *Molecular Biology and Evolution* **21**, 809–818.
- Yoshinaka T, Yano K and Yamaguchi H (1973) Isolation of highly radioresistant bacterium *Arthrobacter radiotolerans* nov. sp. *Agricultural and Biological Chemistry* **37**, 2269–2275.
- Yutin N and Koonin EV (2012) Archaeal origin of tubulin. *Biology Direct* **7**, 1–9.
- Zahnle K, Arndt N, Cockell C, Halliday A, Nisbet E, Selsis F and Sicep NH (2007) Emergence of a habitable planet. *Space Science Reviews* **129**, 35–78.
- Zakhvatkin AA (1949) *The Comparative Embryology of the low Invertebrates*. Moscow, RU: Sources and method of the origin of metazoan development.
- Zaremba-Niedzwiedzka K, Caceres EF, Saw JH, Bäckström D, Juzokaite L, Vancaester E, Seitz KW, Anantharaman K, Starnawski P, Kjeldsen KU, Stott MB, Nunoura T, Banfield JF, Schramm A, Baker BJ, Spang A and Ettema TJG (2017) Asgard archaea illuminate the origin of eukaryotic cellular complexity. *Nature* **541**, 353–358.
- Zhang B (2018) *The Physics of Gamma-Ray Bursts*. Cambridge, UK: Cambridge University Press. ISBN: 978-1-139-22653-0.
- Zhao W, Zhang X, Jia G, Shen YA and Zhu M (2021) The Silurian–Devonian boundary in East Yunnan (South China) and the minimum constraint for the lungfish–tetrapod split. *Science China Earth Sciences* **64**, 1784–1797.
- Zimorski V, Mentel M, Tielens AG and Martin WF (2019) Energy metabolism in anaerobic eukaryotes and Earth’s late oxygenation. *Free Radical Biology and Medicine* **140**, 279–294.
- Zubrin R (1999) *Entering Space: Creating a Spacefaring Civilization*. New York, NY: Putnam Publishing.

Appendix A: Summary of the 49 steps (plus one) of the Drake equation

Step	Drake Par.	Value	Description
1	Drake 1	1.10×10^{10}	Number of stars of the galaxy suitable for life (of spectral class F, G and K)
2	Drake 2	1.80×10^{-1}	Number of planets suitable in the habitable area for star (spectral class F, G and K)
3	Drake 3	1.84×10^{-2}	Fraction of stable planets
4			Multiple star systems
5			Supernova less than 40 ly away
6			Gamma flashes with less than 5000 ly away
7			Superflare of the star
8			Transit of the gassy giants on internal orbits
9			Prolonged meteoric bombardment
10			Instability of the rotation axis
11			Absence of the carbon cycle
12	Drake 4	5.16×10^{-1}	Absence of the planetary magnetic field
13	Drake 5	5.45×10^{-1}	Fraction of planets where life is born
14			The abiological synthesis of biological molecules
15			The concentration of the primordial broth
16			The formation of lipid bags
17			Inclusion in the lipid membranes of chlorophyll
18			The ‘photopump for protons’
19			The formation of nucleic acid filaments
20			The catalytic role of the RNA
21			Determination of roles
22			Cell membrane formation
	Eukaryotes		Emergency of the genetic code
			Fraction of planets where eukaryotes are born
			The evolution of an aerobic bacterium

(Continued)

Appendix A: (Continued.)

Step	Drake Par.	Value	Description
23			The guest–symbiont encounter
24			The formation of the pores and the escape of cytoplasmic extensions
25			The ‘winding’ of the symbionts and the disappearance of the guest’s cell wall
26			The penetration of symbionts in the cytoplasm
27			The migration of DNA from the genome of the symbiont to that of the guest
28			The acquisition of the eukaryotic cytoplasmic membrane
29			Incorporation into a single coating and phagocytosis
30	Drake 5	8.49×10^{-1}	Fraction of planets where animals are born (metazoa)
31	Metazoa		The acquisition of a complex life cycle
32			The aggregation of the zoospores and the formation of the synzoospore
33			The sedentary colony composed of differentiated cells
34	Drake 5	3.48×10^{-2}	The production of collagen
35	ETC		Fraction of planets where technological civilizations (ETC) are born
36			Increased metazoa size (nervous and vascular system)
37			Limb development
38			Conquest of lands above sea level
39			Differentiation of land animals
40			Upright position and manual skills
41			Change of diet and encephal growth
42			Organization of the brain on abstract thinking
43	Drake 6	5.00×10^{-1}	Birth of articulated language and technique
44			Fraction of planets where life decides to communicate
45	Drake 7	7.29×10^{-6}	Fraction of the static ETCs duration ($K < 1.4$)
46			Self-destruction due to evolutionary failure
47			Involuntary technological error
48			Technological insufficiency to face planetary changes
49			Spontaneous involution
50			Artificial genetic transition ended up on a dead track
			Transition of artificial intelligence ended up on a dead track
			Reaching Ω point
	Drake 7	4.64×10^{-3}	Fraction of dynamics ETCs that exceed 7 challenges and become eternal ($K \geq 1.4$)

Appendix B: Percentage of past planets and present for each stage of development

The calculation sequence reported in these tables starts from the first three parameters of Drake, the astronomical ones, providing their probabilistic combination for all the duration of the planet, from 0 to 9.5 Gy.

The subsequent combination with the following vestments, from fourth onwards, takes into account the necessary times when the processes reported in Table 28. Based on those times, the corresponding value of the third parameter is chosen.

Until the sixth parameter, both the number of planets inhabited by life forms during the whole stellar population of 7 Gy, and of those inhabited, is reported. The seventh parameter instead introduces a rigid temporal bond that directly provides us with current ETCs both in the case of static civilizations K1 (7A) and in that of K2 dynamic civilizations (7B).

Finally, we note that the distance values reported in Table 29 are obtained taking into account the following average values of the typical quantities of the galactic disk, that is, without considering the galactic centre (Bulge):

1.13×10^{11}	Average number of disk stars
1.53×10^{13}	Average disk volume (ly^3)
5	Average distance stars (ly)

Appendix B1. Percentage of past planets and present for each stage of development

1'-2'-3' Drake	grandezza sperimentale		frazione minima nel tempo max	frazione massima nel tempo max	componente j media logaritmo	componente j varianza logaritmo	somma media logaritmo	somma varianza logaritmo	media processo tot	scostamento processo tot	MIN pianeti potenzialmente abitabili	MAX pianeti potenzialmente abitabili	
		ΔT	A_j	B_j	μ_j	σ_j^2	μ	σ^2	$\langle X_p \rangle$	σX_p	$\langle XD_p \rangle$	$\langle XD_p \rangle$	
1	Numero di stelle della galassia adatte alla vita (di classe spettrale F, G e K)	anni di durata del pianeta	1,00E+10	1,20E+10	23,1198	0,0028							
2	numero pianeti adatti nella zona abitabile per stella (di classe spettrale F, G e K)		1,60E-01	2,00E-01	-1,7169	0,0041							
3	frazione di pianeti stabili per anni		0,00E+00	1,00E+00	0,0000	0,0000	21,4029	0,0069	1,98E+09	1,65E+08	1,69E+09	2,27E+09	5,4E+08 passo temporale τ MIN = 1.359.230.076 anni τ MAX = 2.016.147.681 anni $p = \exp(-\Delta TMAX/\tau)$
			5,00E+08	6,92E-01	7,90E-01	-0,3067	0,0012	21,0962	0,0081	1,46E+09	1,31E+08	1,23E+09	1,69E+09
			1,00E+09	4,79E-01	6,09E-01	-0,6111	0,0048	20,7918	0,0117	1,08E+09	1,17E+08	8,75E+08	1,28E+09
			1,50E+09	3,32E-01	4,75E-01	-0,9130	0,0107	20,4899	0,0176	7,99E+08	1,06E+08	6,14E+08	9,83E+08
			2,00E+09	2,30E-01	3,71E-01	-1,2126	0,0189	20,1903	0,0258	5,94E+08	9,62E+07	4,28E+08	7,61E+08
			2,50E+09	1,59E-01	2,89E-01	-1,5099	0,0294	19,8930	0,0363	4,44E+08	8,54E+07	2,96E+08	5,92E+08
			3,00E+09	1,10E-01	2,26E-01	-1,8048	0,0420	19,5981	0,0489	3,33E+08	7,45E+07	2,04E+08	4,62E+08
			3,50E+09	7,62E-02	1,76E-01	-2,0975	0,0567	19,3054	0,0636	2,50E+08	6,41E+07	1,39E+08	3,61E+08
			4,00E+09	5,27E-02	1,38E-01	-2,3879	0,0732	19,0150	0,0801	1,89E+08	5,45E+07	9,42E+07	2,83E+08
			4,50E+09	3,65E-02	1,07E-01	-2,6762	0,0916	18,7267	0,0985	1,43E+08	4,59E+07	6,32E+07	2,22E+08
			5,00E+09	2,53E-02	8,37E-02	-2,9623	0,1116	18,4406	0,1185	1,08E+08	3,84E+07	4,17E+07	1,75E+08
			5,50E+09	1,75E-02	6,54E-02	-3,2464	0,1331	18,1566	0,1400	8,24E+07	3,19E+07	2,71E+07	1,38E+08
			6,00E+09	1,21E-02	5,10E-02	-3,5284	0,1559	17,8745	0,1628	6,28E+07	2,64E+07	1,71E+07	1,09E+08
			6,50E+09	8,38E-03	3,98E-02	-3,8085	0,1799	17,5945	0,1868	4,81E+07	2,18E+07	1,03E+07	8,58E+07
			7,00E+09	5,80E-03	3,11E-02	-4,0867	0,2050	17,3163	0,2119	3,68E+07	1,79E+07	5,84E+06	6,78E+07
			7,50E+09	4,01E-03	2,42E-02	-4,3630	0,2308	17,0399	0,2377	2,83E+07	1,47E+07	2,91E+06	5,37E+07
			8,00E+09	2,78E-03	1,89E-02	-4,6376	0,2574	16,7653	0,2643	2,18E+07	1,20E+07	1,03E+06	4,26E+07
			8,50E+09	1,92E-03	1,48E-02	-4,9106	0,2845	16,4923	0,2914	1,68E+07	9,78E+06	-1,24E+05	3,38E+07
			9,00E+09	1,33E-03	1,15E-02	-5,1819	0,3119	16,2210	0,3188	1,30E+07	7,97E+06	-7,98E+05	2,68E+07
			9,50E+09	9,22E-04	8,99E-03	-5,4517	0,3396	15,9512	0,3465	1,01E+07	6,48E+06	-1,15E+06	2,13E+07
4' Drake	grandezza sperimentale		frazione minima nel tempo max	frazione massima nel tempo max	componente j media logaritmo	componente j varianza logaritmo	somma media logaritmo	somma varianza logaritmo	media processo tot	scostamento processo tot	MIN processo tot	MAX processo tot	
		ΔT	A_j	B_j	μ_j	σ_j^2	μ	σ^2	$\langle X_p \rangle$	σX_p	$\langle XD_p \rangle$	$\langle XD_p \rangle$	
1	Numero di stelle della galassia adatte alla vita (di classe spettrale F, G e K)	anni di durata del pianeta	1,00E+10	1,20E+10	23,1198	0,0028	20,3603	0,0490	7,13E+08	1,60E+08	4,36E+08	9,89E+08	712.851.649 712.851.649 pianeti in 7 Ga su un totale di 1.457.862.814
2	numero pianeti adatti nella zona abitabile per stella (di classe spettrale F, G e K)		1,60E-01	2,00E-01	-1,7169	0,0041							91.652.355 pianeti attuali su un totale di 187.439.505
3	frazione di pianeti stabili per anni		9,00E+08	6,92E-01	7,90E-01	-0,3067	0,0012						
4	frazione di pianeti dove nasce la vita		3,22E-01	6,55E-01	-0,7359	0,0409							
5' eucarioti	grandezza sperimentale		frazione minima nel tempo max	frazione massima nel tempo max	componente j media logaritmo	componente j varianza logaritmo	somma media logaritmo	somma varianza logaritmo	media processo tot	scostamento processo tot	MIN processo tot	MAX processo tot	
		ΔT	A_j	B_j	μ_j	σ_j^2	μ	σ^2	$\langle X_p \rangle$	σX_p	$\langle XD_p \rangle$	$\langle XD_p \rangle$	
1	Numero di stelle della galassia adatte alla vita (di classe spettrale F, G e K)	anni di durata del pianeta	1,00E+10	1,20E+10	23,1198	0,0028	18,1358	0,1541	8,12E+07	3,32E+07	2,38E+07	1,39E+08	81.238.609 81.238.609 pianeti in 7 Ga su un totale di 332.630.617
2	numero pianeti adatti nella zona abitabile per stella (di classe spettrale F, G e K)		1,60E-01	2,00E-01	-1,7169	0,0041							34.816.547 pianeti attuali su un totale di 142.555.979
3	frazione di pianeti stabili per anni		3,00E+09	1,10E-01	2,26E-01	-1,8048	0,0420						
4	frazione di pianeti dove nasce la vita		3,22E-01	6,55E-01	-0,7359	0,0409							
5 eucarioti	frazione di pianeti dove nascono eucarioti		2,89E-01	7,09E-01	-0,7264	0,0644							

Appendix B2. Percentage of past planets and present for each stage of development

5* metazoi	grandezza sperimentale		frazione minima nel tempo max	frazione massima nel tempo max	componente j media logaritmo	componente j varianza logaritmo	somma media logaritmo	somma varianza logaritmo	media processo tot	scostamento processo tot	MIN processo tot	MAX processo tot		
		ΔT anni di durata del pianeta	A_j	B_j	μ_j	σ_j^2	μ	σ^2	$\langle X_j \rangle$	σX_j	$\langle X \rangle_A$	$\langle X \rangle_B$		
1	Numero di stelle della galassia adatte alla vita (di classe spettrale F, G e K)		1,00E+10	1,20E+10	23,1198	0,0028	17,2836	0,2026	3,55E+07	1,68E+07	6,36E+06	6,46E+07	35.493.456	20.281.975
2	numero pianeti adatti nella zona abitabile per stella (di classe spettrale F, G e K)		1,60E-01	2,00E-01	-1,7169	0,0041							planeti in 7 Ga su un totale di 188.580.549	planeti attuali su un totale di 107.760.314
3	frazione di pianeti stabili per anni	4,00E+09	5,27E-02	1,38E-01	-2,3879	0,0732								
4	frazione di pianeti dove nasce la vita		3,22E-01	6,55E-01	-0,7359	0,0409								
5 eucarioti	frazione di pianeti dove nascono eucarioti		2,89E-01	7,09E-01	-0,7264	0,0644								
5 metazoi	frazione di pianeti dove nascono metazoi		5,97E-01	9,44E-01	-0,2692	0,0172								
5* CET	grandezza sperimentale		frazione minima nel tempo max	frazione massima nel tempo max	componente j media logaritmo	componente j varianza logaritmo	somma media logaritmo	somma varianza logaritmo	media processo tot	scostamento processo tot	MIN processo tot	MAX processo tot		
		ΔT anni di durata del pianeta	A_j	B_j	μ_j	σ_j^2	μ	σ^2	$\langle X_j \rangle$	σX_j	$\langle X \rangle_A$	$\langle X \rangle_B$		
1	Numero di stelle della galassia adatte alla vita (di classe spettrale F, G e K)		1,00E+10	1,20E+10	23,1198	0,0028	13,5528	0,3909	9,35E+05	6,47E+05	-1,85E+05	2,06E+06	934.994	601.067
2	numero pianeti adatti nella zona abitabile per stella (di classe spettrale F, G e K)		1,60E-01	2,00E-01	-1,7169	0,0041							planeti in 7 Ga su un totale di 142.657.715	planeti attuali su un totale di 91.708.531
3	frazione di pianeti stabili per anni	4,50E+09	3,65E-02	1,07E-01	-2,6762	0,0916								
4	frazione di pianeti dove nasce la vita		3,22E-01	6,55E-01	-0,7359	0,0409								
5 eucarioti	frazione di pianeti dove nascono eucarioti		2,89E-01	7,09E-01	-0,7264	0,0644								
5 metazoi	frazione di pianeti dove nascono metazoi		5,97E-01	9,44E-01	-0,2692	0,0172								
5 CET	frazione di pianeti dove nascono CET		1,25E-02	5,66E-02	-3,4425	0,1700								
6* Drake	grandezza sperimentale		frazione minima nel tempo max	frazione massima nel tempo max	componente j media logaritmo	componente j varianza logaritmo	somma media logaritmo	somma varianza logaritmo	media processo tot	scostamento processo tot	MIN processo tot	MAX processo tot		
		ΔT anni di durata del pianeta	A_j	B_j	μ_j	σ_j^2	μ	σ^2	$\langle X_j \rangle$	σX_j	$\langle X \rangle_A$	$\langle X \rangle_B$		
1	Numero di stelle della galassia adatte alla vita (di classe spettrale F, G e K)		1,00E+10	1,20E+10	23,1198	0,0028	12,8529	0,4045	4,68E+05	3,30E+05	-1,04E+05	1,04E+06	467.518	300.547
2	numero pianeti adatti nella zona abitabile per stella (di classe spettrale F, G e K)		1,60E-01	2,00E-01	-1,7169	0,0041							planeti in 7 Ga su un totale di 142.657.715	planeti attuali su un totale di 91.708.531
3	frazione di pianeti stabili per anni	4,50E+09	3,65E-02	1,07E-01	-2,6762	0,0916								
4	frazione di pianeti dove nasce la vita		3,22E-01	6,55E-01	-0,7359	0,0409								
5 eucarioti	frazione di pianeti dove nascono eucarioti		2,89E-01	7,09E-01	-0,7264	0,0644								
5 metazoi	frazione di pianeti dove nascono metazoi		5,97E-01	9,44E-01	-0,2692	0,0172								
5 CET	frazione di pianeti dove nascono CET		1,25E-02	5,66E-02	-3,4425	0,1700								
6	frazione di pianeti dove la vita decide di comunicare		4,00E-01	6,00E-01	-0,6999	0,0136								

Appendix B3. Percentage of past planets and present for each stage of development

7 ^a A Drake	grandezza sperimentale		frazione minima nel tempo max	frazione massima nel tempo max	componente j media logaritmo	componente j varianza logaritmo	somma media logaritmo	somma varianza logaritmo	media processo tot	scostamento processo tot	MIN processo tot	MAX processo tot	
		ΔT	A_j	B_j	μ_j	σ_j^2	μ	σ^2	$\langle X_0 \rangle$	σX_0	$\langle X_0 \rangle_{\mu}$	$\langle X_0 \rangle_{\sigma}$	
1	Numero di stelle della galassia adatte alla vita (di classe spettrale F, G e K)	anni di durata del pianeta	1,00E+10	1,20E+10	23,1198	0,0028	1,0213	0,4110	3,41E+00	2,43E+00	-8,01E-01	7,62E+00	3
2	numero pianeti adatti nella zona abitabile per stella (di classe spettrale F, G e K)		1,60E-01	2,00E-01	-1,7169	0,0041							pianeti attuali su un totale di 142.657.715
3	frazione di pianeti stabili per anni	4,55E+09	3,65E-02	1,07E-01	-2,6762	0,0916							
4	frazione di pianeti dove nasce la vita		3,22E-01	6,55E-01	-0,7359	0,0409							
5 eucarioti	frazione di pianeti dove nascono eucarioti		2,89E-01	7,09E-01	-0,7264	0,0644							
5 metazoi	frazione di pianeti dove nascono metazoi		5,97E-01	9,44E-01	-0,2692	0,0172							
5 CET	frazione di pianeti dove nascono CET		1,25E-02	5,66E-02	-3,4425	0,1700							
6	frazione di pianeti dove la vita decide di comunicare		4,00E-01	6,00E-01	-0,6999	0,0136							
7	frazione temporale della durata di una civiltà di tipo K1 statica		6,29E-06	8,30E-06	-11,8316	0,0064							

7 ^a B Drake	grandezza sperimentale		frazione minima nel tempo max	frazione massima nel tempo max	componente j media logaritmo	componente j varianza logaritmo	somma media logaritmo	somma varianza logaritmo	media processo tot	scostamento processo tot	MIN processo tot	MAX processo tot	
		ΔT	A_j	B_j	μ_j	σ_j^2	μ	σ^2	$\langle X_0 \rangle$	σX_0	$\langle X_0 \rangle_{\mu}$	$\langle X_0 \rangle_{\sigma}$	
1	Numero di stelle della galassia adatte alla vita (di classe spettrale F, G e K)	anni di durata del pianeta	1,00E+10	1,20E+10	23,1198	0,0028	7,3533	0,6981	2,21E+03	2,22E+03	-1,64E+03	6,07E+03	2.214
2	numero pianeti adatti nella zona abitabile per stella (di classe spettrale F, G e K)		1,60E-01	2,00E-01	-1,7169	0,0041							pianeti attuali su un totale di 142.657.715
3	frazione di pianeti stabili per anni	4,95E+09	3,65E-02	1,07E-01	-2,6762	0,0916							
4	frazione di pianeti dove nasce la vita		3,22E-01	6,55E-01	-0,7359	0,0409							
5 eucarioti	frazione di pianeti dove nascono eucarioti		2,89E-01	7,09E-01	-0,7264	0,0644							
5 metazoi	frazione di pianeti dove nascono metazoi		5,97E-01	9,44E-01	-0,2692	0,0172							
5 CET	frazione di pianeti dove nascono CET		1,25E-02	5,66E-02	-3,4425	0,1700							
6	frazione di pianeti dove la vita decide di comunicare		4,00E-01	6,00E-01	-0,6999	0,0136							
7	frazione temporale della durata di una civiltà di tipo K2 dinamica		1,03E-03	8,25E-03	-5,4996	0,2935							

Appendix C: The calculation of the distribution function of the seventh parameter

Knowing that $\Phi(z)$ is Maccone’s lognormal, the $F_p(\Delta T_p)$ distribution function is written:

$$\left\{ \begin{aligned} \Phi(z) &\equiv \frac{1}{z} \times \frac{1}{\sqrt{2\pi\sigma}} e^{-\frac{(\ln(z)-\mu)^2}{2\sigma^2}} \\ F_p(\Delta T_p) &= \Phi\left(p^{\frac{\Delta T_0}{\Delta T_p}}\right) \times p^{\frac{\Delta T_0}{\Delta T_p}} \times \left(\frac{\Delta T_0 \ln \frac{1}{p}}{\Delta T_p^2}\right). \end{aligned} \right.$$

To derive the above equation with respect to ΔT_p , we use the following formulas:

$$\left\{ \begin{aligned} \frac{d}{dz} \Phi(z) &= \Phi(z) \times \left[\frac{\mu - \ln(z) - \sigma^2}{z\sigma^2}\right] \\ \frac{d}{dy} \left(p^{\frac{y_0}{y}}\right) &= \frac{y_0 \times \ln\left(\frac{1}{p}\right) \times p^{\frac{y_0}{y}}}{y^2} \\ \frac{d}{dy} \left[p^{\frac{y_0}{y}} \times \left(\frac{y_0 \times \ln \frac{1}{p}}{y^2}\right) \right] &= \frac{y_0 \times \ln\left(\frac{1}{p}\right) \times p^{\frac{y_0}{y}}}{y^4} \times y_0 \times \ln\left(\frac{1}{p}\right) - 2y, \end{aligned} \right.$$

where we have set, as a synthetic notation: $\Delta T_p = y$ and $\Delta T_0 = y_0$.

Therefore, we will have:

$$\begin{aligned} \frac{d}{dy} F(y) &= \Phi\left(p^{\frac{y_0}{y}}\right) \times \frac{y_0 \times \ln\left(\frac{1}{p}\right) \times p^{\frac{y_0}{y}}}{y^5 \sigma^2} \\ &\times \left[(-2\sigma^2) \times y^2 + \left(\mu \times y_0 \times \ln\left(\frac{1}{p}\right)\right) \times y + \left(y_0 \times \ln\left(\frac{1}{p}\right)\right)^2 \right] \\ &= 0. \end{aligned}$$

That is to say:

$$(-2\sigma^2) \times y^2 + \left(\mu \times y_0 \times \ln\left(\frac{1}{p}\right)\right) \times y + \left(y_0 \times \ln\left(\frac{1}{p}\right)\right)^2 = 0,$$

and then, selecting only the greater-than-zero solution for y :

$$\left\{ \begin{aligned} y_{MAX} &= C \times \left(y_0 \times \ln\left(\frac{1}{p}\right)\right) \\ C &= \frac{\mu + \sqrt{\mu^2 + 8\sigma^2}}{4\sigma^2} \end{aligned} \right.$$

Finally, at the maximum point, for $F_p(\Delta T_p)$, you will have:

$$\left\{ \begin{array}{l} F(\Delta T_{p\text{MAX}}) = D \times \frac{1}{y_0 \times \ln\left(\frac{1}{p}\right)} \\ D = \frac{\exp\left[-\frac{1}{2\sigma^2} \left(\frac{4\sigma^2}{\sqrt{\mu^2 + 8\sigma^2} + \mu}\right)^2\right]}{\sqrt{2\pi}\sigma \left(\frac{\sqrt{\mu^2 + 8\sigma^2} + \mu}{4\sigma^2}\right)^2} \end{array} \right.$$